Programa de Doctorado "Matemáticas"

PhD Dissertation

Dynamics and Bifurcations in Nonlinear Systems with Hysteresis

Author

Marina Esteban Pérez

Supervisors

Prof. Dr. Enrique Ponce Núñez

Prof. Dr. Francisco Torres Peral

A mis padres y hermanos.
A mis abuelos.

Agradecimientos

Ahora que me encuentro al final de este camino, echo la vista atrás y me doy cuenta de toda la gente que ha contribuido de una manera u otra en él.

Empiezo agradeciendo a mis directores de tesis Enrique y Paco, sin los que este trabajo no hubiese sido posible. Ambos me habéis enseñado no sólo matemáticas, sino también a ser más fuerte. Enrique, gracias por estar siempre ahí en mis momentos de agobio y por tus consejos. Paco, gracias por poner una nota de humor en cada reunión y ayudarme a cada paso. Habéis sido más que unos padres académicos.

Reconocimiento especial merecen mis compañeros del Departamento de Matemática Aplicada II. Javier, por responder todas mis dudas burocráticas. Emilio, porque tú y Enrique me metisteis en este mundo de los Sistemas Dinámicos, para mí eres un gran ejemplo. Fernando, porque a pesar de que me caigas mal, me alegras los congresos y te comes todos los pastelitos. A los que han sido compañeros en la docencia, como Juan Manuel y Bosco, gracias por vuestras muestras de cariño. No puedo olvidarme de Mari Carmen, secretaria del departamento, que ha tenido mucha paciencia conmigo.

Agradezco, como no podría ser de otra manera, a los amigos que me han acompañado desde que empecé el Grado en Matemáticas. Mercedes, Ana, Cristina, Lorena, Bea, Asun, Fran e Ismael, el destino quiso que estuviésemos juntos de principio a fin. Gracias a todos por cada rato de risas, cada tarde en la biblioteca y cada reunión tan 'fantástica'. Especialmente, gracias 'mami' Asun por dejarme aprender de ti y por cuidarme tanto. Si no fuese por ti, yo no estaría aquí porque se me hubiese olvidado presentar los papeles. Poco tiempo después, se cruzaron en mi camino un malagueño y un murciano, a los que les agradezco la poca productividad investigadora y las muchas carcajadas; siempre nos quedarán los 'Pijos, Pan y Habas'.

Gracias a mis amigas del alma, mis 'Tiramis', Irene, Laura, Yolanda, Kris y Salva. Por preguntar infinitas veces de qué va esta tesis y fascinaros sin ni siquiera entenderlo. Gracias por vuestras palabras de aliento y por estar ahí siempre. Sigamos luchando por nuestros sueños tan dispares y tan unidas.

A mi familia entera, millones de gracias. Papá, porque aunque parezca mentira, discutir también desestresa, gracias por sentirte tan orgulloso de mí.

Mamá, mi pilar fundamental, necesitaría diez mil páginas para agradecerte todo lo que haces por mí, gracias por darme lo que necesito sin pedírtelo. Gracias a mis hermanos, Octavín e Irene, por entender cuándo tenía un día malo y saber cambiarlo. A mis abuelas, porque de mi abuela Lupe heredé la perseverancia y de mi abuela Pepa aprendí que todo sacrificio tiene su recompensa, mejor si es tomate. A mis abuelos Julio y Juan, ¡ay, cuánto me gustaría que estuviérais aquí! A mi perro, Flaco, porque aunque no sabe ni qué es una tesis, su cariño me ha reconfortado siempre.

Gracias también a ti, Nano, porque has sido mi vía de escape. Llenas mis días de risas y de amor. Has estado siempre de mi lado, luchando contra mis miedos y haciéndome sentir que contigo, estoy segura. No dejes nunca de hacerlo, te quiero.

Resumen

El principal objetivo de esta tesis es la determinación de soluciones periódicas así como posibles bifurcaciones en una familia de sistemas dinámicos en presencia de histéresis. En particular, analizamos sistemas lineales a trozos en tres dimensiones con dinámica lenta-rápida, que tras la introducción de una no linealidad de tipo histéresis, quedan reducidos a sistemas planos.

En el Capítulo 1 introducimos los sistemas tridimensionales lineales a trozos objeto de estudio, y reducimos su dimensión gracias a una hipótesis de relajación que conduce a una no linealidad de tipo histéresis. Además, presentamos una forma canónica normalizada que nos permite reducir el número de parámetros.

En el Capítulo 2 analizamos el caso en el que el sistema con histéresis no tenga equilibrios aislados, esto es, al menos uno de los autovalores del sistema plano es nulo. Detectamos algunas bifurcaciones relevantes como una bifurcación silla-nodo de órbitas periódicas o una bifurcación del infinito.

En los Capítulo 3 y 4, estudiamos los casos de autovalores reales no nulos, que dan lugar a equilibrios de tipo nodo, silla o nodo impropio. Bifurcaciones como silla-nodo de órbitas periódicas, bifurcaciones homoclínicas y heteroclínicas son descritas analíticamente. Detectamos regiones del plano de parámetros donde la existencia de cuatro órbitas periódicas es posible.

En el Capítulo 5 nos centramos en los casos con autovalores complejos, esto es, cuando los equilibrios son de tipo centro o foco. En el caso centro la dinámica está completamente estudiada y somos capaces de detectar bifurcaciones del mismo tipo que las ya obtenidas en capítulos anteriores. En el caso de equilibrios de tipo foco, encontramos una bifurcación que supone una transición directa a comportamiento caótico, y nuestro objetivo será obtener las condiciones sobre los parámetros que dan lugar a este fenónemo.

Finalmente, tras un capítulo de conclusiones, hemos incluido algunos casos no genéricos en los apéndices A y B.

Summary

The main objective of this thesis is to determine periodic solutions and possible bifurcations in a family of dynamical systems with hysteresis. In particular, we analyze a concrete family of slow-fast piecewise linear systems in three dimensions, which after introducing a hysteretic function, is embedded in two dimensions.

In Chapter 1, we introduce the tridimensional piecewise linear systems to be studied. Then, we reduce their dimension thanks to a relaxation hypothesis. Moreover, we show a normalized canonical form which allows us to decrease the number of parameters.

In Chapter 2, we analyze the case where the hysteretic system has no isolated equilibria, that is, when one of the eigenvalues of the planar system is zero. We detect some relevant bifurcations as a saddle-node bifurcation of periodic orbits and a bifurcation from infinity.

In Chapters 3 and 4, we study the non-zero real eigenvalues cases, giving rise to equilibria of node, saddle or improper node type. Bifurcations as saddle-node of periodic orbits, homoclinic and heteroclinic bifurcations are analytically described. We detect also, some regions on the parameter plane where the existence of four periodic orbits is possible.

In Chapter 5 we focus on the complex eigenvalues case, that is, when the equilibria are centre or focus type. For the centre case, the dynamics is completely determined and we can detect similar bifurcations as the obtained in previous chapters. The focus case is tackled in a different way. In this last case, our aim will be to obtain conditions for which the parameters lead to an instantaneous transition to chaotic behaviour.

Finally, after a conclusions chapter, we include some non-generic cases in appendices A and B.

Contents

Chapter 1

Introduction and preliminaries

1.1 Framework and setting of the problem

Piecewise linear differential systems (PWL systems, for short) are an important class of nonlinear dynamical systems. They frequently appear in many nonlinear engineering devices, which are accurately modelled by piecewise linear vector fields, see [15]. They appear also in mathematical biology, see [12,51–53] where they constitute approximate or toy models. Thus, they must be considered as a significant class of piecewise smooth dynamical systems.

The analysis of planar continuous PWL systems is well established when the number of linear zones is small, see [54] and references therein. However, when the planar vector field is allowed to be discontinuous, not all the problems are completely solved. Thus, for instance, in this case the corresponding adaptation of 16th Hilbert's problem about the number of existing limit cycles, is an open question.

For 3D continuous PWL systems the situation is much less satisfactory. Thus, even to justify the existence of periodic orbits is a difficult problem, which can be tackled in different ways. For instance, we can resort to bifurcation theory, so considering critical situations corresponding to selected values of parameters and study the possible generation of periodic orbits after some small change in a distinguished parameter (the bifurcation parameter), see [6–9, 20, 21, 42]. In any case, the bifurcation analysis of 3D piecewise linear systems is of great relevance for understanding the huge dynamical phenomena one can find in simple nonlinear models. Think for instance of the celebrated Chua's oscillator, see [34], where chaotic regimes have been repeatedly stressed. Typically, for such chaotic or even simple periodic behaviour, the existence of complex eigenvalues is an implicit assumption. Among other contributions, in this work we emphasize that it is also possible to have periodic behaviour, although non-chaotic, by considering dynamical regimes ruled by real eigen-

values.

Our starting point is a generic piecewise linear system with slow-fast dynamics, which appear frequently in several contexts, see [13], [14], [19], [27], [44], [46], [47], [49]. In particular, we consider slow-fast symmetric 3D piecewise linear systems and through a dimensional reduction procedure we obtain a planar symmetric hysteretic system as done for instance in [19]. Our representation for hysteresis is the simplest one, see [37] and [55] for other different models of hysteresis.

The special configuration of the phase space in hysteretic systems makes particularly involved its mathematical analysis. In the seeming elementary 2D case, hysteretic systems could be described as formed by two overlapped sheets with certain transition or jumping lines. In fact, the features of the phase space do not allow to apply the classical results of qualitative theory of differential equations in the plane (Poincaré-Bendixon, index theory,...). This explains that, after the pioneering work on periodic behaviour of hysteretic systems by Andronov and collaborators in [1] (see specially Section 7 of Chapter VIII), a complete and systematic treatment of such systems is not yet available. In particular, a lack of theoretical results on their possible dynamics and bifurcations to be found in these systems is detected. Trying to explain the possibility of chaotic regimes, to the best of our knowledge, the emphasis have been put on dynamics of focus type [36, 46, 47] and less attention has been paid to the possibility of periodic behaviour in presence of real eigenvalues.

As a big part of our achievements, we rigorously show the coexistence of several periodic regimes for symmetric 2D hysteretic systems, by analytically detecting several types of bifurcations. We find saddle-node bifurcations of periodic orbits, pitchfork bifurcations of periodic orbits or even homoclinic and heteroclinic connections. Thus, even dealing with a symmetric vector field, the presence of hysteresis turns out to give rise to a richer structure of periodic orbits than in the case of mere discontinuous planar systems (see [2], [39]) as well as for the case of continuous planar systems with three zones (see [32]). Furthermore, regarding the focus dynamics, we add some contributions to the existing works by showing from a theoretical point of view, the existence of a specific chaotic regime that does not require a discontinuous transition map (see Chapter 5).

1.2 From 3D slow-fast PWL systems to 2D hysteretic systems and vice versa

We start by assuming a symmetric 3D piecewise linear system with the following structure

$$\begin{array}{rcl} \begin{pmatrix} \dot{X} \\ \dot{Y} \end{pmatrix} & = & A_0 \begin{pmatrix} X \\ Y \end{pmatrix} + \mathbf{b}_0 Z, \\ \epsilon \dot{Z} & = & -X + \varphi(Z), \end{array} \tag{1.1}$$

where X, Y, $Z \in \mathbb{R}$ are the states variables, $A_0 = (a_{ij})$ is a 2×2 matrix with coefficients in $\mathbb{R}$, $\mathbf{b}_0 = (b_1, b_2)^T$ is a real vector, $0 < \epsilon \ll 1$ and $\varphi(Z)$ is a continuous piecewise linear function, symmetrical with respect to the origin, defined by

$$\varphi(Z) = \begin{cases} -m(Z + z_0) - x_0, & Z \leqslant -z_0, \\ cZ, & |Z| \leqslant z_0, \\ -m(Z - z_0) + x_0, & Z \geqslant z_0, \end{cases} \tag{1.2}$$

where the parameters c, m, x_0 and z_0 are positive real numbers, and $x_0 = cz_0$. Here, the dot represents the derivative with respect to the time s.

In the limit when $\epsilon \to 0$, the last equation of (1.1) represents a surface which is usually called *critical manifold*. In Figure 1.1 we can see the generic shape of the function $\varphi(Z)$ and the generated surface $X = \varphi(Z)$.

Regarding Figure 1.1, we can define the two half-planes $\mathbf{Z_U}$ and $\mathbf{Z_L}$, namely

$$\begin{array}{l} \mathbf{Z_U} = \{(X, Y, Z) \in \mathbb{R}^3 : X - x_0 + m(Z - z_0) = 0,\ X \leqslant x_0\}, \\ \mathbf{Z_L} = \{(X, Y, Z) \in \mathbb{R}^3 : X + x_0 + m(Z + z_0) = 0,\ X \geqslant -x_0\}, \end{array}$$

or equivalently,

$$\begin{array}{l} \mathbf{Z_U} = \{(X, Y, Z) \in \mathbb{R}^3 : X - x_0 + m(Z - z_0) = 0,\ Z \geqslant z_0\}, \\ \mathbf{Z_L} = \{(X, Y, Z) \in \mathbb{R}^3 : X + x_0 + m(Z + z_0) = 0,\ Z \leqslant -z_0\}. \end{array}$$

The set, $\mathbf{Z_U}$ (resp. $\mathbf{Z_L}$) will be called upper half-plane (resp. lower half-plane). Now, for $\delta \neq 0$ and small, consider a half-plane which is parallel to $\mathbf{Z_U}$

$$\Pi = \{(X, Y, Z) \in \mathbb{R}^3 : X - x_0 + m(Z - z_0) = \delta,\ Z \geqslant z_0\}.$$

If we consider an orbit with initial point (X_0, Y_0, Z_0) on the plane Π and define

$$\delta(s) = X(s) - x_0 + m(Z(s) - z_0)$$

with $X(0) = X_0$, $Z(0) = Z_0$, we see by using the last equation in (1.1) that

$$\begin{array}{rcl} \dot{\delta}(s) & = & \dot{X}(s) + m\dot{Z}(s) \\ & = & \dot{X}(s) + \dfrac{m}{\epsilon}(-X(s) - m(Z(s) - z_0) + x_0) \\ & = & \dot{X}(s) - \dfrac{m}{\epsilon}\delta(s), \end{array}$$

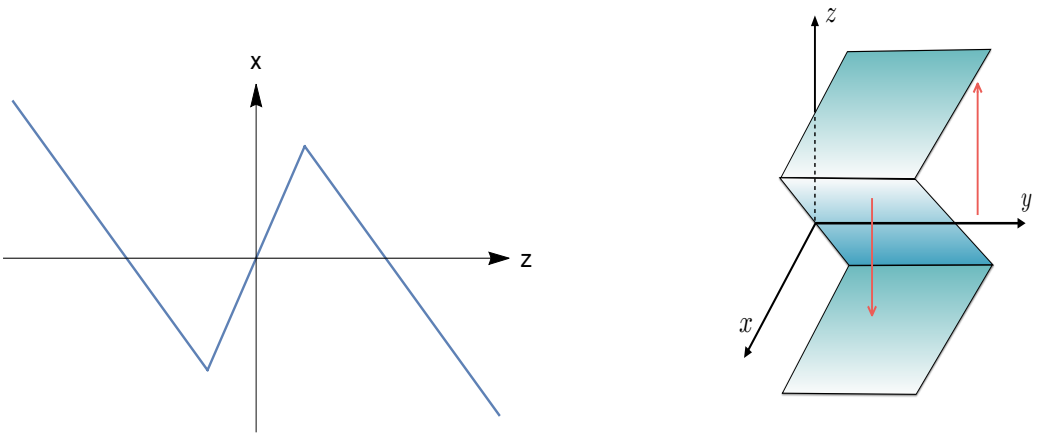

Figure 1.1: Typical graph for $\varphi(Z)$ and surface $X = \varphi(Z)$.

so that, for ϵ sufficiently small, we get

$$\operatorname{sign} \dot{\delta} = -\operatorname{sign} \delta,$$

and so, the half-plane $\mathbf{Z_U}$ is attractive. Something similar occurs for the lower half-plane $\mathbf{Z_L}$. Consequently, the intermediate stripe between $\mathbf{Z_U}$ and $\mathbf{Z_L}$ turns out to be repulsive.

Our main assumption, to be referred as *relaxation hypothesis*, is that we can consider that the motion in $\mathbb{R}^3$ happens only in the two attractive half-planes $\mathbf{Z_U}$ and $\mathbf{Z_L}$ (upper and lower). When an orbit reaches the boundary of one half-plane ($\mathbf{Z_U}$ or $\mathbf{Z_L}$), it jumps instantaneously to the other half-plane by keeping the same values of X and Y and changing only the value of Z. Clearly, the dynamics on each half-plane is essentially two-dimensional; in fact, we can eliminate the third variable by projecting the orbits on the plane $Z = 0$ by using the equation of each half-plane. Then we have on $\mathbf{Z_U}$ for $Z \geqslant z_0$, or equivalently $X \leqslant x_0$, the dynamical system

$$\begin{pmatrix} \dot{X} \\ \dot{Y} \end{pmatrix} = \widetilde{A} \begin{pmatrix} X \\ Y \end{pmatrix} + \widetilde{\mathbf{b}}, \qquad \text{if } X \leqslant x_0, \tag{1.3}$$

and similarly on $\mathbf{Z_L}$ for $Z \leqslant -z_0$, the system

$$\begin{pmatrix} \dot{X} \\ \dot{Y} \end{pmatrix} = \widetilde{A} \begin{pmatrix} X \\ Y \end{pmatrix} - \widetilde{\mathbf{b}}, \qquad \text{if } X \geqslant -x_0, \tag{1.4}$$

where

$$\widetilde{A} = [\tilde{a}_{ij}] = \begin{pmatrix} a_{11} - \dfrac{b_1}{m} & a_{12} \\ \\ a_{21} - \dfrac{b_2}{m} & a_{22} \end{pmatrix}, \quad \widetilde{\mathbf{b}} = [\tilde{b}_i] = \begin{pmatrix} b_1(1 + \dfrac{c}{m})z_0 \\ \\ b_2(1 + \dfrac{c}{m})z_0 \end{pmatrix}.$$

An additional rescaling makes it possible to take $x_0 = 1$ and $z_0 = 1/c$. Starting from these two systems, which form a symmetric pair of dynamical systems, and following the approach in [22], that requires only $a_{12} \neq 0$, the change of variables

$$\begin{pmatrix} x \\ y \end{pmatrix} = \begin{pmatrix} 1 & 0 \\ \tilde{a}_{22} & -\tilde{a}_{12} \end{pmatrix} \begin{pmatrix} X \\ Y \end{pmatrix},$$

allow us to get both systems in Liénard's canonical form[1]. From now on, we represent with a prime, the derivative with respect to the time τ. Thus, without going into the details, there is no loss of generality in considering that the dynamics on $\mathbf{Z_U}$ and $\mathbf{Z_L}$ is ruled by the Liénard system

$$\mathbf{x}' = \mathbf{F}(\mathbf{x}) = \begin{cases} \mathbf{F_U}(\mathbf{x}) = A\mathbf{x} + \mathbf{b}, & \text{for } x \leqslant 1, \\ \mathbf{F_L}(\mathbf{x}) = A\mathbf{x} - \mathbf{b}, & \text{for } x \geqslant -1, \end{cases} \tag{1.5}$$

where A is the matrix

$$A = \begin{pmatrix} t & -1 \\ d & 0 \end{pmatrix},$$

being t the trace and d the determinant of the matrix A, which of course are the same as for the matrix $\widetilde{A}$. Here $\mathbf{x} = (x, y) \in \mathbb{R}^2$, $\mathbf{b} = (b_1, b_2)$ is a constant array, and the hysteretic transition mechanism will be specified later.

As mentioned, our relaxation hypothesis also assures that if some orbit on the half-plane $\mathbf{Z_U}$ arrives at its border, then the orbit jumps to the point with the same (x, y) coordinates on $\mathbf{Z_L}$ and vice versa, leading to a 2D hysteretic system with symmetry. More details on the transition mechanism between the two subsystems will appear later.

We see that there are only two parameters in the new matrix representing the linear part, namely the trace t and the determinant d, plus two parameters b_1 and b_2 responsible for the location of equilibria.

Reciprocally, the simplest 3D piecewise linear system leading to hysteretic system (1.5) under the relaxation hypothesis is

$$\begin{cases} \dot{x} = \left(t + \frac{\beta_1}{m}\right) x - y + \beta_1 z, \\ \dot{y} = \left(d + \frac{\beta_2}{m}\right) x + \beta_2 z, \\ \epsilon \dot{z} = -x + \varphi(z), \end{cases} \tag{1.6}$$

[1]The non-generic case $a_{12} = 0$ is treated for sake of completeness in Appendix A.

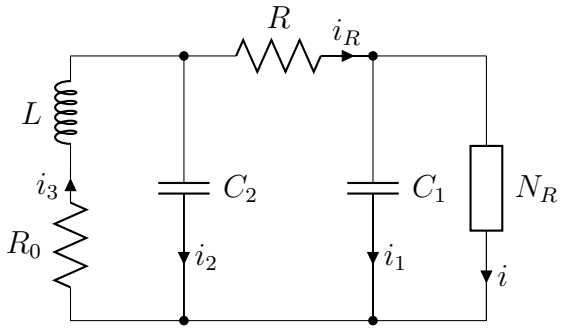

Figure 1.2: The basic scheme of Chua oscillator, including the active nonlinear resistor N_R, sometimes called Chua diode.

where $\varphi(z)$ is as in (1.2) with $x_0 = 1$, $z_0 = 1/c$, and

$$\beta_1 = \frac{cm}{c+m} b_1, \quad \beta_2 = \frac{cm}{c+m} b_2. \tag{1.7}$$

1.2.1 A relevant example

The so-called Chua's oscillator (see for example [11]) is the electronic circuit shown in Figure 1.2. Usually, the dynamics of this circuit is accurately modeled by a 3D continuous piecewise linear vector field with three regions. It is a celebrated circuit whose only active element is a nonlinear resistor N_R also known as Chua's diode. This nonlinear resistor is assembled by means of two equal operational amplifiers (OA) with different polarizations, so that its current-voltage characteristics becomes accurately modeled by a symmetric piecewise linear function. Thus, regarding Figure 1.2, we can write that the current through the nonlinear resistor N_R is

$$i = f(V_i) = G_b V_i + \frac{1}{2}\left(G_a - G_b\right)\left(|V_i + E| - |V_i - E|\right), \tag{1.8}$$

where V_i is the voltage across the resistor N_R, the conductance values G_a, G_b are parameters giving the different slopes of the characteristics (G_a for the central part, G_b for the external parts), and $\pm E$ are the input voltages where there appear *corners* in the graph of the function f.

Taking into account that the voltage v_1 across the capacitor C_1 is equal to

the voltage V_i, the state equations of Chua's oscillator are (see [11])

$$\begin{cases} \dfrac{dv_1}{d\tau} &= \dfrac{1}{C_1}[G(v_2 - v_1) - f(v_1)], \\ \dfrac{dv_2}{d\tau} &= \dfrac{1}{C_2}[G(v_1 - v_2) + i_3], \\ \dfrac{di_3}{d\tau} &= -\dfrac{1}{L}\left(v_2 + R_0 i_3\right), \end{cases} \tag{1.9}$$

where v_1 and v_2 are the voltages across the capacitors C_1 and C_2, i_3 is the current through the inductance L, there appears the conductance $G = 1/R$, and the function f is given in (1.8).

As done in [26], we may write Chua's oscillator equations (1.9) in normalized dimensionless form by making a change of variables. To see that the new 3D system enters our formulation, we take

$$x = -\frac{v_2}{E}, \quad y = \frac{i_3}{EG}, \quad z = \frac{v_1}{E} \quad \text{and} \quad \bar{\tau} = \frac{\tau G}{C_2}.$$

Thus we get the system

$$\begin{cases} \dfrac{dx}{d\bar{\tau}} &= -x - y - z, \\ \dfrac{dy}{d\bar{\tau}} &= \beta_{\mathrm{CO}} x - \gamma_{\mathrm{CO}} y, \\ \dfrac{dz}{d\bar{\tau}} &= \alpha_{\mathrm{CO}}\left[-x - h(z)\right] \end{cases} \tag{1.10}$$

where

$$h(z) = \begin{cases} bx + (b-a), & z < -1, \\ ax, & |z| \leqslant 1, \\ bx - (b-a)], & z > 1, \end{cases}$$

and furthermore the values

$$a = 1 + \frac{G_a}{G}, \quad b = 1 + \frac{G_b}{G}, \quad \alpha_{\mathrm{CO}} = \frac{C_2}{C_1} > 0, \quad \beta_{\mathrm{CO}} = \frac{C_2}{LG^2} > 0,$$

and

$$\gamma_{\mathrm{CO}} = \frac{R_0 C_2}{LG} \geqslant 0.$$

In this way, if we assume that α_{CO} is big, $\epsilon = 1/\alpha_{\mathrm{CO}}$ is small, and identifying $\varphi(z)$ and $-h(z)$, we have the original system (1.1)-(1.2) with

$$c = -a, \quad m = b, \quad z_0 = 1 \quad \text{and} \quad x_0 = -a,$$

where it must be required that $a < 0$ (something usual) and $b > 0$, as in the recent analysis done in [4]. Thus, the theoretical analysis included in this work deserves to be exploited in looking for the dynamical behavior of Chua oscillator when the capacitor ratio C_1/C_2 is sufficiently small.

1.3 The normalized canonical form

Starting from hysteretic system in its general Liénard form (1.5) and resorting again to the results in [22], if we assume $d \neq 0$, then a new linear change of variables and time allows us to rewrite our hysteretic system in a useful canonical form.

Proposition 1.1. *Introducing the modal parameter*

$$\mu = \begin{cases} i & \text{if } \ t^2 - 4d < 0, \\ 0 & \text{if } \ t^2 - 4d = 0, \\ 1 & \text{if } \ t^2 - 4d > 0, \end{cases} \tag{1.11}$$

and the auxiliary parameter

$$\omega = \begin{cases} \dfrac{\sqrt{|t^2 - 4d|}}{2} & \text{if } \ \mu \neq 0, \\ 1 & \text{if } \ \mu = 0, \end{cases}$$

and the normalized semi-trace

$$\gamma = \frac{t}{2\omega},$$

the following statements hold.

(a) The canonical form (1.5) *can be rewritten as*

$$\mathbf{x}' = \begin{pmatrix} 2\gamma & -1 \\ \gamma^2 - \mu^2 & 0 \end{pmatrix} \mathbf{x} + \frac{1}{\omega} \begin{pmatrix} \omega b_1 \\ b_2 \end{pmatrix}$$

(b) If furthermore $d \neq 0$, then the canonical form (1.5) *can be put into the normalized version*

$$\mathbf{x}' = \mathbf{F}(\mathbf{x}) = \begin{cases} \mathbf{F_U}(\mathbf{x}) = A(\mathbf{x} - \mathbf{x_E}), & \text{for } x \leqslant 1, \\ \mathbf{F_L}(\mathbf{x}) = A(\mathbf{x} + \mathbf{x_E}), & \text{for } x \geqslant -1, \end{cases} \tag{1.12}$$

where $\mathbf{x} = (x, y)^T$, $\pm\mathbf{x_E} = \pm(x_E, y_E)^T$ are the equilibria of the subsystems, the superscript T represents transposition and A is the matrix

$$A = \begin{pmatrix} 2\gamma & -1 \\ \gamma^2 - \mu^2 & 0 \end{pmatrix},$$

where μ is the modal parameter defined in (1.11).

Proof. (a) It is enough to consider the change of variables

$$(\bar{x}, \bar{y}, \bar{t}) = (\omega x, y, \omega t).$$

(b) If $d \neq 0$ then $\gamma^2 - \mu^2 \neq 0$ and we can compute the location of the (virtual or real) equilibrium for the upper system, namely

$$x_E = \frac{b_2}{\omega(\mu^2 - \gamma^2)}, \quad y_E = b_1 + 2\gamma x_E,$$

and the conclusion follows.

□

Note that, apart from the modal parameter, in matrix A there is only another parameter (γ) ruling the dynamics. The eigenvalues of the matrix A are $\lambda_\pm = \gamma \pm \mu$, being either real or complex depending on the value of the modal parameter μ.

Remark 1.2. *We note that this normalized canonical form* (1.12) *is just a representative case of the Liénard canonical form, as one can conclude easily by writing in* (1.5)

$$t = 2\gamma, \quad d = \gamma^2 - \mu^2, \quad b_1 = y_E - 2\gamma x_E, \quad b_2 = (\mu^2 - \gamma^2)x_E. \tag{1.13}$$

In what follows, we will use the more general Liénard canonical form (1.5) when the determinant d is equal to zero, and the normalized form given in (1.12) otherwise, taking into account the corresponding value of the parameter μ.

As already mentioned, our main goal is to determine the structure of periodic orbits in symmetric 2D hysteretic systems given by the two planar systems

$$\mathbf{x}' = \mathbf{F_U}(\mathbf{x}), \quad x \leqslant 1, \tag{1.14}$$

and

$$\mathbf{x}' = \mathbf{F_L}(\mathbf{x}), \quad x \geqslant -1, \tag{1.15}$$

where $\mathbf{x} = (x, y)^T \in \mathbb{R}^2$, and the vector fields $\mathbf{F_U}$, $\mathbf{F_L}$ are as in (1.5) or (1.12). We will call the system (1.14) as the upper or S_U-system and for (1.15) we will speak of the lower or S_L-system.

We study first the transition maps to be defined between the *jumping lines* and their main properties regarding the existence of periodic orbits. All the included results will be crucial for analyzing the different cases considered in the rest of this work.

1.4 Transition maps and periodic orbits

In the case of considering the normalized form (1.12), with a non-vanishing determinant, the corresponding equilibrium points will be called virtual when $x_E \geqslant 1$, since they do not belong to the phase space. Otherwise, if $x_E < 1$ then we will speak of real equilibria. In any case, if the eigenvalues are real then both systems S_U and S_L have two invariant manifolds, associated to the eigenvalues $\lambda_+ = \gamma + \mu$ and $\lambda_- = \gamma - \mu$.

Although the hysteretic system is discontinuous in the boundaries $x = \pm 1$, we can define a unique forward solution by selecting adequately the subsystem to be used, upper or lower system, once fixed the initial point $\mathbf{x}_0 = (x_0, y_0)$. Assuming for instance $x_0 < 1$ and adopting the convention of selecting the upper system as the starting one, the corresponding solution is computed by solving the dynamical system $\mathbf{x}' = \mathbf{F_U}(\mathbf{x})$ as long as $x(\tau) \leq 1$. If there exists a time τ_f, such that $x(\tau_f) = 1$ then the point $\mathbf{x}(\tau_f)$ is assumed to be the initial point for a solution of the S_L-system, i.e. the system $\mathbf{x}' = \mathbf{F_L}(\mathbf{x})$. Such an orbit of the lower system with initial point $\mathbf{x}(\tau_f)$ will be followed as long as $x \geqslant -1$. If the orbit does arrive to the line $x = -1$, then the corresponding point will be taken as a new initial point for the upper system.

Obviously, if $x_0 > -1$ and the lower system is selected as the starting one, we could build the solution by solving $\mathbf{x}' = \mathbf{F_L}(\mathbf{x})$ while $x(\tau) \geq -1$. If there exists a time τ_r, such that $x(\tau_r) = -1$ then the point $\mathbf{x}(\tau_r)$ is assumed to be the initial point for a solution of the S_U-system, i.e. the system $\mathbf{x}' = \mathbf{F_U}(\mathbf{x})$, and so on.

In passing from the S_U-system to the S_L-system, we speak of a *fall*, which occurs when an orbit of the S_U-system, called upper orbit, hits the falling line

$$\Sigma_+ = \{(x, y) : x = 1\},$$

see Figure 1.3. Similarly, we define a *rise* when we pass from the S_L-system to the S_U-system, which occurs when an orbit of the S_L-system, called lower orbit, hits the rising line

$$\Sigma_- = \{(x, y) : x = -1\}.$$

Thus, excepting the non-generic cases of linear periodic orbits when there are centre dynamics in the subsystems, any periodic orbit of hysteretic system (1.14)-(1.15) is indeed nonlinear and implies a sequence of falls and rises, having at least two pieces, one corresponding to the an orbit of the S_U-system and another corresponding to an orbit of the S_L-system. Although, when the dynamics is of focus type, periodic orbits with four (or more) transitions are possible, we omit its consideration in the sequel, and so, when we speak of periodic orbits, we assume that they have only two transitions.

Therefore, in looking for periodic orbits there is no loss of generality in taking $\mathbf{x}_0 = (-1, u_-) \in \Sigma_-$ as initial point of an orbit of the upper system. In the case where a periodic orbit intersects the rising line Σ_- in two points, we use the point with the biggest ordinate as the initial point.

If the orbit of the S_U-system through the point $(-1, u_-)$ arrives at a point $(1, u_+)$ in the falling line Σ_+, we can define the evolution map T_U as follows,

$$\begin{array}{rccc} T_U : \Sigma_-^{\text{ad}} \subset \Sigma_- & \to & \Sigma_+ \\ (-1, u_-) & \longrightarrow & (1, u_+), \end{array}$$

where Σ_-^{ad} is the subset of the rising line Σ_- for which the forward orbit of the S_U-system reaches the falling line Σ_+. This evolution map T_U induces a scalar map U, called the *upper transition map*, such that $u_+ = U(u_-)$.

A similar evolution map T_L can be defined for the S_L-system by considering the points belonging to the set $\Sigma_+^{\text{ad}} \subset \Sigma_+$ whose forward orbits reach Σ_- and rise, namely

$$\begin{array}{rccc} T_L : \Sigma_+^{\text{ad}} \subset \Sigma_+ & \to & \Sigma_- \\ (1, l_+) & \longrightarrow & (-1, l_-). \end{array}$$

Also, the evolution map T_L induces a scalar map L, called the *lower transition map*, such that $l_- = L(l_+)$.

If for a certain value p in the domain of the upper transition map U we have that $q = U(p)$ belongs to the domain of the lower transition map L, we can compute the *complete transition map* or *return map* $(L \circ U)(p)$. Therefore, if there exists a pair (p, q) such that

$$q = U(p), \quad p = L(q), \tag{1.16}$$

then $L\,(U(p)) = p$, and so the hysteretic system (1.14)-(1.15) has a nonlinear periodic orbit. Reciprocally, if there exists a nonlinear periodic orbit, then there also exists an associated pair (p, q) such that $q = U(p)$ and $p = L(q)$.

It is worth noting that hysteretic system (1.14)-(1.15) is symmetrical with respect to the origin. Effectively, if we change $\mathbf{x}$ to $-\mathbf{x}$ in the system (1.14), then we obtain the system (1.15), and vice versa.

The maps L and U have some properties inherited from the symmetry of the hysteretic system.

Lemma 1.3. *The following statements hold.*

(a) If $U(p)$ is defined, then $L(-p)$ is also defined and $L(-p) = -U(p)$.

(b) The full transition map $L \circ U$ satisfies

$$L \circ U = (-U) \circ (-U).$$

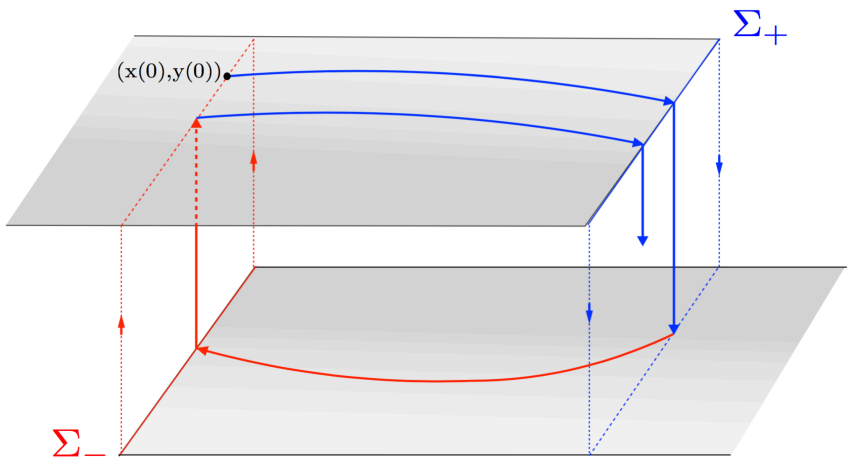

Figure 1.3: The transition mechanism between S_U and S_L systems. We use blue colour for the pieces of the solutions of the upper system and red colour for the pieces of solutions of the lower one. We can see also the falls at the line Σ_+ and the rises at the line Σ_-.

Proof. If $U(p)$ is well defined, taking $q = U(p)$ we obtain $T_U(-1, p) = (1, q)$. From the symmetry with respect to the origin the equality $T_L(1, -p) = (-1, -q)$ follows. Then $-q = -U(p) = L(-p)$ and statement (a) is shown.
From statement (a) we get $L\left(U(p)\right) = -U\left(-U(p)\right)$, and statement (b) follows. □

Proposition 1.4. *Periodic orbits of system* (1.14)-(1.15) *come in pairs, excepting the case where the periodic orbit is itself symmetrical with respect the origin.*

Proof. If we assume that the pair (p, q) determines a periodic orbit, applying Lemma 1.3 we can write

$$L(U(-q)) = L(-L(q)) = L(-p) = -U(p) = -q,$$

then the pair $(-q, -p)$ corresponds to the periodic orbit which is its symmetrical with respect to the origin.

□

The stability of periodic orbits is determined by the derivative

$$\frac{d}{dp}(L \circ U)(p) = \frac{d}{dp}((-U) \circ (-U))(p) =$$

$$= \frac{dU}{dp}(-U(p))\frac{dU}{dp}(p) = \frac{dU}{dp}(-q)\frac{dU}{dp}(p).$$

Consequently, periodic orbits are stable when

$$\left|\frac{dU}{dp}(-q)\frac{dU}{dp}(p)\right| < 1. \tag{1.17}$$

In the particular case that $q = U(p) = -p$ the periodic orbit is self-symmetrical with respect to the origin. Therefore symmetric periodic orbits are determined by the condition

$$U(p) + p = 0. \tag{1.18}$$

According to (1.17), the stability of a symmetrical periodic orbit is given by the inequality

$$\left|\frac{dU}{dp}(p)\frac{dU}{dp}(p)\right| = \left|\frac{dU}{dp}(p)\right|^2 < 1,$$

or equivalently when

$$\left|\frac{dU}{dp}(p)\right| < 1. \tag{1.19}$$

Remark 1.5. *Clearly, the symmetry with respect to the origin allows us to restrict the analysis to only one of the subsystems, say the S_U-system. Thus, if the pair (u_-, u_+) with $u_+ \neq -u_-$, satisfies the equations*

$$\begin{cases} U(u_-) &= u_+, \\ U(-u_+) &= -u_-, \end{cases} \tag{1.20}$$

then, such a pair represents a non-symmetric periodic orbit. In what follows, we will use the condition (1.20) *instead of* (1.16)*. Of course, in the specific case of symmetric periodic orbits, we only must consider the equation*

$$U(u) + u = 0. \tag{1.21}$$

Proposition 1.6. *Assume that Σ_-^{ad} is a connected set. If the map U is continuous and there exists a pair of non-symmetric periodic orbits, then there exists a third periodic orbit, which is symmetric.*

Proof. Assuming that (p, q) and $(-q, -p)$, determine a pair of non-symmetric periodic orbits, then from (1.20) we have

$$\begin{aligned} U(p) &= q, \\ U(-q) &= -p, \end{aligned}$$

so that

$$\begin{aligned} U(p) + p &= p + q, \\ U(-q) - q &= -(p + q). \end{aligned}$$

Therefore, the function $U(u) + u$ takes opposite values in p and $-q$. Consequently, applying the Intermediate Value Theorem to the function $U(u) + u$ we deduce the existence of at least one value u_s in the interval determined by p and $-q$ such that $U(u_s) + u_s = 0$, and a third periodic orbit exists, which is symmetric.

□

1.5 Some auxiliary functions and parameters

Next, we give a necessary condition for the existence of non-symmetric periodic orbit, by introducing the auxiliary functions

$$f(u) = U(u) - u, \quad g(u) = U(u) + u. \tag{1.22}$$

Proposition 1.7. *If system* (1.14)-(1.15) *has a non-symmetric periodic orbit, then the following statements hold.*

(a) The function $f(u)$ given in (1.22) *is non injective.*

(b) The function $g(u)$ given in (1.22) *takes opposite values in two different points.*

Proof. Since equations (1.20) imply the equalities

$$f(u_-) = f(-u_+), \quad g(u_-) = -g(-u_+)$$

both statements follow directly.

□

Corollary 1.8. *Suppose that Σ_-^{ad} is a connected set. If there exists a non-symmetric periodic orbit for system* (1.5)*, then the transition map U satisfies $U'(u) = 1$ for some u such that $(-1, u) \in \Sigma_-^{ad}$.*

Proof. From Proposition 1.7(a), function f is non-injective and so there exists a value u such that $f'(u) = 0$. From (1.22) the conclusion follows. □

Writing an explicit expression of the map U, that is, giving u_+ in terms of u_-, is not possible excepting rather particular cases. Then, we consider instead a parametric expression of the transition map U in terms of the flight time τ, that is, we will look for some functions $u_-(\tau)$, $u_+(\tau)$ to be specified later. The flight time τ belongs to either a bounded interval $\mathcal{I} = (0, \tau_M]$, to be precise later, see Remark 1.11, or to the unbounded interval $\mathcal{I} = (0, \infty)$. Accordingly,

the functions f and g in (1.22) will be substituted by their analogous functions η and κ, namely

$$\eta(\tau) = u_+(\tau) - u_-(\tau), \quad \kappa(\tau) = u_+(\tau) + u_-(\tau). \tag{1.23}$$

Using this notation, the number of symmetric periodic orbits will be determined by the number of zeroes of function $g(u)$ or $\kappa(\tau)$.

Proposition 1.9. *Suppose that Σ_-^{ad} is a connected set. If $\kappa'(\tau) \neq 0$ for all $\tau \in \mathcal{I}$, then $g'(u) \neq 0$, or equivalently $U'(u) \neq -1$ for all u such that $(-1, u) \in \Sigma_-^{ad}$ so that, the maximum number of symmetric periodic orbits is one.*

Proof. The number of zeroes of functions g or κ determines the number of symmetric periodic orbits. If $g'(u) \neq 0$ (or $\kappa'(u) \neq 0$), from (1.22) $U'(u) \neq -1$ and so the function g is monotone and the maximum number of zeroes is one. □

Now, we introduce some distinguished points, which will be necessary in the sequel.

Definition 1.10. *The points where $x' = 0$ for the upper system $\mathbf{x}' = \mathbf{F_U}(\mathbf{x})$ at the lines Σ_- and Σ_+, will be called* contact points *and denoted by $(-1, u_-^c)$ and $(1, u_+^c)$ respectively.*

When there exist real eigenvalues leading to invariant straight lines, the point where the invariant line of the upper system with bigger slope intersects Σ_-, will be denoted as $(-1, u_-^*)$; while the point where the invariant line of the upper system with smaller slope intersects Σ_+, will be denoted as $(1, u_+^*)$.

Remark 1.11. *As we will see, by analyzing all the possible cases, the parameter τ belongs to a bounded interval $\mathcal{I} = (0, \tau_M]$ in the cases in which the tangency at the line Σ_+ has a* visible *character and there exists an orbit of the upper system starting at a point $(-1, u_-) \in \Sigma_-$ arriving to the contact point $(1, u_+^c)$. We say that the tangency is visible when the tangent orbit, if extended in $\mathbb{R}^2$ without falling, is locally on the left of Σ_+, see Figure 1.4.*

The visibility condition amounts to the inequality $x'' < 0$ at the contact point. A simple characterization of such a condition follows.

Lemma 1.12. *The contact point of system* (1.5) *at the line Σ_+ is visible when $d + b_2 > 0$.*

Proof. It suffices to compute

$$x'' = t(tx - y + b_1) - (dx + b_2) = (t^2 - d)x - ty + tb_1 - b_2,$$

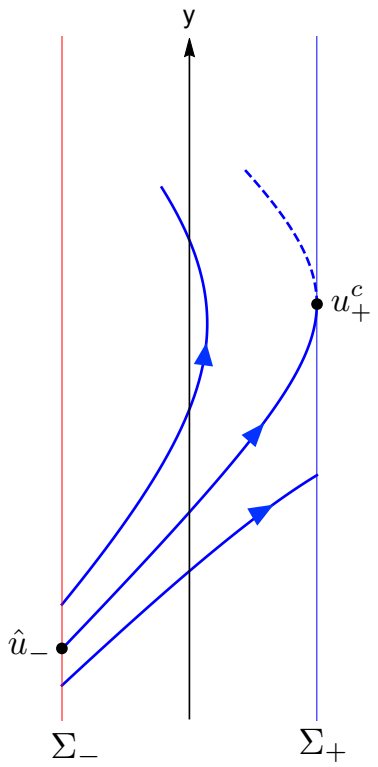

Figure 1.4: Sketch of the cases in which an orbit starting on a point $(-1, \hat{u}_-)$ of the line Σ_- tangentially gets the line Σ_+ at the point $(1, u_c^+)$

and put $(x, y) = (1, t + b_1)$, which is the quoted contact point. We get

$$x'' \,|_{(1,u_+^c)} = -d - b_2,$$

and the conclusion follows.

□

The maximum value of the flight time τ_M will correspond to certain orbit through a point at the line Σ_-, to be referred as $(-1, \hat{u}_-)$, arriving tangentially to the line Σ_+, at the point $(1, u_+^c)$, see Figure 1.4. The study of such maximum value τ_M will be done later for each case.

Regarding the shape of the symmetric periodic orbits, the following definition is useful.

Definition 1.13. *We speak of lens-like symmetric periodic orbits for those which only use the hysteresis band, that is the central zone $x \in [-1, 1]$. Thus, at the initial point $(-1, u_-)$ we must have $x' \geqslant 0$ for system S_U.*

Analogously, symmetric periodic orbits are called of cloud type when they use the zones $x < -1$ and $x > 1$. Therefore, we must have $x' < 0$ at their initial point $(-1, u_-)$ for system S_U.

In order to get a complete view of the structure of periodic orbits in terms of parameters, it is of paramount relevance to detect the bifurcations giving rise to the appearance or disappearance of such periodic orbits. We also consider as a bifurcation the case where, by moving some parameter, a periodic orbit persists but changing its stability or its qualitative shape (for instance, passing from cloud to lens type).

While the bifurcation catalogue is rather well established for smooth systems (see [25] and [28]), next we introduce some specific bifurcations of periodic orbits for our hysteretic systems. These bifurcations, which are not standard ones, will be referred as *arrival-grazing bifurcation* and *departure-grazing bifurcation*. The contact points defined in Definition 1.10 are crucial for such bifurcations of periodic orbits in hysteretic systems.

Definition 1.14. *We speak of an* arrival-grazing periodic orbit bifurcation *when, by moving some parameter, an existing symmetric periodic orbit of lens type arrives on the line* Σ_+ *at the contact point* $(1, u_+^c)$*, to disappear.*

Definition 1.15. *We define a* departure-grazing periodic orbit bifurcation *when, a change in some parameters produces that an orbit of lens type, becomes tangent to the line* Σ_-*, at the contact point* $(-1, u_-^c)$*, giving rise to a cloud type periodic orbit.*

Note that while in a departure-grazing bifurcation the periodic orbit persists and only changes its shape, in an arrival-grazing bifurcation there is a change in the number of periodic orbits.

In the sequel, we will also need the auxiliary parameter defined for $x_E \neq 1$

$$\rho = \frac{x_E + 1}{x_E - 1}, \tag{1.24}$$

so that

$$\begin{array}{rcll} 0 \leqslant & \rho & < 1, & \text{if} \quad x_E \leqslant -1, \\ -1 \leqslant & \rho & < 0, & \text{if} \quad -1 < x_E \leqslant 0, \\ -\infty < & \rho & < -1, & \text{if} \quad 0 < x_E < 1, \\ 1 < & \rho & < \infty, & \text{if} \quad 1 < x_E. \end{array} \tag{1.25}$$

Chapter 2

Systems with a zero eigenvalue

In this chapter, we deal with the hysteretic system given in (1.5) which corresponds to the intermediate situation between node and saddle dynamics, namely the case with at least one zero eigenvalue. The material of this chapter is essentially the same as of the reference [17], submitted for publication.

The presence of zero eigenvalues is generically associated to the absence of equilibrium points along with the existence of degenerate singular points at infinity. Excepting one rather degenerate situation where non-isolated periodic orbits are possible, we will see that all the periodic orbits inherit the symmetry respect to the origin. Under certain additional assumptions to be specified later, it is allowed to define a return map around the invariant manifold at infinity, so that bifurcations of periodic orbits at infinity naturally appear, see theorems 2.3 and 2.6 below. Other bifurcations leading to a change in the number of periodic orbits are reported and characterized, namely saddle-node bifurcations of periodic orbits (two periodic orbits of different stability type collide to disappear) and grazing bifurcations (one periodic orbit grazes the jumping or transition lines of the phase space and disappear). Note that our problem is completely different from the case of planar relay feedback systems considered in [23]. In fact, the dynamical richness coming from the hysteresis mechanism is greater than the one originated by a single discontinuity line.

As already mentioned, here we will focus our attention to the existence of periodic orbits in the degenerate case $d = \det(A) = 0$, which apart from its intrinsic interest, appears as a bridge configuration between the case of saddle-dynamics [16] and the node dynamics [18]. In fact, regarding the associated 3D-dynamical system, it is easy to check that this configuration appears when the system has a pitchfork bifurcation of equilibria at infinity (see [29]). Under the hypothesis $\det(A) = 0$, we generically do not have equilibria, neither real nor virtual ones. But in some more degenerate cases we can also have an

infinity of non-isolated equilibria forming two half-straight lines.

2.1 Main results of the chapter

Under our essential hypothesis $\det(A) = 0$, putting $t = \lambda$ and $d = 0$, the Liénard form of the hysteretic global system (1.5) leads to the equations

$$\begin{cases} x' &= \lambda x - y \pm b_1, \\ y' &= \pm b_2, \end{cases} \qquad \pm x \leqslant 1, \tag{2.1}$$

with the transition between both sub-systems as indicated in Chapter 1. We exclude for the moment the case $b_2 = 0$, which is rather degenerate as then we have straight lines of equilibria. Then, we pay attention before to the main case without equilibria, that is $b_2 \neq 0$, assuming also the generic condition $\lambda \neq 0$. Next result gives the asymptotic behaviour of the upper system in (2.1) when considered as if it were defined in the whole plane.

Lemma 2.1. *The upper system in (2.1) with $\lambda \neq 0$ and $b_2 \neq 0$, when considered in the whole plane $\mathbb{R}^2$, has the invariant straight line ISL $y = \lambda x + b_1 - b_2/\lambda$ which is attractive for $\lambda < 0$ and repulsive for $\lambda > 0$.*

Proof. The invariance of the straight line ISL is direct. In fact, after some computations, we can calculate the solutions of (2.1), namely

$$\begin{aligned} x(\tau) &= e^{\lambda\tau} x_0 + \frac{1}{\lambda}\left(y_0 - b_1 + b_2\tau + \frac{b_2}{\lambda}\right) + \frac{e^{\lambda\tau}}{\lambda}\left(b_1 - y_0 - \frac{b_2}{\lambda}\right), \\ y(\tau) &= y_0 + b_2\tau, \end{aligned} \tag{2.2}$$

where (x_0, y_0) is a given initial point. We see that the limit

$$\lim_{\tau\to\pm\infty}\left(y(\tau) - \lambda x(\tau) - b_1 + \frac{b_2}{\lambda}\right) = \lim_{\tau\to\pm\infty}\left[e^{\lambda\tau}\left(y_0 - \lambda x_0 - b_1 + \frac{b_2}{\lambda}\right)\right]$$

vanishes for $\lambda < 0$ and $\tau \to +\infty$ (getting attractivity) and also for $\lambda > 0$ and $\tau \to -\infty$, deducing then its repulsive character. □

We recall that the *contact points* $(-1, u_-^c)$ and $(1, u_+^c)$ of the upper system in (2.1) at the lines Σ_- and Σ_+ respectively, are the points of $\Sigma_\mp$ where $x' = 0$. Simple computations show that

$$u_-^c = -\lambda + b_1, \quad u_+^c = \lambda + b_1.$$

For $b_2 \neq 0$ and $\lambda \neq 0$ we define also the point $(-1, u_-^*)$, where the line ISL intersects Σ_-, namely

$$u_-^* = -\lambda + b_1 - \frac{b_2}{\lambda}.$$

Symmetric periodic orbits with initial point at the line Σ_- with $u_- \leqslant u_-^c$, satisfy $x' \geqslant 0$ and so they will be of lens type. Analogously, symmetric periodic orbits starting in a point $(-1, u_-)$ with $u_- \geqslant u_-^c$ will be of cloud type, see Definition 1.13.

In the remaining analysis, for the global visualization of the dynamical behaviour of our hysteretic systems including the points near infinity, it turns out very useful to compactify the phase space, see Section 2.9.1 of [32]. Thus, we will plot some orbits in the so-called Poincaré disk

$$\mathbb{D} = \{(x_{\mathbb{D}}, y_{\mathbb{D}}) : x_{\mathbb{D}}^2 + y_{\mathbb{D}}^2 \leqslant 1\}$$

by considering the change of variables

$$(x_{\mathbb{D}}, y_{\mathbb{D}}) = \frac{1}{1 + \sqrt{1 + x^2 + y^2}}(x, y),$$

for every $(x, y) \in \mathbb{R}^2$, see for instance Figures 2.1, 2.2, 2.8 and 2.9 below.

2.1.1 The double zero eigenvalue case

Our first results concern the non-generic case $\lambda = 0$, that is, the case with a double zero eigenvalue. After studying for $b_2 < 0$ the stability of the 'infinity manifold' in Proposition 2.2, by considering the corresponding Poincaré disk, we characterize the bifurcation set of this case in Theorem 2.3.

First, in Figures 2.1 and 2.2 we show two Poincaré disks corresponding to different signs of the parameter b_2. A detailed analysis, not to be included here, confirms that for $\lambda = 0$ there appear two singular points at $(\pm 1, 0)$ in the boundary $\partial\mathbb{D}$ of the Poincaré disk $\mathbb{D}$. We see that, when $b_2 > 0$, the singular points have an elliptic character giving rise to an infinity of homoclinic orbits and heteroclinic ones between both of them. However, when $b_2 < 0$, these singular points do not preclude the existence of a return map near infinity, as shown next. Note that, not being the involved dynamics of focus type, the techniques used in the proof of the next result to study the orbits near the infinity are different from the ones considered in [30].

Proposition 2.2. *Considering hysteretic system (2.1) for $\lambda = 0$ and $b_2 < 0$, namely*

$$\begin{cases} x' &= -y \pm b_1, \\ y' &= \pm b_2, \end{cases} \qquad \pm x \leqslant 1 \tag{2.3}$$

the infinity manifold is always monodromic, that is, it is possible to define a global return map in a neighbourhood of infinity. Furthermore, the infinity manifold becomes attractive when $b_1 \leqslant 0$, being repulsive for $b_1 > 0$.

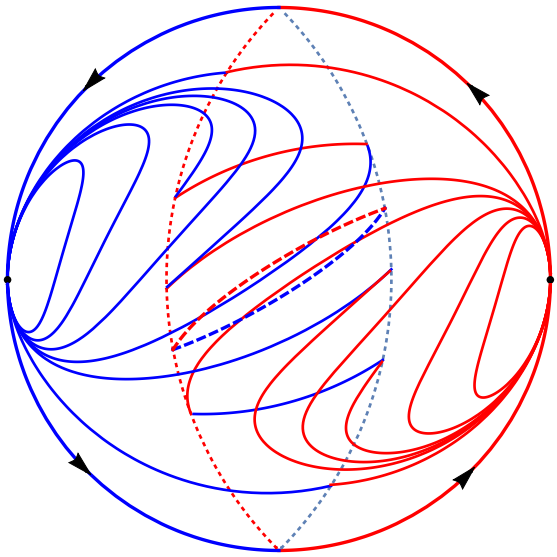

Figure 2.1: The Poincaré disk for $\lambda = 0$, $b_1 > 0$ and $b_2 > 0$. Note the singular points at $(\pm 1, 0) \in \partial\mathbb{D}$. We can see a global view of the dynamical behaviour, including the one near the infinity where an infinite number of homoclinic and heteroclinic orbits between the singular points, and one unstable periodic orbit exist.

Proof. We start by computing the transition map U, since as said before, the map L is not needed due to the symmetry of the problem. In the line $x = 1$, we see that $x' \geqslant 0$ only if $y \leqslant b_1$ so that we must have $u_+ \leqslant b_1$. System (2.3) can be integrated to obtain as general solution

$$(b_1 - y)^2 + 2b_2 x = C.$$

Thus, orbits starting at $(-1, u_-)$ and arriving at $(1, u_+)$ will satisfy

$$(b_1 - u_-)^2 - 2b_2 = (b_1 - u_+)^2 + 2b_2,$$

and so

$$u_+ = U(u_-) = b_1 - \sqrt{(u_- - b_1)^2 - 4b_2}, \tag{2.4}$$

since the other root cannot satisfy the condition $u_+ \leqslant b_1$, and so $\mathrm{Dom}(U) = \mathbb{R}$.

To work in a neighbourhood of infinity, we do the change of variables $r_- = 1/u_-$, $r_+ = -1/u_+$. Then, after some elementary algebra, we obtain

$$r_+ = R(r_-) = \frac{r_-}{\Delta(r_-)}, \text{ where } \Delta(r_-) = \sqrt{(1 - b_1 r_-)^2 - 4b_2 r_-^2} - b_1 r_-.$$

Of course, we have $R(0) = 0$ and we see that for $0 < r_- \ll 1$ the upper return map near infinity is well defined as it is the lower return map, so that the infinity manifold is monodromic as assured in the statement of the proposition.

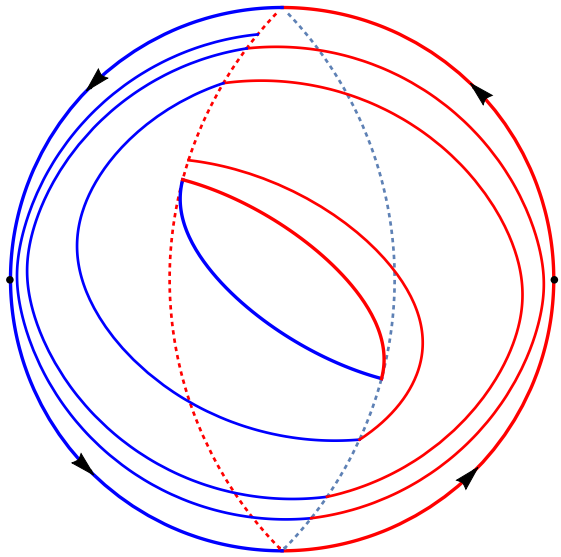

Figure 2.2: The Poincaré disk for $\lambda = 0$, $b_1 > 0$ and $b_2 < 0$. Note the singular points at $(\pm 1, 0) \in \partial\mathbb{D}$. We can see a global view of the dynamical behaviour, including the one near the infinity where one stable periodic orbit becomes the global attractor.

To compute the derivatives of the function R, we write the equality

$$R(r_-)\Delta(r_-) = r_-,$$

and so from

$$R'(r_-)\Delta(r_-) + R(r_-)\Delta'(r_-) = 1,$$

we get $R'(0) = 1$, so that the infinity manifold is non-hyperbolic. With the same procedure, we obtain $R''(0) = 4b_1$. For the case $b_1 = 0$, we have

$$R(r_-) \mid_{b_1=0} = \frac{r_-}{\sqrt{1 - 4b_2 r_-^2}}, \quad R'''(0) \mid_{b_1=0} = 12b_2,$$

and the conclusion follows. □

We note that the stability of the infinity manifold for $b_2 < 0$ and $\lambda = 0$ changes at the critical value $b_1 = 0$, what suggest the existence of a bifurcation. Next result characterizes all the situations with $b_2 \neq 0$ and shows that, as expected, such a bifurcation is associated to a periodic orbit of great amplitude.

Theorem 2.3. *Considering system (2.3) for $b_2 \neq 0$, the following statements hold.*

(a) The system can have periodic orbits only if $b_1 > 0$ and, if they exist, then all of them are symmetric.

(b) There exist periodic orbits only for $b_1 > 0$ and $b_2 \leqslant b_1^2$.

(c) For $b_2 < 0$, at $b_1 = 0$ the system undergoes a periodic orbit bifurcation from infinity, so that for small $b_1 > 0$ there appears a stable symmetric periodic orbit of great size and cloud type.

(d) For $b_1 > 0$, at $b_2 = b_1^2$ the system undergoes an arrival-grazing periodic orbit bifurcation, so that for $b_2 > b_1^2$ there are no periodic orbits, while for small $b_1^2 - b_2 > 0$, there exists a symmetric unstable periodic orbit of lens type. This periodic orbit comes from a critical periodic orbit which is tangent to both lines $\Sigma_\pm$ at the points $(\pm 1, \pm b_1)$.

(e) For $b_1 > 0$, at $b_2 = -b_1^2$ the system undergoes an departure-grazing periodic orbit bifurcation, so that for $b_2 < -b_1^2$ there exists a symmetric stable periodic orbit of cloud type, while for small $b_2 + b_1^2 > 0$ such a periodic orbit becomes of lens type keeping its symmetry and stability properties.

Proof. We start by remarking that the domain for the map U obtained in (2.4) is

$$\mathrm{Dom}(U) = \begin{cases} \mathbb{R}, & \text{if } b_2 < 0, \\ \{u_- \in \mathbb{R} : u_- \leqslant b_1 - 2\sqrt{b_2}\}, & \text{if } b_2 > 0, \end{cases}$$

and so Σ_-^{ad} is always a connected set. Furthermore, the derivative of the transition map U in its domain, is

$$U'(u_-) = -\frac{u_- - b_1}{\sqrt{(u_- - b_1)^2 - 4b_2}}. \tag{2.5}$$

Here, as $b_2 \neq 0$, by Corollary 1.8 we cannot have non-symmetric periodic orbits. The condition for having a symmetric periodic orbit is, see (1.21),

$$\sqrt{(u_- - b_1)^2 - 4b_2} = u_- + b_1,$$

which leads to

$$u_- = -\frac{b_2}{b_1} = -u_+. \tag{2.6}$$

The condition $u_+ \leqslant b_1$ gives now $\frac{b_2}{b_1} \leqslant b_1$, that is $b_2 \leqslant b_1^2$ for $b_1 > 0$, and $b_2 \geqslant b_1^2$ for $b_1 < 0$. Clearly, if $b_2 < 0$ and $b_1 > 0$, symmetric periodic orbits are not possible. The case $b_2 > 0$ and $b_1 < 0$ can be also excluded as we need $u_- \leqslant b_1 - 2\sqrt{b_2}$, that is

$$-\frac{b_2}{b_1} \leqslant b_1 - 2\sqrt{b_2},$$

which is impossible, as the left hand side is positive and the right hand side is negative. Statements (a) and (b) are shown.

Regarding statement (c), it suffices to consider expression (2.6) by taking limits when b_1 tends to zero from above, and to note that $x' < 0$ at $(-1, u_-)$ assures the cloud type for the periodic orbit. The stability comes from (2.5).

The limit situation of statement (d) corresponds to the case $u_+ = u_+^c = b_1$ and so to the previous definition of arrival-grazing periodic orbit bifurcation. The involved periodic orbits are unstable as $b_2 > 0$ in (2.5). Statement (e) is analogous, and the proof is complete.

□

According to Theorem 2.3, the complete bifurcation for $\lambda = 0$ in the parameter plane (b_1, b_2) appears in Figure 2.1.1. In the quoted figure, the different regions between bifurcation curves where a periodic orbit exists appear labelled with C and a subscript (s=stable, u=unstable) and a superscript (l=lens, c=cloud) indicating the type of periodic orbit. Furthermore, the bifurcation curves are indicated with AG and DG for the arrival and departure grazing bifurcations respectively.

Remark 2.4. *When $b_1 > 0$, the hysteretic system in (2.3) undergoes at $b_2 = 0$ a rather degenerate bifurcation. Then the transition map U is the identity restricted to the interval $(-b_1, b_1)$. There also appears a continuum of equilibrium points at the line $y = \pm b_1$ for $\pm x < 1$. Taking into account Theorem 2.3, we conclude that this degenerate bifurcation leads to a stability change for the symmetric periodic orbit of lens type that exists when $|b_2|$ is small. Thus, the stable periodic orbit for $b_2 < 0$ becomes unstable for $b_2 > 0$. The degeneration at $b_2 = 0$, $b_1 > 0$ produces a 'bracelet' of non-symmetric periodic orbits around the symmetric periodic orbit that passes through the point $(-1, 0)$ and $(1, 0)$.*

2.1.2 The single zero eigenvalue case

Now, we return to the most general case $\lambda \neq 0$, that is, we focus on the generic hysteretic system (2.1). First, we will study the domain $\mathrm{Dom}(U)$ of the transition map U, by recalling some distinguished points defined in Definition 1.10, see figures 2.4 and 2.5.

Regarding Figure 2.4, where $b_2 < 0$, the two cases $\lambda < 0$ and $\lambda > 0$ are sketched. In the left panel ($\lambda < 0$), we see that the transition map U is defined for all $u_- \in \mathbb{R}$. However, when $\lambda > 0$, the orbits starting in Σ_- with $u_- \geqslant u_-^*$ cannot intersect Σ_+, and the domain of U turns to be bounded from above. In both cases there is not a maximum value for the flight time τ, so that $\mathcal{I} = (0, \infty)$.

Consider now Figure 2.5 where the cases with $b_2 > 0$ are sketched. Here the domain of U is always bounded from above as there exists one orbit that

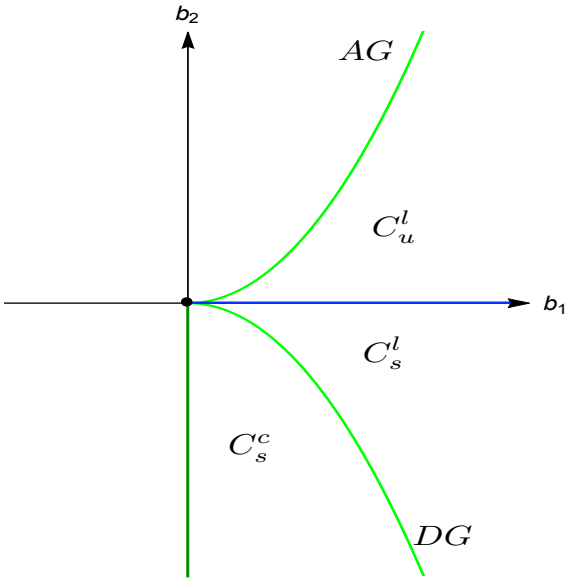

Figure 2.3: The bifurcation set for $\lambda = 0$ in the parameter plane (b_1, b_2) according to Theorem 2.3. The curves in green represent the grazing bifurcation, in this case there is an arrival and a departure grazing bifurcations of periodic orbits. The blue and dark green lines are more degenerated bifurcations; in particular, the dark green line represents the bifurcation from infinity at $b_1 = 0$ for $b_2 < 0$, while for $b_2 = 0$ and $b_1 > 0$ the global system has a bracelet of periodic orbits, as emphasized in Remark 2.4.

spends a maximal time τ_M in going from $(-1, \hat{u}_-)$ to $(1, u_+^c)$, which acts as the uppermost falling orbit. Thus, every orbits starting at the line Σ_- with $u_- > \hat{u}_-$ cannot reach the line Σ_+. Orbits starting at Σ_- with $u_- < \hat{u}_-$ reach Σ_+ with a flight time $\tau < \tau_M$. Note that $\hat{u}_- = U^{-1}(u_+^c)$.

Accordingly, we get

$$\mathrm{Dom}(U) = \begin{cases} \{u_- \in \mathbb{R} : u_- \leqslant u_-^*\}, & \text{if } b_2 < 0 \text{ and } \lambda > 0, \\ \mathbb{R}, & \text{if } b_2 < 0 \text{ and } \lambda < 0, \\ \{u_- \in \mathbb{R} : u_- < \hat{u}_-\}, & \text{if } b_2 > 0, \end{cases} \tag{2.7}$$

and so Σ_-^{ad} is always a connected set.

Since it is not possible to write an explicit expression of u_+ in terms of u_-, we obtain the parametric expression of the transition map U in terms of the flight time τ, by considering a starting point $(-1, u_-) \in \Sigma_-^{ad}$ and imposing that the orbit corresponding to this point reaches Σ_+ in a point $(1, u_+)$. We follow so a similar approach to the introduced in [1] for a different case. So,

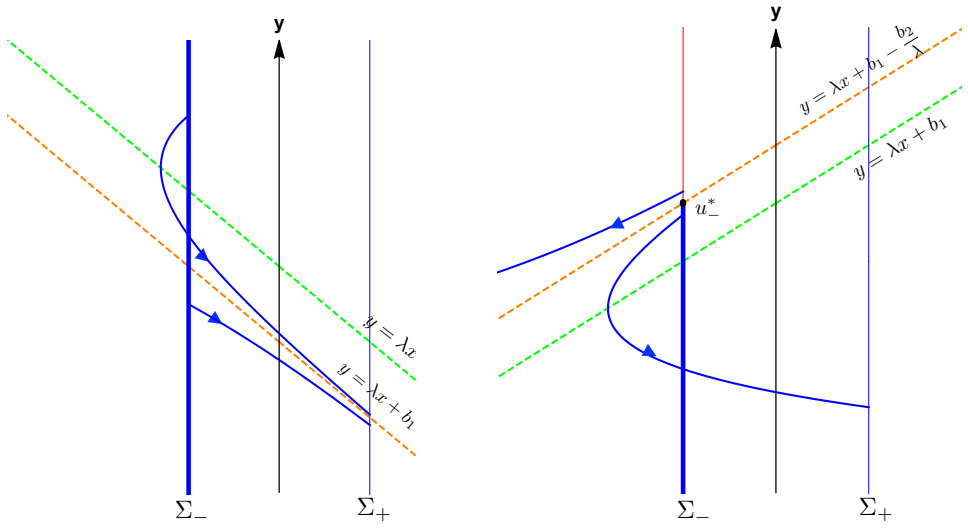

(a) (b)

Figure 2.4: Some orbits of the upper system for $b_2 < 0$ and $\lambda \neq 0$. The dashed straight lines correspond to the invariant straight line ISL (in orange) and the vertical isocline (in green). It is emphasized with a thick line the admissible subset Σ_-^{ad} for the map T_U according to (2.7). (a) The case $\lambda < 0$; (b) the case $\lambda > 0$.

using the expression in (2.2), we get

$$\begin{aligned} u_-(\tau) &= b_1 + \frac{\lambda^2 - b_2 - b_2\lambda\tau + e^{\lambda\tau}(\lambda^2 + b_2)}{\lambda(1 - e^{\lambda\tau})}, \\ u_+(\tau) &= b_1 + \frac{\lambda^2 - b_2 + e^{\lambda\tau}(\lambda^2 + b_2 - b_2\lambda\tau)}{\lambda(1 - e^{\lambda\tau})}. \end{aligned} \tag{2.8}$$

Note that the parameter b_1 represents for the map U only a translation of its graph along the direction of the main bisector in the plane (u_-, u_+).

In the following lemma we give the condition satisfied by τ_M such that $\mathcal{I} = (0, \tau_M]$.

Lemma 2.5. *Consider system* (2.1) *with* $b_2 > 0$ *and* $\lambda \neq 0$. *Then, there exists a maximum value* $\tau = \tau_M$ *of the flight time such that* $\tau \in \mathcal{I} = (0, \tau_M]$. *Furthermore,* $u'_-(\tau_M) = 0$ *and the value* τ_M *is the only solution of equation*

$$(e^{-\lambda\tau} + \lambda\tau - 1)b_2 - 2\lambda^2 = 0. \tag{2.9}$$

Proof. The maximum value of the flight time τ_M exists in the cases in which the contact point at the line Σ_+ has a visible character and there exists an orbit of the upper system that arrives to such a point, see Remark 1.11. If $b_2 > 0$

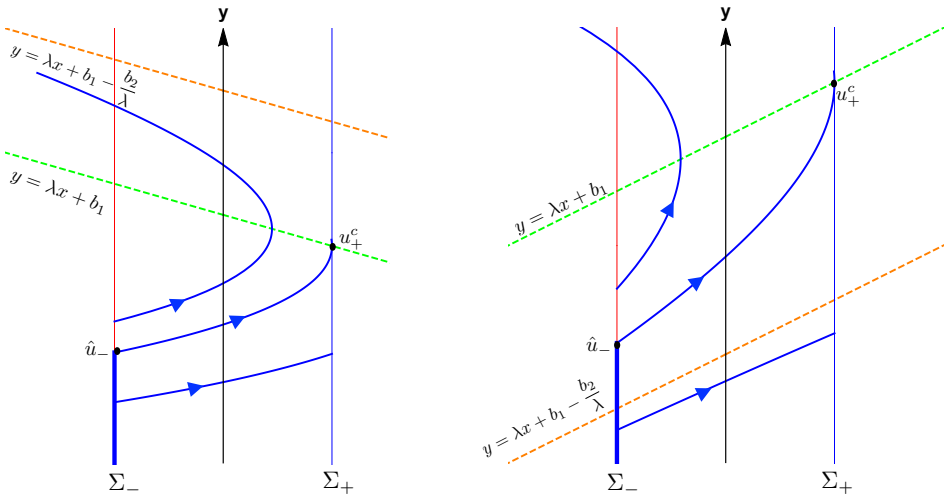

(a) (b)

Figure 2.5: Some orbits of the upper system for $b_2 > 0$ and $\lambda \neq 0$. The dashed straight lines correspond to the invariant straight line ISL (in orange) and the vertical isocline (in green). The admissible subsets Σ_-^{ad} for the map T_U regarding (2.7) are emphasized with a thick line. (a) The case $\lambda < 0$; (b) the case $\lambda > 0$.

we have $x'' = -b_2 < 0$ and by Lemma 1.12, the existence of τ_M is guaranteed. Since orbits starting at $(-1, u_-)$ with $u_- > u_-(\tau_M)$ do not arrive at Σ_+, and orbits which satisfy $u_- < u_-(\tau_M)$ have a flight time $\tau < \tau_M$ arriving at a point in Σ_+ with $u_-+ < u_+^c$; we have that $u_-(\tau_M)$ is the maximum value of the transition map U, and so $u'_-(\tau_M) = 0$. Then, to obtain the equation (2.9), it suffices to impose $u_+(\tau) = u_+^c = \lambda + b_1$. Effectively,

$$b_1 + \frac{\lambda^2 - b_2 + e^{\lambda\tau}(\lambda^2 + b_2 - b_2\lambda\tau)}{\lambda(1 - e^{\lambda\tau})} = \lambda + b_1$$

is equivalent to

$$b_2 + e^{\lambda\tau}(b_2\lambda\tau - b_2 - 2\lambda^2) = 0$$

and (2.9) follows. □

Due to the fact that symmetric periodic orbits are determined by equation (1.21), in this chapter we establish the existence of symmetric periodic orbits by studying the zeroes of the function

$$g(u) = U(u) + u = 2(b_1 - b_{\text{ref}}(\tau, \gamma)), \tag{2.10}$$

where we have introduced the reference function

$$b_{\text{ref}}(\tau, \gamma) = \frac{b_2}{\lambda} - \frac{(1 + e^{\lambda\tau})}{2(1 - e^{\lambda\tau})}(2\lambda - b_2\tau). \tag{2.11}$$

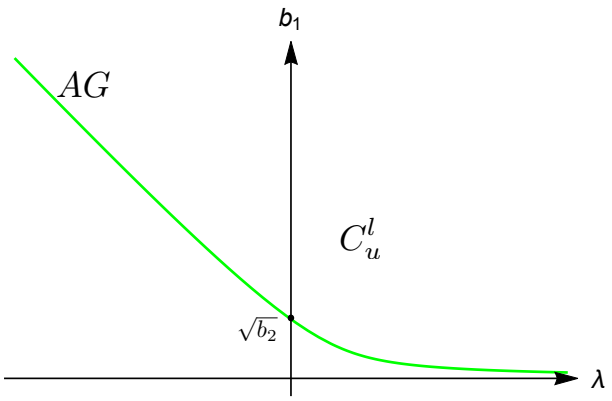

Figure 2.6: The bifurcation set for the case $b_2 > 0$, according to Theorem 2.6, in the parameter plane (λ, b_1). Here, we show the arrival-grazing bifurcation curve $b_1 = b_{AG}(\lambda)$ labelled as AG.

Assuming that the value τ_M is defined, see Lemma 2.5, then using (2.11) we define the function

$$b_{AG}(\lambda) = b_{\text{ref}}(\tau_M, \lambda). \tag{2.12}$$

Assuming also that exists a value $\tau_{SN} \in \mathcal{I}$ such that $g'(u_-(\tau_{SN})) = 0$, then τ_{SN} is the only solution of equation

$$[\lambda\tau_{SN} - \sinh(\lambda\tau_{SN})]b_2 - 2\lambda^2 = 0. \tag{2.13}$$

Using again (2.11), we introduce the function

$$b_{SN}(\lambda) = b_{\text{ref}}(\tau_{SN}, \lambda). \tag{2.14}$$

Both functions b_{AG} and b_{SN} are key points in stating the following result whose proof appears in Section 2.2.

Theorem 2.6. *Assume that $b_2 \neq 0$, and $\lambda \neq 0$ in system (2.1) and consider functions $b_{AG}(\lambda)$ and $b_{SN}(\lambda)$ defined in* (2.12) *and* (2.14) *respectively. Then, the following statements hold.*

(a) If there exists a periodic orbit, then it is symmetrical with respect to the origin.

(b) If $b_2 > 0$, then for $b_1 < b_{AG}(\lambda)$ there are no periodic orbits at all, while for $b_1 \geqslant b_{AG}(\lambda)$ there exists an unstable periodic orbit

(c) If $b_2 < 0$ and $\lambda < 0$, then there exists always one stable periodic orbit.

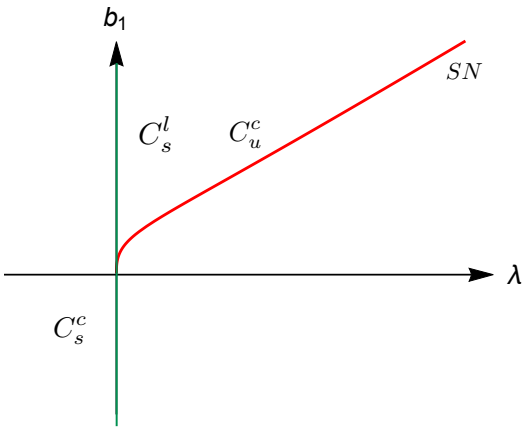

Figure 2.7: The bifurcation set for $b_2 < 0$, according to Theorem 2.6, in the parameter plane (λ, b_1). We can see that all the bifurcation curves are organized around the high-codimension point at the origin of the parameter plane (λ, b_1). The saddle-node bifurcation curve in red, emerges at the origin from the bifurcation at infinity line, which occurs at $\lambda = 0$ for $b_1 \geqslant 0$.

(d) Consider $b_2 < 0$ and $\lambda > 0$. If $b_1 < b_{SN}(\lambda)$, then there are no periodic orbits; if $b_1 = b_{SN}(\lambda)$, then there is one periodic orbit which is non-hyperbolic; finally, if $b_1 > b_{SN}(\lambda)$, then there exist two periodic orbits with opposite stability.

(e) If $b_2 < 0$ then for $\lambda = 0$ the system undergoes a periodic orbit bifurcation from infinity with different character depending on the sign of b_1. Thus, when $b_1 \leqslant 0$ there are no periodic orbits for $\lambda > 0$ and there appears a stable periodic orbit of great size and cloud type for small $\lambda < 0$. Otherwise, when $b_1 > 0$ there exists a stable periodic orbit for $\lambda < 0$ and when $\lambda > 0$ and small there appears a new unstable periodic orbit of great size and cloud type. These two periodic orbits coexist in the parameters region described in the statement (d).

Regarding statement (b) of Theorem 2.6, we see that for $b_1 = b_{AG}(\lambda)$, the hysteretic system (1.5) undergoes an arrival-grazing bifurcation of periodic orbits. From statement (d), we deduce the existence of a saddle-node bifurcation of periodic orbits, where two periodic orbits of different stability character collide to disappear. Clearly, such a bifurcation can be seen in a reverse sense, that is there appear a non-hyperbolic symmetric periodic orbit which gives rise to two different periodic orbits.

In Figures 2.6 and 2.7 we show the bifurcation sets in the parameter plane (λ, b_1) as deduced from the previous Theorem, taking into account the sign

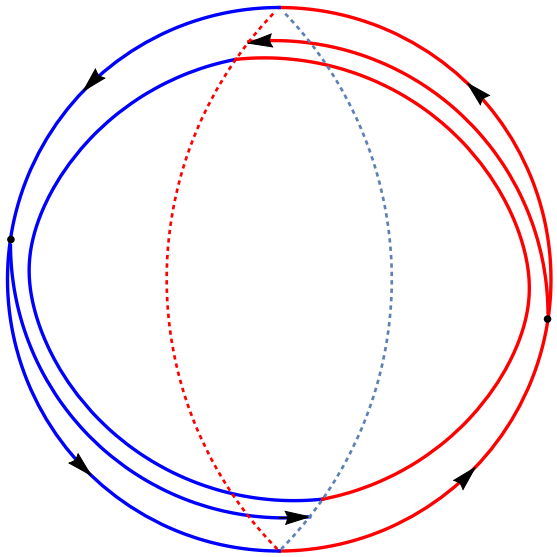

Figure 2.8: Poincaré disk for the case where both b_1 and λ are negative, showing that a stable symmetric periodic orbit of great size exists.

of b_2. Note that for $b_2 > 0$ the curve defined in (2.12), which represents an arrival-grazing bifurcation of periodic orbits can be extended in a continuous way to the point $(0, \sqrt{b_2})$, which was predicted by Proposition 2.3(d).

In Figures 2.8 and 2.9, we show two Poincaré disks illustrating the periodic orbits that appear through the bifurcation from infinity in the case $b_2 < 0$, according to Theorem 2.6. We remark the existence of two different periodic orbits, both symmetrical with respect to the origin, in the region with $\lambda > 0$ and $b_1 > b_{SN}(\lambda)$. Note that the singular points at infinity, where the invariant straight lines emerge from, appear at the point

$$\left(\pm\frac{1}{\sqrt{1+\lambda^2}}, \pm\frac{\lambda}{\sqrt{1+\lambda^2}}\right) \in \partial\mathbb{D}.$$

2.1.3 An illustrative example

We finish this section by showing the usefulness of above results by considering an illustrative example. It is well known that to prove the existence of periodic orbits for 3D piecewise linear systems is a difficult task which is far from being solved. We will see that in cases where the relaxation hypothesis can be assumed, some periodic orbits in a family of 3D piecewise linear dynamical systems can be detected.

Using equations (1.6)-(1.7) in Chapter 1 with $m = 1$, $\varphi(z)$ as in (1.2), and

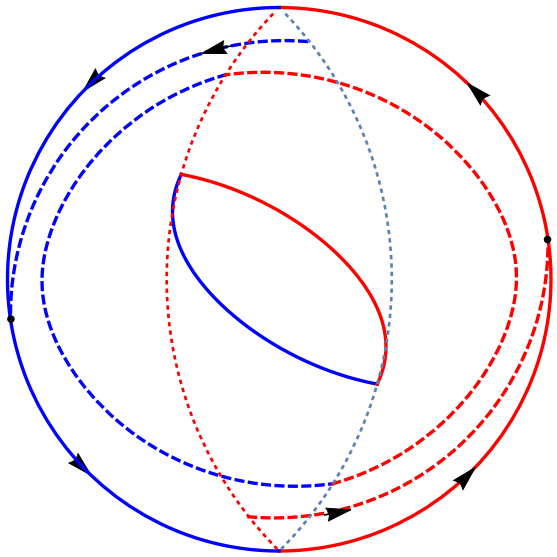

Figure 2.9: Poincaré disk for the case with both b_1 and λ positive, where two orbits are coexisting, and the big one is unstable.

$z_0 = 1/c$, $x_0 = 1$, we can see that the 3D system

$$\begin{cases} \dot{x} = (\lambda + \beta_1)x - y + \beta_1 z, \\ \dot{y} = \beta_2 x + \beta_2 z, \\ \epsilon \dot{z} = -x + \varphi(z) \end{cases} \tag{2.15}$$

leads, by the relaxation hypothesis, to system (2.1) with parameters

$$b_1 = \beta_1 \frac{1+c}{c}, \quad b_2 = \beta_2 \frac{1+c}{c}.$$

Taking now $\beta_1 = 0.5$, $\beta_2 = -0.5$, $c = 1$ and $\lambda = 0.15$ we get that $b_1 = 1$ and $b_2 = -1$ in system (2.1), and so Theorem 2.6 guarantees the existence of a stable periodic orbit surrounded by a unstable periodic orbit. Following similar ideas to the approach in [19], we can expect the existence of periodic orbits in system (2.15) for ϵ sufficiently small. Effectively, if we simulate now system (2.15) for the corresponding values, we see that orbits clearly approach a stable periodic orbit which is in perfect correspondence with the one of the hysteretic system, see Figures 2.10 and 2.11. In fact, this periodic orbit persists even when we slightly perturb the 3D system allowing the determinant not to be zero.

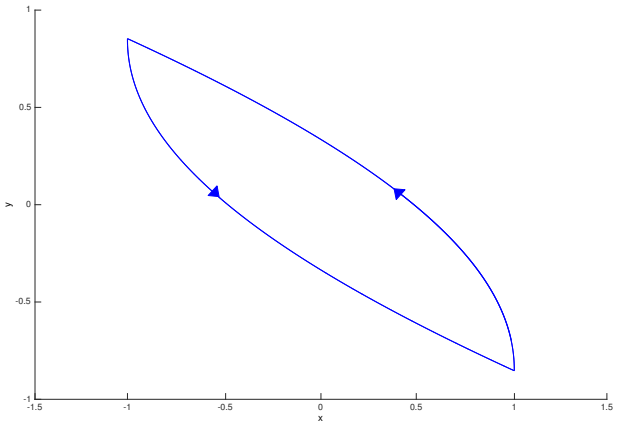

Figure 2.10: The stable symmetric periodic orbit of hysteretic system (2.1) for $b_1 = 1$, $b_2 = -1$ and $\lambda = 0.15$. These values of the parameters correspond to the region above the line $b_{SN}(\lambda)$ showed in Figure 2.7.

2.2 Proof of Theorem 2.6

In this section, we prove Theorem 2.6 step by step. First, we compute the derivative of the transition map U as defined in (2.8), namely

$$U'(u_-) = \frac{u'_+(\tau)}{u'_-(\tau)} = \frac{2\lambda^2 - b_2\lambda\tau + b_2(e^{\lambda\tau} - 1)}{2\lambda^2 - b_2\lambda\tau + b_2(1 - e^{-\lambda\tau})}. \tag{2.16}$$

For proving statement (a), we use Corollary 1.8 and the derivative of U in (2.16), getting a direct contradiction with the equation $U'(u) = 1$.

Due to the fact that symmetric periodic orbits are determined by equation (1.21), in the following we establish the existence of symmetric periodic orbits by studying the zeros of the function $g(u) = U(u) + u$.

The following lemma is useful to prove the remaining statements.

Lemma 2.7. *Consider system* (1.5). *The following statement hold.*

(i) If $b_2 > 0$, $\lambda \neq 0$, *then* $U'(u) > 1$ *for all* $u \in \mathrm{Dom}(U)$. *Moreover*

$$\lim_{\tau\to 0} U'(u_-(\tau)) = 1, \quad \lim_{\tau\to\tau_M} U'(u_-(\tau)) = +\infty, \tag{2.17}$$

where τ_M *is defined in* (2.9).

(ii) If $b_2 < 0$, $\lambda < 0$, *then* $|U'(u)| < 1$ *for all* $u \in \mathrm{Dom}(U)$. *Moreover,*

$$\lim_{\tau\to 0} U'(u_-(\tau)) = 1, \quad \lim_{\tau\to\infty} U'(u_-(\tau)) = 0. \tag{2.18}$$

(iii) If $b_2 < 0$, $\lambda > 0$, *then* $g''(u) < 0$ *for all* $u \in \mathrm{Dom}(U)$.

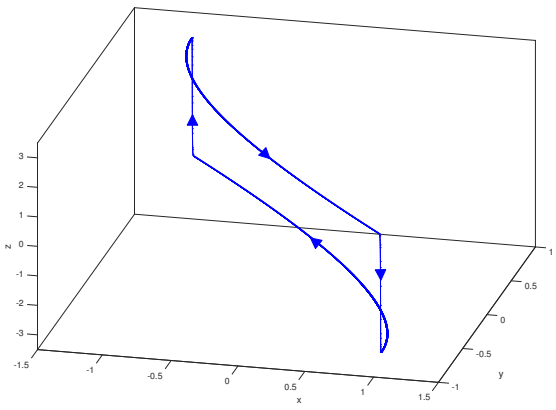

Figure 2.11: The corresponding periodic orbit for the 3D continuous piecewise linear system (2.15) for $\beta_1 = 0.5$, $\beta_2 = -0.5$, $c = 1$, $\lambda = 0.15$ and $\epsilon = 0.001$.

Proof. (i) It is easy to see that $U'(u_-(\tau)) \to 1$ as $\tau \to 0$. Then, we will prove the second limit in statement (i) by showing that $u'_-(\tau_M) = 0$ and $u'_+(\tau_M) > 0$. The derivative of u_- with respect to the time τ is

$$u'_-(\tau) = \frac{b_2(e^{\lambda\tau} - \lambda\tau e^{\lambda\tau} - 1) + 2\lambda^2 e^{\lambda\tau}}{(1 - e^{\lambda\tau})^2}. \tag{2.19}$$

If $\tau = \tau_M$, from (2.9) we get

$$b_2 = \frac{2\lambda^2}{e^{-\lambda\tau_M} + \lambda\tau_M - 1}, \tag{2.20}$$

and directly we obtain $u'_-(\tau_M) = 0$. However, for $u'_+(\tau)$ we have,

$$u'_+(\tau) = \frac{e^{\lambda\tau}}{(1 - e^{\lambda\tau})^2}[b_2(e^{\lambda\tau} - 1 - \lambda\tau) + 2\lambda^2].$$

Substituting the value of b_2 from (2.20), we get

$$u'_+(\tau_M) = \frac{2\lambda^2 e^{\lambda\tau_M}}{1 + e^{\lambda\tau_M}(\lambda\tau_M - 1)}.$$

Now, it is easy to see that $u'_+(\tau_M) \neq 0$ for $\lambda \neq 0$. Since $U'(u_-(\tau)) \to 1$ as $\tau \to 0$ and $U'(u_-(\tau)) \to +\infty$ as $\tau \to \tau_M$, using that $U'(u) \neq 1$ for all $u \in \mathrm{Dom}(U)$, we get that $U'(u) > 1$ in its domain, and statement (i) is done.

(ii) We see first by contradiction that $U'(u) \neq -1$. Using (2.16), condition $U'(u) = -1$ is equivalent to

$$b_2 = \frac{2\lambda^2}{\lambda\tau - \sinh(\lambda\tau)}. \tag{2.21}$$

Since $\text{sign}(\lambda\tau - \sinh(\lambda\tau)) = -\text{sign}(\lambda)$ for $\tau > 0$, solutions of $U'(u) = -1$ only exist when b_2 and λ have opposite signs, which is a contradiction. Now, using (2.16) again, equalities (2.18) are direct. As we know that $U'(u_-(\tau)) \neq 1$ for all $\tau > 0$, $|U'(u)| < 1$ for all $u \in \text{Dom}(U)$ and statement (ii) follows.

(iii) We determine the sign of the second derivative of $g(u)$, by using

$$\frac{d}{d\tau}\left(\frac{d}{du_-}U(u_-(\tau))\right) = \frac{d^2}{du_-^2}[g(u_-(\tau))]\frac{du_-}{d\tau}. \tag{2.22}$$

Since $e^{\lambda\tau} - \lambda\tau e^{\lambda\tau} - 1 \leqslant 0$ and using (2.19), we obtain $u'_-(\tau) \geqslant 0$. Then, using (2.16), we get after some computations

$$\text{sign}\, g''(u) = \text{sign}\frac{d}{d\tau}\left(\frac{d}{du_-}U(u_-(\tau))\right) = -\text{sign}\, h(\tau),$$

where

$$h(\tau) = \lambda(2\lambda - b_2\tau)\cosh\left(\frac{\lambda\tau}{2}\right) + 2b_2\sinh\left(\frac{\lambda\tau}{2}\right).$$

As $h(0) = 2\lambda^2 > 0$ and $h'(\tau) > 0$ for all τ, the concavity of the function g is proved.

□

The next step is to proof statement (b). From Lemma 2.7(i) we obtain $g'(u) > 2$, and so g is increasing and it has at most one zero. Noting that $g(u_-(\tau_M)) = g(\hat{u}_-)$, we have

$$\lim_{u\to-\infty} g(u) = -\infty, \quad g(u) \leqslant g(\hat{u}_-) = 2(b_1 - b_{AG}(\lambda)),$$

where $b_{AG}(\gamma)$ is defined in (2.12). According to the value of b_1 different cases appear. If $b_1 < b_{AG}(\lambda)$, then the function g does not vanish and there are no periodic orbits. If $b_1 \geqslant b_{AG}(\lambda)$, then $g(\hat{u}_-) \geqslant 0$, and so the function g has one zero and system (1.5) has one periodic orbit, which is unstable because $U'(u) > 1$. Moreover, from statement (d) of Theorem 2.3 we see that the definition of $b_{AG}(\gamma)$ can be extended to $\lambda = 0$, so that $b_{AG}(0) = \sqrt{b_2}$. Furthermore, when $\lambda \to \pm\infty$, we obtain $\lambda\tau_M \to \pm\infty$. Then, the following limits hold

$$\lim_{\lambda\to+\infty} b_{AG}(\lambda) = 0, \quad \lim_{\lambda\to-\infty} b_{AG}(\lambda) = +\infty,$$

as shown in Figure 2.6.

Regarding statement (c), from Lemma 2.7(ii) and Proposition 1.9, we get $g'(u) > 0$, and so the maximum number of symmetric periodic orbits is one. Since the function $g(u)$ is continuous, injective and it takes all the values in

$\mathbb{R}$, we obtain that $g(u)$ has always a zero, which corresponds to a symmetric periodic orbit of system (1.5). The stability of such an orbit follows from Lemma 2.7(ii), and statement (c) is shown.

Next, we will prove statement (d) of Theorem 2.6. From Lemma 2.7(iii), the function g is concave down and since $b_2\lambda < 0$, we see that equation (2.13) has a unique solution $\tau = \tau_{SN}$, so that the maximum value of function g is

$$g(u_-(\tau_{SN})) = 2(b_1 - b_{SN}(\lambda)),$$

where $b_{SN}(\lambda)$ is defined in (2.14). Then, if $b_1 < b_{SN}(\lambda)$, the maximum value of $g(u)$ is negative and there is no solution of equation (1.21); if $b_1 = b_{SN}(\lambda)$, there exists one symmetric periodic orbit which is non-hyperbolic, while for $b_1 > b_{SN}(\lambda)$ there exist two symmetric periodic orbit with opposite stabilities. Statement (d) is shown.

Now, we will show some properties of the function $b_{SN}(\lambda)$ to justify the graph for the periodic orbits saddle-node bifurcation curve in Figure 2.7. The function $b_{SN}(\lambda)$ is continuous and when $\lambda \to \infty$, the product $\lambda\tau_{SN}(\lambda) \to \infty$. Then, it is easy to see from (2.14) that

$$\lim_{\lambda\to\infty} b_{SN}(\lambda) = \infty.$$

The limit of $b_{SN}(\lambda)$ when $\lambda \to 0^+$ is more involved. When $\lambda \to 0^+$, the limit of the product $v(\lambda) = \lambda\tau_{SN}(\lambda)$ could be any non-negative number or ∞. But, regarding equation (2.13), we know that $v(\lambda)$ satisfies the condition,

$$v - \sinh(v) = \frac{2\lambda^2}{b_2}. \tag{2.23}$$

Thus, $\lim_{\lambda\to 0^+} v(\lambda) = 0$. The expansion in λ of (2.23) also tells us that $v(\lambda) = \mathcal{O}(\lambda^{2/3})$ and so $\tau_{SN}(\lambda) = \mathcal{O}(\lambda^{-1/3})$ for λ small, see (2.13), that is $\tau_{SN} \to \infty$ when $\lambda \to 0^+$. Then, using (2.13) in the expression of b_{SN} in (2.14), we have that

$$\lim_{\lambda\to 0^+} b_{SN}(\lambda) = \lim_{\lambda\to 0^+} \lambda \left(\frac{2(1 - e^{\lambda\tau_{SN}}) + (1 + e^{\lambda\tau_{SN}})\sinh(\lambda\tau_{SN})}{(1 - e^{\lambda\tau_{SN}})(\lambda\tau_{SN} - \sinh(\lambda\tau_{SN}))} \right).$$

Since $\lambda\tau_{SN} \to v$, such a limit is equivalent to

$$\lim_{\lambda\to 0^+} b_{SN}(\lambda) = \lim_{v\to 0} \frac{v}{\tau_{SN}} \frac{2(1 - e^v) + (1 + e^v)\sinh v}{(1 - e^v)(v - \sinh v)}.$$

Doing some computations, we get

$$\lim_{\lambda\to 0^+} b_{SN}(\lambda) = \lim_{v\to 0} \frac{v}{\tau_{SN}} \frac{(e^v - 1)^2}{e^{2v} - 2ve^v - 1} = \lim_{v\to 0} \frac{v}{\tau_{SN}} \frac{3v^2}{v^3} = 0.$$

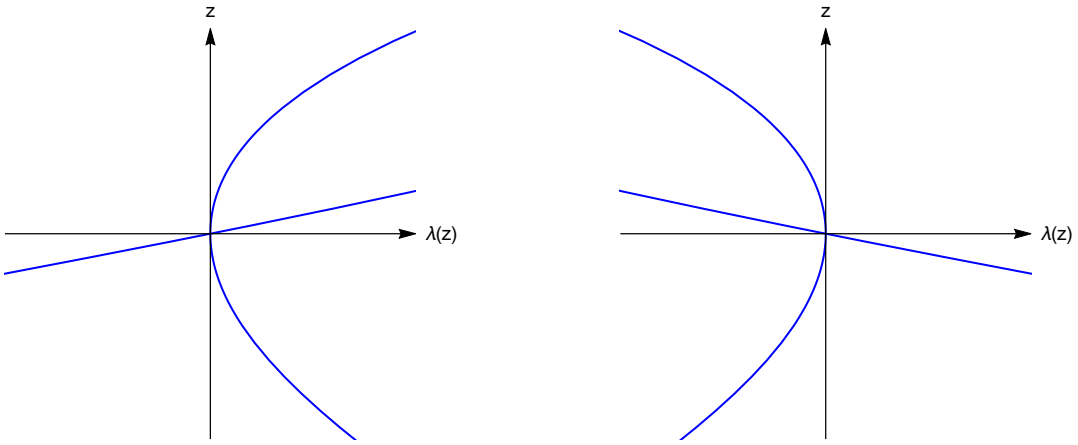

(a) (b)

Figure 2.12: The solutions for the equation $h(z, \lambda) = 0$ near the origin, see (2.25), for the cases (a) $b_1 > 0$ and (b) $b_1 < 0$. Only branches in the first and third quadrants represent valid periodic orbits for our hysteretic system.

We conclude that the bifurcation curve of a saddle-node bifurcation of periodic orbits emerges from the origin in the parameter plane (λ, b_1), as we show in Figure 2.7.

Finally, we show the proof of statement (e). The existence of symmetric periodic orbits is given by the condition $\kappa(\tau) = 0$, see (1.23). We will prove first that the solutions of this equation with respect to the parameter λ, undergoes a pitchfork bifurcation without symmetry for $\lambda = 0$ when $b_2 < 0$. To this end, we introduce the following pitchfork bifurcation lemma where the usually assumed symmetry of the vector field is not required; in fact, this lemma is an improved version of Theorem 2.1 in [48] which is stated here without proof, for the sake of brevity. In what follows, to clarify the notation, we use subscripts when taking derivatives respect to different variables.

Lemma 2.8. *Consider a first-order autonomous equation,*

$$\frac{dz}{d\tau} = h(z, \lambda), \quad \tau > 0.$$

Suppose that $(z, \lambda) = (0, 0)$ is a bifurcation point, and let $h(z, \lambda)$ be an analytic function of z and λ in a neighbourhood of the origin, so that

$$h(0, 0) = h_z(0, 0) = 0.$$

If $h_\lambda(0, 0) = 0$, $h_{zz}(0, 0) = 0$ and $h_{z\lambda}(0, 0) \neq 0$, $h_{zzz}(0, 0) \neq 0$, then a pitchfork bifurcation is produced at the point $(z, \lambda) = (0, 0)$.

Now, the condition for the existence of symmetric periodic orbits $\kappa(\tau) = 0$ is equivalent, from relations (2.8), to

$$(b_1\lambda - b_2)\tanh\left(\frac{\lambda\tau}{2}\right) - \lambda^2 + b_2\frac{\lambda\tau}{2} = 0, \tag{2.24}$$

where only the solutions with $\tau > 0$ represent valid periodic orbits. To simplify condition (2.24), we do a rescaling in time in system (2.1) which allows us to assume $b_2 = -1$ without loss of generality. Also, the variable change $z = \lambda\tau/2$ in (2.24) suggest to introduce the function

$$h(z, \lambda) := (1 + b_1\lambda)\tanh z - \lambda^2 - z, \tag{2.25}$$

so that the condition (2.24) is reduced to $h(z, \lambda) = 0$. Consider first the case $b_1 \neq 0$. It is easy to see that function $h(z, \lambda)$ in (2.25), satisfies the conditions in Lemma 2.8, and so equation $h(z, \lambda) = 0$ can have up to three solutions. Consider a solution branch $\lambda(z)$ with Taylor series $\lambda(z) = a_0 + a_1 z + a_2 z^2 + \mathcal{O}(z^3)$. Putting this expression in the equation $h(z, \lambda) = 0$, we obtain the coefficients a_i, getting the two following expansions for $\lambda(z)$, namely

$$\lambda_1(z) = b_1 z - \frac{1}{3b_1}z^2 + \mathcal{O}(z^3), \tag{2.26}$$

and

$$\lambda_2(z) = \frac{1}{3b_1}z^2 + \mathcal{O}(z^3). \tag{2.27}$$

Since $z = \lambda\tau/2$ and we need $\tau > 0$, we only have to consider as significative solutions those solutions with $\text{sign}(z) = \text{sign}(\lambda)$. Thus, when $b_1 > 0$, we obtain two significative solutions for $\lambda > 0$ and only one significative solution for $\lambda < 0$. If $b_1 < 0$, we have no significative solution for λ positive and just one for $\lambda < 0$. See Figure 2.12.

Clearly, the number of valid periodic orbits changes at $\lambda = 0$ from 2 to 1 if $b_1 > 0$ and from 0 to 1 if $b_1 < 0$ and it is associated to the branch in (2.27). Let us see that the appearing periodic orbit at $\lambda = 0$ comes from infinity by showing that its period tends to infinity when $\lambda \to 0^+$. We undo in (2.27) the variable change along the previous solutions. The flight time of the periodic orbit that appears when either $b_1 > 0$ and $\lambda > 0$ and small, or for $b_1 < 0$ and $\lambda < 0$ and small, satisfies $\tau = \mathcal{O}(|\lambda|^{-1/2})$. Thus, $\tau \to \infty$ if $\lambda \to 0$ from above when $b_1 > 0$ or below when $b_1 < 0$. It is easy to see that, under these conditions, $u_-(\tau) \to +\infty$ and $u_+(\tau) \to -\infty$. Then, we conclude the great size of the orbit that appears in the case $\lambda = 0$ with $b_1 \neq 0$.

The case $b_1 = 0$ needs a specific treatment because Lemma 2.8 does not apply and we cannot use expressions in (2.26) or (2.27). For $b_1 = 0$ equation $h(z, \lambda) = 0$ becomes

$$\tanh z - z - \lambda^2 = 0,$$

and using Taylor series we get

$$-\frac{z^3}{3} - \lambda^2 + \mathcal{O}(z^5) = 0.$$

Then, we can obtain the solution $z(\lambda) = \mathcal{O}(\lambda^{2/3})$ and undoing the variable change we get that $\tau = \mathcal{O}(|\lambda|^{-1/3})$, so that $\tau \to \infty$ when $\lambda \to 0$. The same conclusion as before about the great size of the bifurcating periodic orbit follows, and statement (e) is proved.

Chapter 3

Systems with single non-zero real eigenvalues

In this chapter, we consider a hysteretic system of either saddle or node type with symmetry. The following content is essentially the same as of the reference [18], submitted for publication.

As in the previous chapter, we study the properties of the transition map U to detect periodic orbits and their bifurcations. Here, we will have always equilibria, being real or virtual. We deal from the beginning with the system (1.12) with $\mu = 1$, and $|\gamma| < 1$ for the saddle cases, while for the node ones we must take $|\gamma| > 1$. So that, system (1.12) leads to the systems S_U and S_L, see (1.14)-(1.15), namely

$$\left\{ \begin{array}{rcl} x' & = & 2\gamma(x \mp x_E) - (y \mp y_E), \\ y' & = & (\gamma^2 - 1)(x \mp x_E). \end{array} \right. \qquad \mp x \geqslant -1 \tag{3.1}$$

First, we compute the solution of the upper system S_U

$$\left(\begin{array}{c} x(\tau) - x_E \\ y(\tau) - y_E \end{array} \right) = e^{A\tau} \left(\begin{array}{c} x(0) - x_E \\ y(0) - y_E \end{array} \right), \tag{3.2}$$

where

$$e^{A\tau} = e^{\gamma\tau} \left(\begin{array}{cc} \mathrm{ch}\tau + \gamma \mathrm{sh}\tau & -\mathrm{sh}\tau \\ (\gamma^2 - 1)\mathrm{sh}\tau & \mathrm{ch}\tau - \gamma \mathrm{sh}\tau \end{array} \right)$$

and we adopt the notation ch and sh for the functions hyperbolic cosine and hyperbolic sine. Furthermore, in what follows we will use extensively the function

$$\psi_\gamma(\tau) = \mathrm{ch}\tau + \gamma \mathrm{sh}\tau. \tag{3.3}$$

Taking $(-1, u_-) \in \Sigma_-^{ad}$ as initial point of an orbit, we can assure that the quoted orbit reaches, after a time τ, the line Σ_+ at the point $(1, u_+)$. Then,

from (3.2), the following parametric representation for the map $u_+ = U(u_-)$ is obtained,

$$\begin{aligned} u_-(\tau) &= y_E + \frac{(x_E-1)e^{-\gamma\tau} - (x_E+1)\psi_\gamma(\tau)}{\mathrm{sh}\tau}, \\ u_+(\tau) &= y_E - \frac{(x_E+1)e^{\gamma\tau} - (x_E-1)\psi_{-\gamma}(\tau)}{\mathrm{sh}\tau}, \end{aligned} \tag{3.4}$$

where the flight time τ belongs to either a bounded interval $\mathcal{I} = (0, \tau_M]$ or to the interval $\mathcal{I} = (0, \infty)$ which will be specified in Lemma 3.5.

Therefore, for each pair (p, q) that determines a periodic orbit, where $p = u_-(\tau_1)$ and $q = u_+(\tau_1)$, the twin periodic orbit is determined by the pair $(-q, -p)$ where $-q = u_-(\tau_2)$ and $p = -u_+(\tau_2)$. Hence, periodic orbits correspond to solutions of the system

$$\begin{cases} u_-(\tau_2) + u_+(\tau_1) = 0, \\ u_-(\tau_1) + u_+(\tau_2) = 0. \end{cases} \tag{3.5}$$

Note from (1.17) that a periodic orbit is stable when

$$\left|\frac{dU}{dp}(-q)\frac{dU}{dp}(p)\right| = \left|\frac{u'_+(\tau_1)u'_+(\tau_2)}{u'_-(\tau_1)u'_-(\tau_2)}\right| < 1.$$

Symmetric periodic orbits with respect to the origin, are determined according to (1.18) by the equality

$$U(p) + p = u_-(\tau_1) + u_+(\tau_1) = 0,$$

and from (1.19) its stability is given by the inequality

$$\left|\frac{dU}{dp}(p)\right| = \left|\frac{u'_+(\tau_1)}{u'_-(\tau_1)}\right| < 1.$$

3.1 Main results of the chapter

The non-generic case $\gamma^2 = 1$ is analyzed separately because the condition that allows us to obtain the canonical form (1.12) is violated. In this case, it is easy to see that $u_+(\tau) = u_-(\tau)$ and then the equalities $U(u) = u$ and $L(u) = u$ trivially follow, for all u on their respective domains.

Proposition 3.1. *When $\gamma^2 = 1$ there are periodic orbits only if either $\gamma = 1$ and $y_E - 2(1 + x_E) > 0$ or $\gamma = -1$ and $y_E + 2(1 + x_E) > 0$. In such cases, there exists a bounded continuum of invariant closed curves.*

Proof. If $\gamma^2 = 1$, then $U(u_-) = u_-$ and $L(u_+) = u_+$ within their respective domains and all the trajectories are horizontal straight lines.

When $\gamma = 1$, the straight line $2(x - x_E) - (y - y_E) = 0$ is full of equilibria. The map U is defined for $u_- < y_E - 2(1 + x_E)$ and the map L is defined for $u_+ > -y_E + 2(1 + x_E)$, so we have $L(U(u_-)) = u_-$ for

$$-[y_E - 2(1 + x_E)] < u_- < y_E - 2(1 + x_E),$$

which is only possible if the last term is positive.

Analogously, when $\gamma = -1$ and $y_E+2(1+x_E) > 0$ we obtain $L(U(u_-)) = u_-$ for

$$-[y_E + 2(1 + x_E)] < u_- < y_E + 2(1 + x_E),$$

otherwise there are no periodic orbits. The proposition is shown.

□

Next, we give a first result about existence of symmetric periodic orbits.

Proposition 3.2. *Assume that $\gamma^2 \neq 1$. If either $|x_E| \geqslant 1$ or $\gamma x_E \geqslant 0$ with $|\gamma| + |x_E| \neq 0$, then the following statements hold.*

(a) System (3.1) only can have symmetric periodic orbits.

(b) When $u'_-(\tau) \neq 0$ for all $\tau \in \mathcal{I}$, we have

$$\frac{dU}{du} = \frac{u'_+(\tau)}{u'_-(\tau)} \neq 1.$$

Proof. From statements (a) and (b) of Lemma 3.14 in Section 3.2 the derivative of the function $\eta(\tau) = u_+(\tau) - u_-(\tau)$ does not vanish for all $\tau \in \mathcal{I}$, and so the function $\eta(\tau)$ is injective. According to Proposition 1.7, the existence of non-symmetric periodic orbits is precluded and statement (a) is shown. Statement (b) follows from the inequality $\eta'(\tau) \neq 0$, and the proof is done.

□

Remark 3.3. *In the specific case $\gamma = x_E = 0$ and $y_E > 1$ (see Theorem 3.9(a)), it is easy to show the existence of a pair of homoclinic orbits bounding a continuum of periodic orbits. Otherwise, non-symmetric periodic orbits can only exist when $|x_E| < 1$ and $\gamma x_E < 0$.*

Next, we show, without proof, the behaviour of the functions $u_-(\tau)$ and $u_+(\tau)$ when $\tau \to 0^+$.

Lemma 3.4. *The functions $u_-(\tau)$, $u_+(\tau)$ given in (3.4) and the corresponding function $U(u)$ satisfy the following properties*

$$\lim_{\tau\to 0^+} u_-(\tau) = \lim_{\tau\to 0^+} u_+(\tau) = -\infty, \quad \lim_{u\to-\infty} U(u) = -\infty,$$

$$\lim_{u\to-\infty} \frac{dU}{du} = \lim_{\tau\to 0^+} \frac{u'_+(\tau)}{u'_-(\tau)} = 1.$$

According to Definition 1.10, the contact point at the falling line, $(1, u_+^c)$, is characterized by the condition $x'(\tau) = 0$, so that

$$u_+^c = y_E + 2\gamma(1 - x_E). \tag{3.6}$$

As explained in Chapter 1, by analyzing all the possible cases, the parameter τ belongs a bounded interval $\mathcal{I} = (0, \tau_M]$ in the cases in which the above contact point at the line Σ_+ has a visible character, see Lemma 1.12. In the following lemma, we give the characterization of such a maximum value τ_M.

Lemma 3.5. *If system* (3.1) *has an equilibrium point, which is one of the following four cases,*

(a) a real node outside the hysteresis band ($x_E < -1$, $|\gamma| > 1$),

(b) a stable node inside the hysteresis band ($|x_E| < 1$, $\gamma < -1$),

(c) a virtual saddle outside the hysteresis band ($x_E > 1$, $|\gamma| < 1$),

(d) a stable node on the line Σ_- ($x_E = -1$, $\gamma < -1$),

then, there exists a maximum value $\tau = \tau_M$ for the flight time such that $\tau \in \mathcal{I} = (0, \tau_M]$. Furthermore, $u'_-(\tau_M) = 0$ and the value τ_M is the only solution of equation

$$\rho = \beta(\tau) := e^{-\gamma\tau}\psi_\gamma(\tau), \tag{3.7}$$

where the parameter ρ and the function ψ_γ are defined in (1.24) and (3.3)*, respectively.*

Proof. Let us study when the contact point at the line Σ_+ has a visible character. Following Lemma 1.12 and relations in (1.13) it is necessary to have

$$x'' \,|_{(1,u_+^c)} = (\gamma^2 - 1)(x_E - 1) < 0.$$

Taking into account Remark 1.11, the case where $x_E \in (-1, 1)$ with $\gamma > 1$ must be excluded, and so the existence of the value τ_M is guaranteed in the four quoted cases. By definition, $u_-(\tau_M)$ corresponds to the maximum value

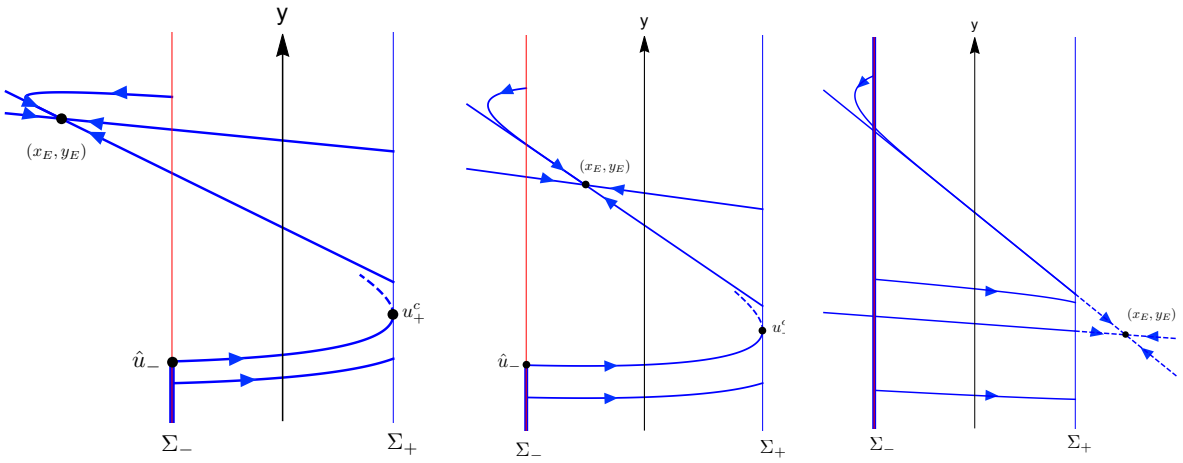

Figure 3.1: The stable node cases. (a) The real stable node outside the hysteresis band. (b) The real stable node inside the hysteresis band. (c) The virtual stable node. The thick part of the line Σ_- corresponds to the set Σ_-^{ad}.

of the transition map U, so that $u'_-(\tau_M) = 0$. Finally, to get equation (3.7), it suffices to impose that $u_+(\tau) = u_+^c$, namely

$$y_E - \frac{(x_E+1)e^{\gamma\tau} - (x_E-1)\psi_{-\gamma}(\tau)}{\mathrm{sh}\tau} = y_E + 2\gamma(1-x_E).$$

Introducing now the parameter ρ given in (1.24), we have

$$\rho = e^{-\gamma\tau}[2\gamma\mathrm{sh}\tau + \psi_{-\gamma}(\tau)]$$

and (3.7) follows.

□

Due to the fact that symmetric periodic orbits are determined by equation (1.18), in the following we establish the existence of symmetric periodic orbits by studying the zeroes of the function

$$g(u) = U(u) + u = 2[y_E - y_{\mathrm{ref}}(\tau,\gamma)], \tag{3.8}$$

where we have introduced the reference function

$$y_{\mathrm{ref}}(\tau,\gamma) = \gamma x_E + \frac{x_E\mathrm{sh}(\gamma\tau) + \mathrm{ch}(\gamma\tau) + \mathrm{ch}\tau}{\mathrm{sh}\tau}. \tag{3.9}$$

The analysis of periodic orbits is splitted into several cases, taking into account the location, topological type and stability of equilibria. Within each case, we choose the parameters γ and y_E as main bifurcation parameters.

3.1.1 The stable node case

Here, we assume that the equilibria of both sub-systems S_U and S_L are either real or virtual stable nodes, see Fig 3.1. In the cases where the value τ_M is defined, see Lemma 3.5, by using (3.9) we define the function

$$y_{AG}(\gamma) = y_{\text{ref}}(\tau_M, \gamma). \tag{3.10}$$

Also, in the cases where there exists a value $\tau_P \in \mathcal{I}$ such that the derivative of the function $\eta(\tau) = u_+(\tau) - u_-(\tau)$ vanishes, see Lemma 3.14, we get that τ_P is the only solution of equation

$$\rho = \frac{1 - e^{-\gamma\tau}\psi_\gamma(\tau)}{-1 + e^{\gamma\tau}\psi_{-\gamma}(\tau)}, \tag{3.11}$$

and using (3.9) we introduce the function

$$y_P(\gamma) = y_{\text{ref}}(\tau_P, \gamma). \tag{3.12}$$

According to Definition 1.10, the contact point at the rising line, $(-1, u_-^c)$, is characterized by the condition $x'(\tau) = 0$, so that

$$u_-^c = y_E - 2\gamma(1 + x_E). \tag{3.13}$$

if there exists a value $\tau_{DG} \in \mathcal{I}$ such that $u_-(\tau_{DG}) = u_-^c$ with $x'' > 0$ at the point $(-1, u_-^c)$, see Lemma 3.12, we get that τ_{DG} is the only solution of the equation

$$\rho = \frac{-e^{-\gamma\tau}}{\text{ch}\tau - \gamma\text{sh}\tau}, \tag{3.14}$$

and using again (3.9) we introduce the function

$$y_{DG}(\gamma) = y_{\text{ref}}(\tau_{DG}, \gamma). \tag{3.15}$$

The three functions y_{AG}, y_P and y_{DG} are crucial in stating our main results. Next, we show our findings for the stable node case.

Theorem 3.6 (**Stable node case**). *Assume that $\gamma < -1$ in system* (3.1) *and consider functions $y_{AG}(\gamma)$, $y_P(\gamma)$ and $y_{DG}(\gamma)$ defined in* (3.10), (3.12) *and* (3.15) *respectively. Then, the following statements hold.*

(a) If $x_E \leqslant 0$, then non-symmetric periodic orbits are impossible. Furthermore, for $y_E < y_{AG}(\gamma)$ there are no periodic orbits while for $y_E \geqslant y_{AG}(\gamma)$ there is one symmetric periodic orbit which is unstable.

(b) If $0 < x_E < 1$, then the following cases arise.

(b1) If $y_E < y_{AG}(\gamma)$, then there are no periodic orbits.

(b2) If $y_{AG}(\gamma) \leqslant y_E < y_P(\gamma)$, then there is only one periodic orbit, which is unstable and symmetric.

(b3) If $y_E = y_P(\gamma)$, then there is only one periodic orbit, which is non hyperbolic and symmetric.

(b4) If $y_E > y_P(\gamma)$, then there is one symmetric periodic orbit, which is stable.

(c) If $x_E \geqslant 1$, then non-symmetric periodic orbits are impossible and there exists one symmetric periodic orbit which is stable. If $y_E < y_{DG}(\gamma)$, then such a symmetric periodic orbit is of cloud type while for $y_E \geqslant y_{DG}(\gamma)$ it is of lens type.

Regarding statement (b) of Theorem 3.6, it should be noticed the existence of three different bifurcations. On the one hand, for $y_E = y_{AG}(\gamma)$ system (3.1) undergoes an arrival-grazing bifurcation of periodic orbits which implies the appearance of an unstable lens-type symmetric periodic orbit, see Definition 1.14. On the other hand, for $y_E = y_P(\gamma)$ a stability change is produced for the existing symmetric periodic orbit. This stability change is associated to a pitchfork bifurcation of periodic orbits, so that for $y_E > y_P(\gamma)$ there appears a symmetric pair of non-symmetric unstable periodic orbits. We will not give a rigorous proof of this last assertion, even though it has been checked extensively by simulation. However, for some specific values of the parameter γ, which simplify the computations, see Appendix B, we have rigorously proved the existence of such a pitchfork bifurcation of periodic orbits. Finally, a departure-grazing periodic orbit bifurcation appears for $y_E = y_{DG}(\gamma)$ involving a change in the shape from cloud to lens type of an existing periodic orbit, see Definition 1.15. These above three bifurcation curves are plotted in figures 3.7, 3.8, 3.9 and 3.10 labelled with AG, P and DG respectively.

In the open regions between bifurcation curves on figures 3.7, 3.8, 3.9 and 3.10, we label with $C^{\{l,c\}}_{\{s,u\}}$ when a periodic orbit exists. The subscript stands for its stability character (s =stable, u =unstable) and the superscript does for its shape (l =lens, c =cloud). If the periodic orbit is non-symmetric, it has a companion, so that we add an upper bar to indicate such a pair. We emphasize that in Figure 3.8 there exists a parameter region with four periodic orbits, as a consequence of the pitchfork bifurcation that the system undergoes in the region with $\gamma > 1$, once we have crossed the SN bifurcation.

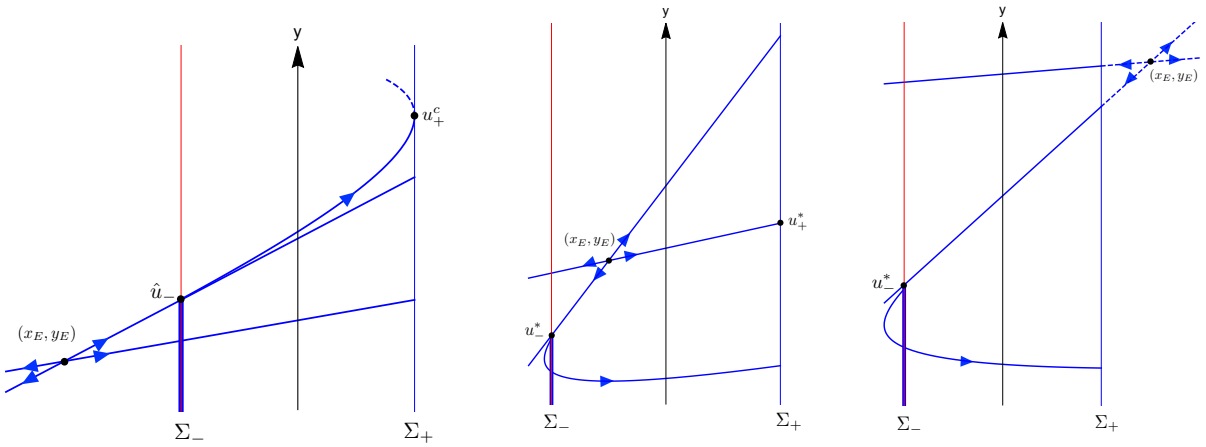

Figure 3.2: The unstable node cases. (a) The real unstable node outside the hysteresis band. (b) The real unstable node inside the hysteresis band. (c) The virtual unstable node. The thicker part of Σ_- corresponds to Σ_-^{ad}.

3.1.2 The unstable node case

Next, we assume that both sub-systems S_U and S_L have an unstable node either real or virtual that is, we assume $\gamma > 1$, see Fig. 3.2. Before giving our next result, we introduce the distinguished point $(-1, u_-^*)$ where the invariant manifold of the S_U-system with bigger slope (corresponding to the lowest eigenvalue) intersects the line Σ_-. A direct computation shows that

$$u_-^* = y_E - (\gamma + 1)(x_E + 1). \tag{3.16}$$

In the cases where there exists a value $\tau_{SN} \in \mathcal{I}$ such that the derivative of the function $\kappa(\tau) = u_+(\tau) + u_-(\tau)$ vanishes, see Lemma 3.13, we get that τ_{SN} is the only solution of equation

$$\rho = \frac{1 + e^{-\gamma\tau}\psi_\gamma(\tau)}{1 + e^{\gamma\tau}\psi_{-\gamma}(\tau)}. \tag{3.17}$$

Using again (3.9), we introduce the function

$$y_{SN}(\gamma) = y_{\text{ref}}(\tau_{SN}, \gamma), \tag{3.18}$$

which is needed to state our next result.

Theorem 3.7 (**Unstable node case**). *Assume that $\gamma > 1$ in system* (3.1) *and consider functions $y_{AG}(\gamma)$, $y_P(\gamma)$, $y_{DG}(\gamma)$ and $y_{SN}(\gamma)$ defined in* (3.10), (3.12), (3.15) *and* (3.18) *respectively. Then, the following statements hold.*

(a) If $x_E \leqslant -1$, then non-symmetric periodic orbits are impossible. Furthermore, for $y_E < y_{AG}(\gamma)$ there are no periodic orbits while for $y_E \geqslant y_{AG}(\gamma)$ there is one symmetric periodic orbit which is unstable.

(b) If $-1 < x_E < 0$, then the following cases arise.

(b1) If $y_E < y_{SN}(\gamma)$, then there are no periodic orbits.

(b2) If $y_E = y_{SN}(\gamma)$, then there is one symmetric periodic orbit which is non hyperbolic.

(b3) f $y_{SN}(\gamma) < y_E < y_P(\gamma)$, then there are two symmetric periodic orbits with opposite stabilities. If $y_E < y_{DG}(\gamma)$, then such periodic orbits are clouds, while for $y_{DG}(\gamma) \leqslant y_E$ one of the periodic orbits changes to a lens type.

(b4) If $y_E = y_P(\gamma)$, then there are one unstable symmetric periodic orbit and one non-hyperbolic symmetric periodic orbit.

(b5) If $y_E > y_P(\gamma)$, then there are two unstable symmetric periodic orbits.

(c) If $x_E \geqslant 0$, then non-symmetric periodic orbits are impossible. Furthermore, if $y_E < y_{SN}(\gamma)$, then there are no periodic orbits; if $y_E = y_{SN}(\gamma)$, then there is one periodic orbit which is non hyperbolic; finally, if $y_E > y_{SN}(\gamma)$, then there are two periodic orbits with opposite stabilities being both of cloud type if $y_E < y_{DG}(\gamma)$ and of different shape if $y_E \geqslant y_{DG}(\gamma)$.

Regarding statement (a) of Theorem 3.7, we conclude that for $y_E = y_{AG}(\gamma)$ the hysteretic system undergoes an arrival-grazing bifurcation of periodic orbits, see Definition 1.14. From statements (b) and (c), we deduce the existence of a departure-grazing periodic orbit bifurcation, see Definition 1.15, and a saddle-node bifurcation of periodic orbits, where two periodic orbits of different stability character collide to disappear. Obviously, such a saddle-node bifurcation, as seen in a reverse sense, can be described by saying that for a critical value of parameters, there appears a non-hyperbolic symmetric periodic orbit giving rise to two different periodic orbits. Also, from statement (b) we deduce the appearance of another bifurcation of periodic orbits, where one of the two existing periodic orbits changes its stability. As in Theorem 3.6, we use the subscript P for this bifurcation, which turns out to be a pitchfork bifurcation of periodic orbits, so that a symmetric pair of non-symmetric stable periodic orbits appears for $y_E > y_P(\gamma)$, see Figure 3.11, leading to a configuration with four different periodic orbits. Accordingly, the different bifurcation curves appear in the bifurcation sets of Figure 3.7, 3.8, 3.9 and 3.10, labelled with AG, SN, DG and P respectively.

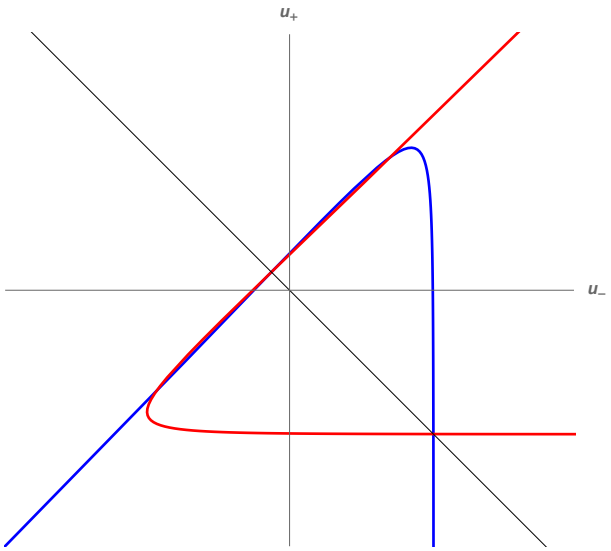

Figure 3.3: The transition map U (in blue) and its symmetrical with respect to the diagonal of the second quadrant (in red). Here we have chosen the parameters $(x_E, y_E) = (-0.65, 2)$ and $\gamma = 1.5$. Each intersection between the two curves represent a periodic orbit. In particular, for these values of the parameters we have four periodic orbits as Theorem 3.7 assures.

3.1.3 The saddle case

Next, we assume that the dynamics of both sub-systems S_U and S_L are of saddle type, that is we take $|\gamma| < 1$, see Figure 3.4. In this case, the point $(-1, u_-^*)$ introduced in (3.16) is the intersection point of the stable manifold with the line Σ_-. Then, apart from the points $(1, u_+^c)$ and $(-1, u_-^c)$ defined in (3.6) and (3.13), an additional distinguished point is introduced. The point $(1, u_+^*)$, where the unstable manifold of the S_U-system intersects the line Σ_+. It is easy to get

$$u_+^* = y_E + (\gamma - 1)(1 - x_E).$$

Also, for $x_E < 1$, which corresponds to the cases sketched in Figures 3.4(a) and 3.4(b), taking into account that

$$g(u_-^*) := \lim_{u \to u_-^*} g(u) = u_+^* + u_-^* = 2(y_E - 1 - \gamma x_E),$$

we introduce the function

$$y_{HT}(\gamma) = 1 + \gamma x_E. \tag{3.19}$$

We are in position to state our main last results, which are more involved than the previous ones and they are splitted into two different theorems.

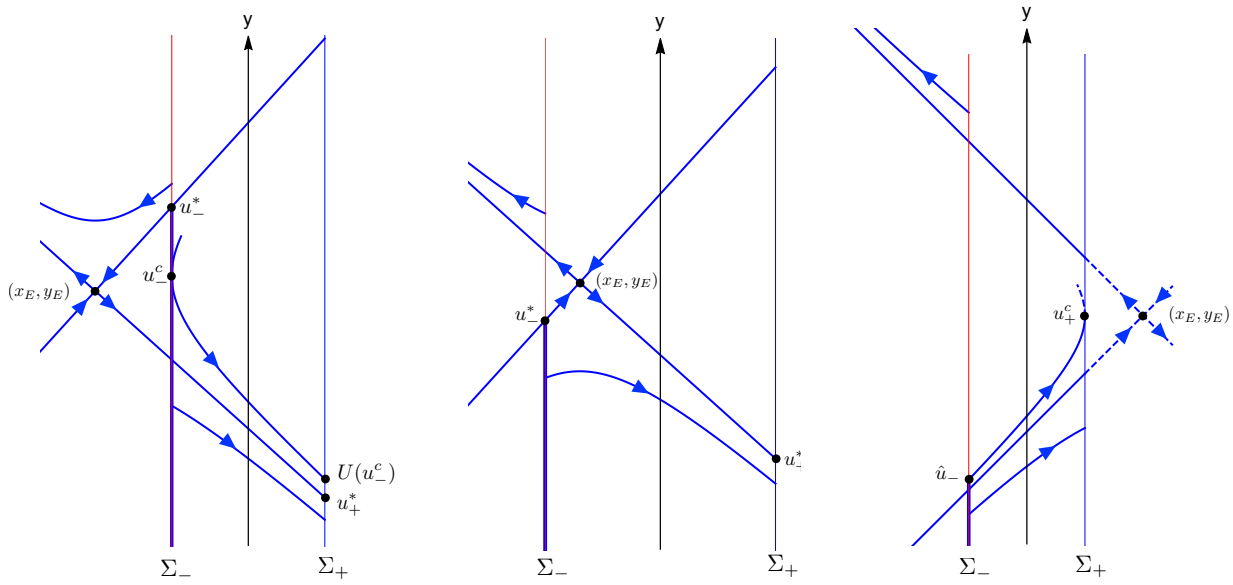

Figure 3.4: The saddle cases. (a) The real saddle outside the hysteresis band. (b) The real saddle inside the hysteresis band. (c) The virtual saddle.

Theorem 3.8 (Saddle outside the hysteresis band). *Assume that* $|\gamma| < 1$ *and* $|x_E| \geqslant 1$ *in system* (3.1)*, and consider functions* $y_{AG}(\gamma)$*,* $y_{DG}(\gamma)$*,* $y_{SN}(\gamma)$ *and* $y_{HT}(\gamma)$*, as defined in* (3.10)*,* (3.15)*,* (3.18) *and* (3.19) *respectively. Then, non-symmetric periodic orbits are impossible and the following statements hold.*

(a) If $x_E < -1$*, then the following cases arise.*

(a1) Consider $-1 < \gamma \leqslant 0$*. If* $y_E = y_{HT}(\gamma)$ *then there exists a double heteroclinic connection, so that for* $y_E < y_{HT}(\gamma)$ *there are no periodic orbits, while for* $y_E > y_{HT}(\gamma)$ *there exists one stable symmetric periodic orbit. Moreover, if* $y_E < y_{DG}(\gamma)$*, then such a symmetric periodic orbit is of cloud type while for* $y_E \geqslant y_{DG}(\gamma)$ *it is of lens type.*

(a2) If $0 < \gamma < 1$*, the following cases arise.*

(a2.1) If $y_E < y_{SN}(\gamma)$*, then there are no periodic orbits.*

(a2.2) If $y_E = y_{SN}(\gamma)$*, then there exists one symmetric periodic orbit which is non-hyperbolic.*

(a2.3) If $y_{SN}(\gamma) < y_E < y_{HT}(\gamma)$*, then there exist two symmetric periodic orbits with opposite stability. Moreover, if* $y_E < y_{DG}(\gamma)$*, then the two existing periodic orbits are of cloud type while for* $y_E \geqslant y_{DG}(\gamma)$ *they are of lens type.*

(a2.4) *If $y_E = y_{HT}(\gamma)$, then there exists a double heteroclinic connection and one symmetric periodic orbit which is stable.*

(a2.5) *If $y_E > y_{HT}(\gamma)$, then there exists one stable symmetric periodic orbit.*

(b) *If $x_E > 1$, then for $y_E < y_{AG}(\gamma)$ there are no periodic orbits at all, while for $y_E \geqslant y_{AG}(\gamma)$ there is only one periodic orbit which is unstable.*

(c) *Consider $|x_E| = 1$. If $y_E = y_{HT}(\gamma)$ then there exists a double heteroclinic connection, so that for $y_E < y_{HT}(\gamma)$ there are no periodic orbits, while for $y_E > y_{HT}(\gamma)$ there exists one stable symmetric periodic orbit.*

When the saddle is inside the hysteresis band, homoclinic orbits are possible. Thus, if there exists an orbit of the upper system that joins the intersection points of the invariant manifolds of the lower saddle, we have an homoclinic connection. Such a closed curve is non-symmetric and so it will have a companion homoclinic connection associated to the upper saddle, see Figure 3.6(b).

Computing the invariant manifolds of the lower saddle, we get that

$$\begin{aligned} u_L &= -y_E + (\gamma - 1)(x_E - 1), \\ u_R &= -y_E + (\gamma + 1)(x_E + 1). \end{aligned} \tag{3.20}$$

are the ordinates of their intersection points with Σ_- and Σ_+ respectively. Imposing the existence of the above connection, see the details in Section 3.2, we get that the flight time τ_H of the orbit is the positive solution of the equation

$$\rho = \mu(\tau) := \frac{e^{-\gamma\tau} - e^{-\tau}}{e^{-\tau} - e^{\gamma\tau}}, \tag{3.21}$$

which exists only for $\gamma x_E \leqslant 0$. This determines, by using (3.9), the function

$$y_H(\gamma) = y_{\text{ref}}(\tau_H, \gamma), \tag{3.22}$$

which plays an important role in our last result.

Theorem 3.9 (**Saddle inside the hysteresis band**). *Assume that $|\gamma| < 1$ and $|x_E| < 1$ in system* (3.1) *and consider functions $y_P(\gamma)$, $y_{SN}(\gamma)$, $y_{HT}(\gamma)$ and $y_H(\gamma)$, as defined in* (3.12), (3.18), (3.19) *and* (3.22) *respectively. Then, the following statements hold.*

(a) *If $\gamma = x_E = 0$, then for $y_E < 1$ there are no closed orbits; for $y_E = 1$ there appears a symmetric heteroclinic orbit; and for $y_E > 1$ there exists a bounded continuum of periodic orbits ending in a symmetric pair of homoclinic connections.*

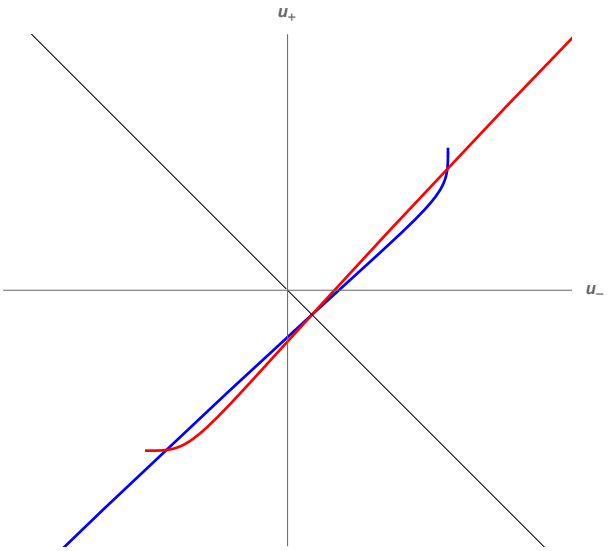

Figure 3.5: The transition map U (in blue) and its symmetrical with respect to the diagonal of the second quadrant (in red). Here we have chosen the parameters $(x_E, y_E) = (-0.65, 1.5)$ and $\gamma = 0.6$. Each intersection between the two curves represent a periodic orbit. In particular, for these values of the parameters we have three periodic orbits as Theorem 3.9 assures.

(b) When $|\gamma| + |x_E| \neq 0$, regarding symmetric periodic orbits, the following cases arise.

(b.1) If $y_E < y_{HT}(\gamma)$, then there are no periodic orbits.

(b.2) If $y_E = y_{HT}(\gamma)$, then there exists one double heteroclinic connection.

(b.3) If $y_E > y_{HT}(\gamma)$, then there exists one symmetric periodic orbit. Moreover, if $\gamma x_E \geqslant 0$, then such a periodic orbit is stable when $\gamma + x_E < 0$ and unstable when $\gamma + x_E > 0$. If $\gamma x_E < 0$, then the stability of this orbit is related to the function $y_P(\gamma)$, namely

(i) if $-1 < x_E < 0$ then the existing periodic orbit is unstable for $y_E < y_P(\gamma)$, non-hyperbolic for $y_E = y_P(\gamma)$ and stable for $y_E > y_P(\gamma)$.

(ii) if $0 < x_E < 1$ then the periodic orbit is stable for $y_E < y_P(\gamma)$, non-hyperbolic for $y_E = y_P(\gamma)$ and unstable for $y_E > y_P(\gamma)$.

(c) When $|\gamma| + |x_E| \neq 0$, there exists a symmetric pair of non-symmetric homoclinic connections for all the values of γ between 0 and $-x_E$ and $y_E = y_H(\gamma)$. The graph of $y_E = y_H(\gamma)$ has the vertical asymptote at $\gamma = -x_E$.

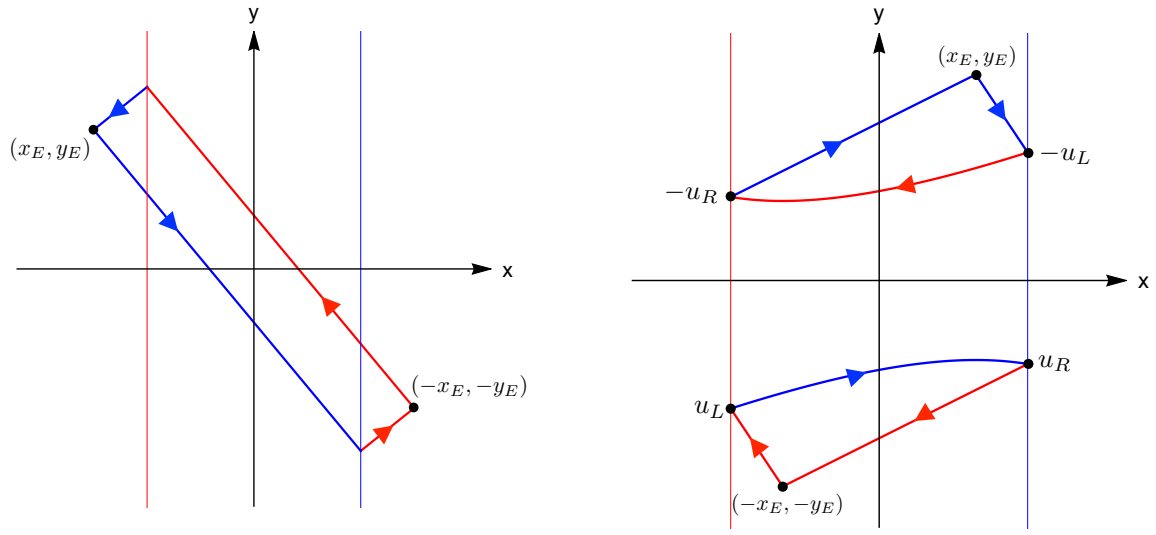

(a) (b)

Figure 3.6: (a) The double heteroclinic connection. (b) The two homoclinic connections. As before, lines in blue correspond to orbits of the S_U system, while lines in red correspond to orbits of the S_L system. The points u_L and u_R are defined in (3.20).

Regarding theorems 3.8 and 3.9, we detect some bifurcation curves. First, the line $y_E = y_{HT}(\gamma)$ denotes a double heteroclinic connection, associated to the generation or annihilation of a symmetric periodic orbit. Second, the line $y_E = y_{SN}(\gamma)$, indicates for $x_E < -1$ a saddle-node bifurcation of periodic orbits. Third, there appear a curve $y_E = y_H(\gamma)$ for $|x_E| < 1$, where we have a pair of homoclinic connections. Fourth, the lines $y_{AG}(\gamma)$ and $y_{DG}(\gamma)$ represent, when $x_E > 1$ an arrival-grazing bifurcation of periodic orbits and when $x_E < -1$ a departure-grazing periodic orbit bifurcation, respectively. Finally, for $y_E = y_P(\gamma)$ and $|x_E| < 1$, there appears a stability change in a symmetric periodic orbit which is associated to a pitchfork bifurcation of periodic orbits as in the node cases. All these bifurcation curves are labelled with HT, SN, H, AG, DG and P in figures 3.7, 3.8 and 3.9, 3.10.

3.1.4 An illustrative example

We show the usefulness of the obtained results by considering an illustrative example. It is well known that assure the existence of periodic orbits in tridimensional piecewise linear systems is a difficult issue. We will detect some periodic orbits, when the relaxation hypothesis can be assumed for a family of

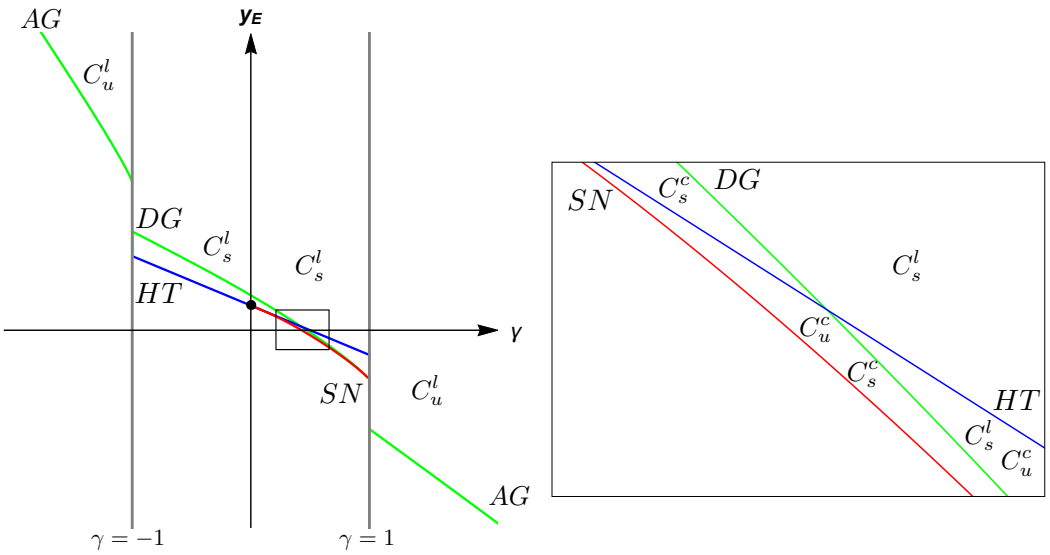

Figure 3.7: The bifurcation set for $x_E \leqslant -1$. We label the bifurcation curves and the open regions with different periodic orbits as explained in the text. In the right panel, a magnification of the square in the left panel is shown.

3D piecewise linear systems.

Using equations (1.6)-(1.7) in Chapter 1 with $m = 1$, function $\varphi(z)$ as in (1.2), and $x_0 = 1$, $z_0 = 1/c$, we obtain that the system

$$\begin{cases} \dot{x} = (2\gamma + \beta_1)x - y + \beta_1 z, \\ \dot{y} = (\gamma^2 - 1 + \beta_2)x + \beta_2 z, \\ \dot{z} = \dfrac{1}{\varepsilon}[-x + \varphi(z)], \end{cases} \tag{3.23}$$

leads, by the relaxation hypothesis, to system (3.1) for

$$x_E = -\frac{\beta_2}{\gamma^2 - 1}\frac{1+c}{c}, \quad y_E = \frac{1+c}{c}\left(\beta_1 - \frac{2\gamma\beta_2}{\gamma^2 - 1}\right).$$

Taking now $\beta_1 = 2.63333$, $\beta_2 = 0.541667$, $\gamma = 1.5$ and $c = 2$, we obtain that $x_E = -0.65$ and $y_E = 2$ in system (3.1), and so Theorem 3.7 guarantees the existence of a pair of stable non-symmetric periodic orbits and two unstable symmetric periodic orbits. Following a similar idea to the approach appearing in [19], we can expect for system (3.23) the existence of a pair of non-symmetric periodic orbits, if ε is sufficiently small. Effectively, if we simulate system (3.23) for the corresponding values of the parameters given before, then we detect two stable periodic orbits, which is in agreement with the results obtained for the hysteretic system, see figures 3.11 and 3.12.

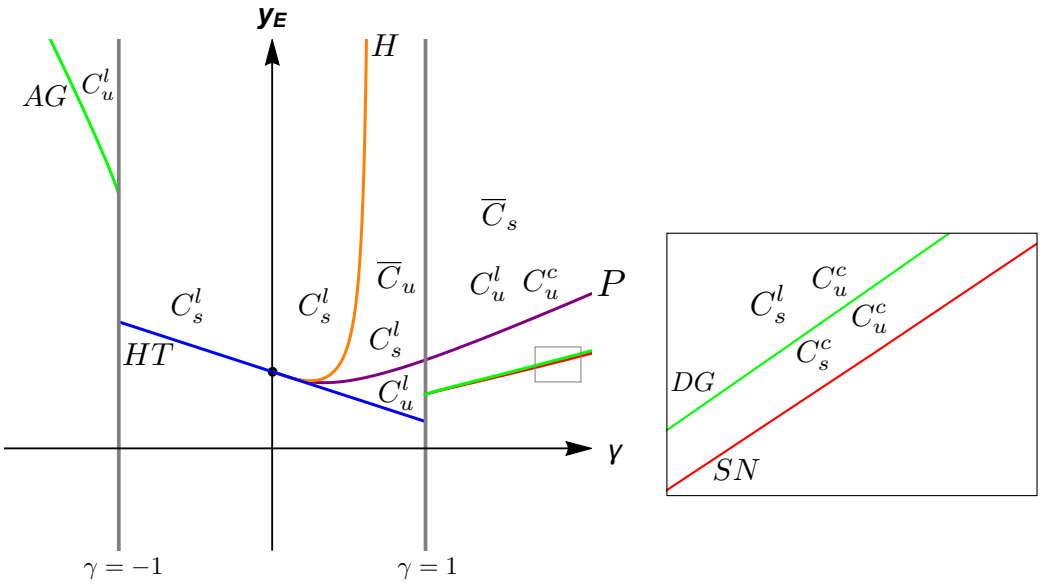

Figure 3.8: The bifurcation set for $-1 < x_E < 0$. We label the bifurcation curves and the open regions with different periodic orbits as explained in the text. In the right panel, a magnification of the square in the left panel is shown.

3.2 Proof of the main results

In this section we start by giving some results regarding the properties of the previously introduced functions $U(u)$, $g(u)$, $\kappa(\tau)$ and $\eta(\tau)$, which are of relevance in the analysis of existence and stability of periodic orbits. Next, we include the proofs of main theorems in the spirit of looking for the conditions that guarantee the different bifurcations. Using the quoted functions we translate our problem in hysteretic system to a standard problem in smooth bifurcation theory, see [15], [25] or [28].

Direct computations show that the two first derivatives of functions $u_-(\tau)$ and $u_+(\tau)$ defined in (3.4) are

$$\begin{aligned} u'_-(\tau) &= \frac{(x_E+1)-(x_E-1)e^{-\gamma\tau}\psi_\gamma(\tau)}{\mathrm{sh}^2\tau}, \\ u'_+(\tau) &= -\frac{(x_E-1)-(x_E+1)e^{\gamma\tau}\psi_{-\gamma}(\tau)}{\mathrm{sh}^2\tau}, \end{aligned} \tag{3.24}$$

and

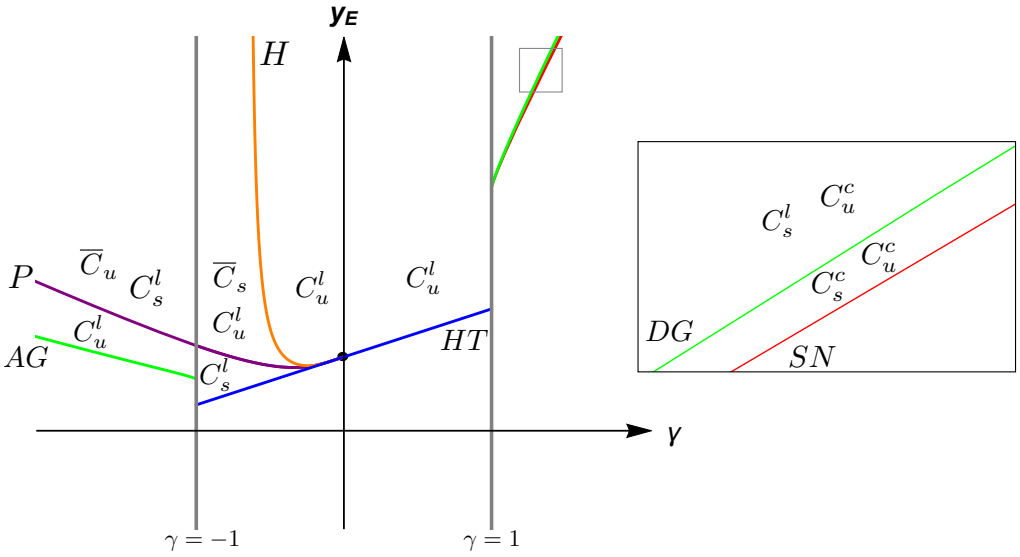

Figure 3.9: The bifurcation set for $0 < x_E < 1$. The different labels are explained in the text. In the right panel, a magnification of the square in the left panel is shown.

$$u''_-(\tau) = \frac{(x_E-1)e^{-\gamma\tau}[1+\psi_\gamma(\tau)^2] - 2(x_E+1)\mathrm{ch}\tau}{\mathrm{sh}^3\tau},$$
$$u''_+(\tau) = \frac{2(x_E-1)\mathrm{ch}\tau - (x_E+1)e^{\gamma\tau}[1+\psi_{-\gamma}(\tau)^2]}{\mathrm{sh}^3\tau}. \tag{3.25}$$

We start by giving some properties of the parametrization of the transition map U and the functions η and κ defined in (1.23).

Lemma 3.10. *If either $\gamma^2 = 1$ or $\gamma = x_E = 0$ in system (3.1), then the functions $u_\pm$ satisfy the equality $u_+(\tau) = u_-(\tau)$.*

If $\gamma^2 \neq 1$ or $|\gamma| + |x_E| \neq 0$, then the following properties hold for $\tau > 0$.

(a) If $|x_E| \leqslant 1$ and $\gamma \geqslant -1$ or $(1-x_E)(1-\gamma^2) \geqslant 0$, then $u'_-(\tau) > 0$.

(b) If $(1-x_E)(1-\gamma^2) < 0$ and there exists a value τ_M such that $u'_-(\tau_M) = 0$, then $u'_-(\tau) > 0$ for all $\tau \in (0, \tau_M)$.

(c) Under hypotheses of statements (a) or (b), there exists $\varepsilon > 0$ such that $\kappa'(\tau) > 0$ for $\tau \in (0, \varepsilon)$.

Proof. The first assertion about the cases $\gamma^2 = 1$ or $\gamma = x_E = 0$ is direct.

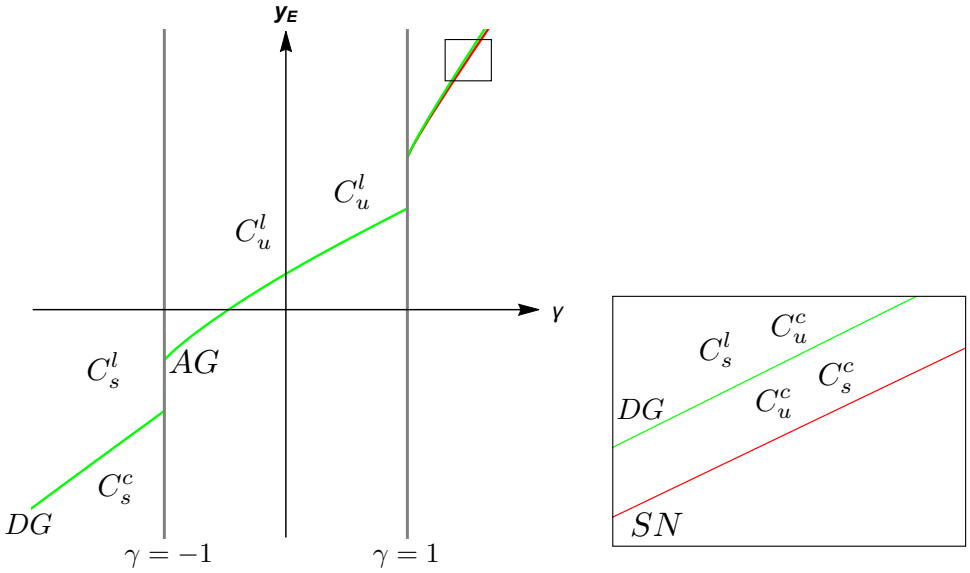

Figure 3.10: The bifurcation set for $x_E \geqslant 1$. The different labels are explained in the text. In the right panel, a magnification of the square in the left panel is shown.

Regarding the remaining cases, from (3.24), we get

$$\operatorname{sign} u'_-(\tau) = \operatorname{sign} f(\tau),$$

where

$$f(\tau) = (x_E + 1) - (x_E - 1)e^{-\gamma\tau}\psi_\gamma(\tau),$$

and

$$f(0) = 2, \quad f'(\tau) = (1 - x_E)(1 - \gamma^2)e^{-\gamma\tau}\mathrm{sh}\tau.$$

Considering now statement (a), if $|x_E| \leqslant 1$ and $\gamma \geqslant -1$, the conclusion follows. If $(1 - x_E)(1 - \gamma^2) = 0$, then $x_E = 1$ so that $u'_-(\tau) > 0$. If the condition $(1 - x_E)(1 - \gamma^2) > 0$ holds, then $f'(\tau) > 0$, which implies $f(\tau) > 0$, and so $u'_-(\tau) > 0$ and statement (a) is shown.

Regarding statement (b), if $(1 - x_E)(1 - \gamma^2) < 0$ then $f'(\tau) < 0$. Taking into account that $f(0) = 2$ and $f(\tau_M) = 0$, we conclude that $f(\tau) > 0$ and consequently $u'_-(\tau) > 0$ for $0 < \tau < \tau_M$. Statement (b) follows.

To prove statement (c), from Lemma 3.4 we obtain

$$\lim_{u\to-\infty} U'(u) = \lim_{u\to-\infty} \frac{dU}{du} = \lim_{\tau\to 0^+} \frac{u'_+(\tau)}{u'_-(\tau)} = 1,$$

so that under the hypotheses of statements (a) or (b), there exists a value $\varepsilon > 0$ such that for $\tau \in (0, \varepsilon)$, we have $u'_-(\tau) > 0$ and $\operatorname{sign} u'_+(\tau) = \operatorname{sign} u'_-(\tau)$. Then, statement (c) follows and the proof is complete.

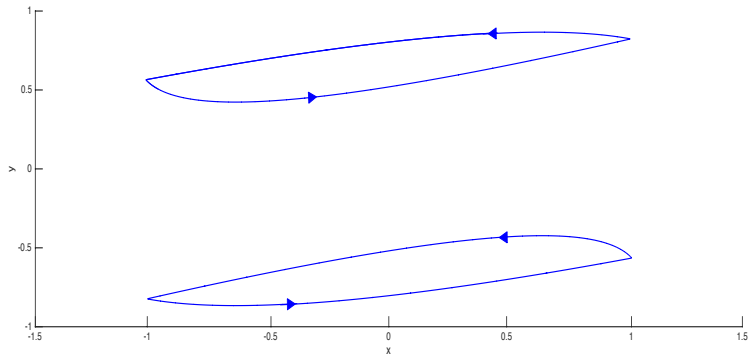

Figure 3.11: The stable non-symmetric periodic orbits of hysteretic system (3.1) for $x_E = -0.65$, $y_E = 2$ and $\gamma = 1.5$. These values of the parameters correspond to the region above the line $y_P(\gamma)$, for $\gamma > 1$, showed in Figure 3.8.

□

Lemma 3.11. *The following statements hold for the function $g(u)$ given in (3.8) and u belonging to its domain.*

(a) If $\gamma > 1$ and $x_E \geqslant 0$, then $g''(u) < 0$.

(b) If $0 < \gamma < 1$ and $x_E \leqslant -1$, then $g''(u) < 0$.

Proof. From Lemma 3.10, $u'_-(\tau) > 0$ and by computing the derivative

$$\frac{d}{d\tau}\left(\frac{dU}{du_-}\right) = \frac{d^2U}{du_-^2}\frac{du_-}{d\tau} = \frac{d}{d\tau}\left(\frac{u'_+(\tau)}{u'_-(\tau)}\right)$$

we get

$$\operatorname{sign}\frac{d^2g}{du_-^2} = \operatorname{sign}\frac{d^2U}{du_-^2} = \operatorname{sign}\left(\frac{d}{d\tau}\left(\frac{u'_+(\tau)}{u'_-(\tau)}\right)\right).$$

In the specific case $x_E = 1$ we get

$$\operatorname{sign} g''(u) = \operatorname{sign}(1-\gamma^2), \tag{3.26}$$

while for $x_E \neq 1$ using (3.25), we get

$$\frac{d}{d\tau}\left(\frac{u'_+(\tau)}{u'_-(\tau)}\right) = \frac{(1-\gamma^2)e^{\gamma\tau}h(\rho)\operatorname{sh}\tau}{[\rho e^{\gamma\tau} - \psi_\gamma(\tau)]^2},$$

and then

$$\operatorname{sign}\frac{d^2g}{du_-^2} = \operatorname{sign}[(1-\gamma^2)h(\rho)] \tag{3.27}$$

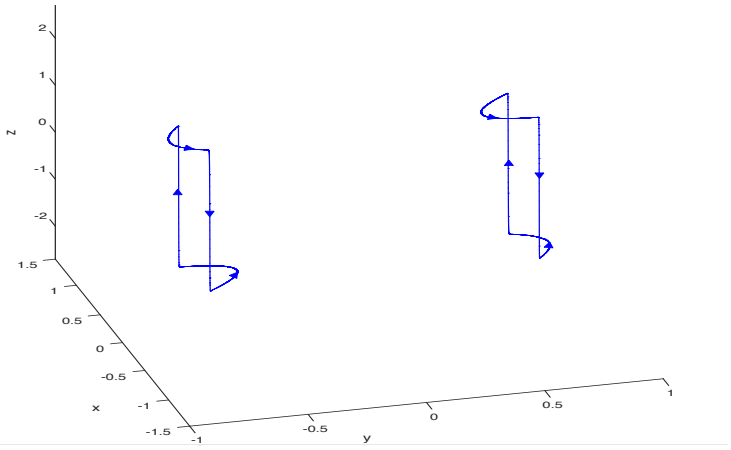

Figure 3.12: The corresponding periodic orbits for the 3D continuous piecewise linear system (3.23) for $\beta_1 = 2.63333$, $\beta_2 = 0.541667$, $c = 2$, $\gamma = 1.5$ and $\varepsilon = 0.001$.

where $h(\rho) = \rho^2 e^{2\gamma\tau} - 2\gamma\rho e^{\gamma\tau}\mathrm{sh}\tau - 1$ is a quadratic function in the variable ρ. If $x_E = -1$, then $\rho = 0$ and the conclusion follows. For $x_E \neq -1$, the function h vanishes at two values $\rho^- < 0 < \rho^+$ such that $h(\rho) < 0$ for $\rho \in (\rho^-, \rho^+)$ and $h(\rho) \geqslant 0$ otherwise. In addition,

$$\begin{aligned} &h(0) = -1, \\ &\operatorname{sign} h(-1) = \operatorname{sign}[\mathrm{sh}(\gamma\tau) + \gamma\mathrm{sh}\tau] = \operatorname{sign}(\gamma), \\ &\operatorname{sign} h(1) = \operatorname{sign}[\mathrm{sh}(\gamma\tau) - \gamma\mathrm{sh}\tau] = \operatorname{sign}[\gamma(\gamma^2 - 1)]. \end{aligned} \tag{3.28}$$

Regarding statement (a), if $x_E = 1$, we get from (3.26) that $g''(u) < 0$. When $x_E \neq 1$, from (3.28) we obtain

$$-1 < \rho^- < \rho^+ < 1,$$

and then $h(\rho) > 0$ for $\rho \in (-\infty, -1) \cup (1, \infty)$ or, according to the definition of ρ in (1.24), $h(\rho) > 0$ for $x_E \in (0, 1) \cup (1, \infty)$. Thus, from (3.27) we get $g''(u) < 0$ and statement (a) is shown.

Assuming now that $x_E < -1$ and $0 < \gamma < 1$, then from (3.28) we obtain

$$-1 < \rho^- < 1 < \rho^+,$$

and so $h(\rho) < 0$ for $\rho \in (0, 1)$, or equivalently, $h(\rho) < 0$ for $x_E < -1$. Then, from (3.27) we get $g''(u) < 0$ and statement (b) is shown.

□

Lemma 3.12. *Consider system* (3.1) *with* $\gamma^2 \neq 1$. *Then, there exists a value* τ_{DG} *for the flight time such that* $u_-(\tau_{DG}) = u_-^c$ *with* $x'' > 0$ *at the point* $(-1, u_-^c)$ *when one of the following statements holds*

(a) *If* $x_E = 1$ *and* $\gamma > 1$. *Furthermore, in this case we have that the value* $\tanh(\tau_{DG}) = 1/\gamma$ *and the derivative* $u'_+(\tau_{DG}) = 0$.

(b) *If* $x_E \neq 1$, *then the condition* $u_-(\tau_{DG}) = u^c_-$ *is equivalent to the equation*

$$\rho = \omega(\tau) := \frac{-e^{-\gamma\tau}}{\mathrm{ch}\tau - \gamma\mathrm{sh}\tau}. \tag{3.29}$$

The above equation has a unique solution $\tau = \tau_{DG}$ *only in the following three cases.*

(i) If $|\gamma| < 1$ *and* $x_E < -1$.

(ii) If $|\gamma| > 1$ *and* $x_E > 1$.

(iii) If $\gamma > 1$ *and* $|x_E| < 1$.

Furthermore, $u'_+(\tau_{DG}) = 0$.

Proof. Let us study when the derivative x'' at the contact point $(-1, u^c_-)$ is positive. The quoted derivative x'' is given by

$$x''|_{(-1,u^c_-)} = (\gamma^2 - 1)(1 + x_E),$$

which is positive only if either $x_E > -1$ with $|\gamma| > 1$ or $x_E < -1$ with $|\gamma| < 1$. The case where $-1 < x_E \leqslant 1$ with $\gamma < -1$ must be excluded because the orbit starting at the point $(-1, u^c_-)$ does not arrive at the falling line Σ_+. Thus, the existence of the value τ_{DG} is guaranteed in the stated cases. By definition, $u_+(\tau_{DG})$ is the maximum value of the image of the transition map U, so that any orbit of the upper system arrives at a point of the line Σ_+ satisfying $u_+ \leqslant u_+(\tau_{DG})$, then $u'_+(\tau_{DG}) = 0$.

If $x_E = 1$, then the condition $u_-(\tau) = u^c_-$ implies $\tanh(\tau_{DG}) = 1/\gamma$. If $x_E \neq 1$, imposing the condition $u_-(\tau) = u^c_-$ we get

$$y_E + \frac{(x_E - 1)e^{-\gamma\tau} - (x_E + 1)(\mathrm{ch}\tau + \gamma\mathrm{sh}\tau)}{\mathrm{sh}\tau} = y_E - 2\gamma(1 + x_E).$$

Taking into account the definition of the parameter ρ in (1.24), equation (3.29) follows.

□

Lemma 3.13. *Assuming* $\gamma^2 \neq 1$, *the following statements hold for function* $\kappa'(\tau) = u'_+(\tau) + u'_-(\tau)$.

(a) *If* $|\gamma| < 1$ *and either* $|x_E| \leq 1$ *or* $\gamma x_E > 0$, *then* $\kappa'(\tau) > 0$ *for all* $\tau \in \mathcal{I}$.

(b) If $x_E = 1$, then the condition $\kappa'(\tau) = 0$ is equivalent to the equation

$$\nu(\tau) := 1 + e^{\gamma\tau}\psi_{-\gamma}(\tau) = 0, \tag{3.30}$$

and it has a (unique) solution $\tau = \tau_{SN}$ only if $\gamma > 1$. Furthermore, $\operatorname{sign}\kappa'(\tau) = \operatorname{sign}(\tau_{SN} - \tau)$.

(c) If $x_E \neq 1$, then the condition $\kappa'(\tau) = 0$ is equivalent to the equation

$$\rho = \alpha(\tau) := \frac{1 + e^{-\gamma\tau}\psi_{\gamma}(\tau)}{1 + e^{\gamma\tau}\psi_{-\gamma}(\tau)}. \tag{3.31}$$

The above equation has a (unique) solution $\tau = \tau_{SN}$ only in the following four cases.

(i) If $\gamma > 1$ and $x_E > -1$.

(ii) If $0 < \gamma < 1$ and $x_E < -1$.

(iii) If $-1 < \gamma < 0$ and $x_E > 1$.

(iv) If $\gamma < -1$ and $x_E < 1$.

Furthermore, $\operatorname{sign}\kappa'(\tau) = \operatorname{sign}(\tau_{SN} - \tau)$.

Proof. Introducing the functions

$$h_1(\tau) = (x_E + 1)[1 + e^{\gamma\tau}\psi_{-\gamma}(\tau)], \quad h_2(\tau) = (x_E - 1)[1 + e^{-\gamma\tau}\psi_{\gamma}(\tau)],$$

from the derivatives (3.24) we get

$$\kappa'(\tau) = \frac{h_1(\tau) - h_2(\tau)}{\operatorname{sh}^2\tau}.$$

Next, we study the sign of the derivative of the function $h(\tau) = h_1(\tau) - h_2(\tau)$, where

$$h'(\tau) = (1 - \gamma^2)\operatorname{sh}\tau[(x_E + 1)e^{\gamma\tau} - (x_E - 1)e^{-\gamma\tau}]$$

or equivalently,

$$h'(\tau) = 2(1 - \gamma^2)\operatorname{sh}\tau[\operatorname{ch}(\gamma\tau) + x_E\operatorname{sh}(\gamma\tau)].$$

For $\gamma = 0$, we get $h'(\tau) = 2\operatorname{sh}\tau > 0$. When either $|x_E| \leq 1$, or $\gamma x_E > 0$ we have $\operatorname{sign} h'(\tau) = \operatorname{sign}(1 - \gamma^2)$. Then, since $h(0) = 4$, statement (a) follows.

Regarding the remaining statements, it is easy to see that the condition $\kappa'(\tau) = 0$ is equivalent to (3.30) if $x_E = 1$ and to equation (3.31) otherwise.

If $x_E = 1$, we study the solutions of equation (3.30). We get, after some computations that

$$\nu(\tau) = 1 + \frac{e^{\gamma\tau}}{2}[(1-\gamma)e^{\tau} + (1+\gamma)e^{-\tau}].$$

When $\gamma < 1$, then $\nu(\tau) > 0$ for all τ. Since $\nu'(\tau) = (1-\gamma^2)\mathrm{sh}\tau e^{\gamma\tau}$, $\nu(0) = 2$, and for $\gamma > 1$ we have $\nu(\tau) \to -\infty$ when $\tau \to \infty$, we conclude that $\nu(\tau)$ only vanishes at some value $\tau = \tau_{SN}$ when $\gamma > 1$. Statement (b) is shown.

If $x_E \neq 1$, we study the existence of solutions for equation (3.31) by analyzing the properties of function α. First, note that $\alpha(0) = 1$ for all γ. When $\gamma = 0$, the function α is constant, so that $\alpha(\tau) \equiv 1$.

Observe also that the function $\alpha(\tau)$ is not defined when its denominator

$$\nu(\tau) = 1 + e^{\gamma\tau}\psi_{-\gamma}(\tau)$$

vanishes. From the proof of statement (b), we obtain that the denominator of $\alpha(\tau)$ only vanishes if $\gamma > 1$ at some point, say $\tau = \hat{\tau}$.

The derivative of function $\alpha(\tau)$ is

$$\alpha'(\tau) = \frac{2(\gamma^2-1)\mathrm{sh}\tau[\mathrm{sh}(\gamma\tau) + \gamma\mathrm{sh}\tau]}{[1 + e^{\gamma\tau}\psi_{-\gamma}(\tau)]^2},$$

and so $\operatorname{sign}\alpha'(\tau) = \operatorname{sign}[\gamma(\gamma^2-1)]$.

When $\gamma > 1$, we have

$$\lim_{\tau\to\widehat{\tau}^-} \alpha(\tau) = \infty, \quad \lim_{\tau\to\widehat{\tau}^+} \alpha(\tau) = -\infty, \quad \lim_{\tau\to\infty} \alpha(\tau) = 0.$$

For $\gamma < 1$, we have

$$\lim_{\tau\to\infty} \alpha(\tau) = \begin{cases} -\infty, & \text{if} \quad \gamma < -1, \\ +\infty, & \text{if} \quad -1 < \gamma < 0, \\ 0, & \text{if} \quad 0 < \gamma < 1, \end{cases}$$

To conclude the proof, we take into account the definition of ρ in (1.24) and analyze the four cases of statement (c), once we know the sign of the derivative $\alpha'(\tau)$.

(i) If $\gamma > 1$ then the function α is increasing and takes values in the set $(1,\infty) \cup (-\infty, 0)$. Hence equation (3.31) only has solutions when the parameter $\rho \in (1,\infty) \cup (-\infty, 0)$ that is, when $x_E > -1$.

(ii) If $0 < \gamma < 1$ then the function α is decreasing and satisfies $0 < \alpha(\tau) < 1$. Hence equation (3.31) has solutions only when $0 < \rho < 1$ that is, when $x_E < -1$.

(iii) If $-1 < \gamma < 0$ then the function α is increasing and satisfies $1 < \alpha(\tau) < \infty$. Hence equation (3.31) has solutions only when $1 < \rho < \infty$ that is, when $x_E > 1$.

(iv) If $\gamma < -1$ then the function α is decreasing and satisfies $-\infty < \alpha(\tau) < 1$. Hence equation (3.31) has solutions only when $-\infty < \rho < 1$ that is, when $x_E < 1$.

Statement (c) is shown and the proof is complete.

□

Lemma 3.14. *Assuming $\gamma^2 \neq 1$, the following statements hold for the function $\eta'(\tau) = u'_+(\tau) - u'_-(\tau)$.*

(a) If either $|x_E| \geqslant 1$ or $\gamma x_E \geqslant 0$ with $x_E \neq 0$, then $\operatorname{sign}\eta'(\tau) = \operatorname{sign}[(1-\gamma^2)x_E]$.

(b) If $x_E = 0$, then $\operatorname{sign}\eta'(\tau) = \operatorname{sign}[\gamma(1-\gamma^2)]$.

(c) If $x_E \neq 1$, then the condition $\eta'(\tau) = 0$ is equivalent to the equation

$$\rho = \delta(\tau) := \frac{1 - e^{-\gamma\tau}\psi_\gamma(\tau)}{-1 + e^{\gamma\tau}\psi_{-\gamma}(\tau)}, \tag{3.32}$$

which has a (unique) solution $\tau = \tau_P$ if the two conditions $|x_E| < 1$ and $\gamma x_E < 0$ hold. Furthermore,

$$\operatorname{sign}\eta'(\tau) = \operatorname{sign}[(\gamma^2 - 1)(\tau - \tau_P)x_E].$$

Proof. Introducing the new functions

$$h_1(\tau) = (x_E - 1)[-1 + e^{-\gamma\tau}\psi_\gamma(\tau)], \quad h_2(\tau) = (x_E + 1)[-1 + e^{\gamma\tau}\psi_{-\gamma}(\tau)],$$

from the derivatives (3.24) we get

$$\eta'(\tau) = \frac{h_1(\tau) + h_2(\tau)}{\operatorname{sh}^2\tau}.$$

Next, we study the sign of the derivative of the function $h(\tau) = h_1(\tau) + h_2(\tau)$, obtaining

$$\begin{aligned} h'(\tau) &= (1-\gamma^2)\operatorname{sh}\tau[(x_E - 1)e^{-\gamma\tau} + (x_E + 1)e^{\gamma\tau}] \\ &= 2(1-\gamma^2)\operatorname{sh}\tau[x_E\operatorname{ch}(\gamma\tau) + \operatorname{sh}(\gamma\tau)]. \end{aligned}$$

If $|x_E| \geqslant 1$ or $\gamma x_E \geqslant 0$ with $x_E \neq 0$, we obtain $\operatorname{sign} h'(\tau) = \operatorname{sign}[(1-\gamma^2)x_E]$, and statement (a) follows.

If $x_E = 0$, then $\operatorname{sign} h'(\tau) = \operatorname{sign}[\gamma(1-\gamma^2)]$. Since $h(0) = 0$, statement (b) is shown.

Regarding statement (c), it is direct to see that the condition $\eta'(\tau) = 0$ is equivalent to equation (3.32). Next, we study the existence of solutions for equation (3.32), under the assumptions $|x_E| < 1$ and $\gamma x_E < 0$.

First, note that the denominator of the function $\delta(\tau)$ only vanishes at $\tau = 0$. Since the function δ satisfies

$$\lim_{\tau\to 0}\delta(\tau) = -1, \quad \lim_{\tau\to\infty}\delta(\tau) = \begin{cases} -\infty, & \text{if} \quad \gamma < 0, \\ -1, & \text{if} \quad \gamma = 0, \\ 0, & \text{if} \quad \gamma > 0, \end{cases}$$

and its derivative

$$\delta'(\tau) = \frac{2(\gamma^2-1)\mathrm{sh}\tau(\mathrm{sh}\gamma\tau - \gamma\mathrm{sh}\tau)}{[-1+e^{\gamma\tau}\psi_{-\gamma}(\tau)]^2}$$

does not vanishes, we get $\operatorname{sign}\delta'(\tau) = \operatorname{sign}(\gamma)$. To conclude the proof, we take into account the definition of ρ given in (1.24) and use the sign of $\delta'(\tau)$ to analyze the following cases.

(i) If $\gamma > 0$ then the function δ is monotone increasing with $-1 < \delta(\tau) < 0$. Hence equation (3.32) has solutions only when $-1 < \rho < 0$, that is when $-1 < x_E < 0$.

(ii) If $\gamma = 0$ then the $\delta(\tau) = -1$. Hence equation (3.32) has solutions only when and $\rho = -1$, that is when $x_E = 0$.

(iii) If $\gamma < 0$ then the function δ is monotone decreasing with $-\infty < \delta(\tau) < -1$. Hence equation (3.32) has only solutions when $-\infty < \rho < -1$, that is $0 < x_E < 1$.

In these cases, equation (3.32) has a unique positive solution τ_P. Furthermore, the function $h(\tau) = h_1(\tau) + h_2(\tau)$, satisfies $h(0) = h'(0) = 0$ and $h''(0) = 2(1-\gamma^2)x_E$, so we can conclude that $\eta'(\tau_P) = 0$ and

$$\operatorname{sign}\eta'(\tau) = \begin{cases} \operatorname{sign}[(1-\gamma^2)x_E] \text{ for } 0 < \tau < \tau_P, \\ \\ \operatorname{sign}[(\gamma^2-1)x_E] \text{ for } \tau_P < \tau. \end{cases}$$

Statement (c) is shown and the proof is complete. □

3.2.1 Proof of Theorem 3.6

When $x_E < 1$, (the real node cases), the admissible domain for the map T_U is the set

$$\Sigma_-^{\rm ad} = \left\{(-1, u_-) : u_- \leqslant U^{-1}(u_+^c) = \hat{u}_-\right\},$$

where the point $(1, u_+^c)$ is introduced in (3.6). Then, the map $g(u)$ is defined for $u \leqslant \hat{u}_- = u_-(\tau_M)$ and the parameter τ belongs to the interval $(0, \tau_M]$, see Lemma 3.5.

(a) If $x_E \leqslant 0$, then $\gamma x_E \geqslant 0$ and from Proposition 3.2, only symmetric periodic orbits are possible. From lemmas 3.5 and 3.10(b), there exists $\tau_M > 0$ such that $u'_-(\tau) > 0$ for $\tau \in (0, \tau_M)$. Thus, from Lemma 3.14(a) or (b) we get $\eta'(\tau) > 0$ and consequently $U'(u) > 1$. Then, the derivative $g'(u) = U'(u) + 1 > 2$, and so the function g is increasing and it has at most one zero. Note that

$$\lim_{u\to-\infty} g(u) = -\infty, \quad g(u) \leqslant g(\hat{u}_-) = 2(y_E - y_{AG}(\gamma)),$$

where we have used (3.8) and (3.10). According to the value of y_E, different cases arise.

(*i*) If $y_E < y_{AG}(\gamma)$, then the function g does not vanish and system (3.1) has no periodic orbits.

(*ii*) If $y_E \geqslant y_{AG}(\gamma)$, then $g(\hat{u}_-) \geqslant 0$, and so the function g has one zero and system (1.12) has one symmetric periodic orbit which is unstable because $U'(u) > 1$.

Statement (a) is shown.

(b) If $0 < x_E < 1$, from lemmas 3.5 and 3.10(b), we have $u'_-(\tau) > 0$ for $\tau \in (0, \tau_M)$. From Lemma 3.10(c), there exists $\varepsilon > 0$ such that $g'(u) = \kappa'(\tau)/u'_-(\tau) > 0$ for $\tau \in (0, \varepsilon)$. Next, we study $\operatorname{sign}\kappa'(\tau)$ for $\tau \in (0, \tau_M)$. From Lemma 3.13(c), we obtain $\kappa'(\tau_{SN}) = 0$ where τ_{SN} satisfies the condition $\rho = \alpha(\tau_{SN})$, see (3.17). Recall that τ_M satisfies the condition $\rho = \beta(\tau_M)$, see (3.7). Since,

$$\alpha(\tau) - \beta(\tau) = -\frac{(1+\gamma^2)\mathrm{sh}^2\tau}{1 + e^{\gamma\tau}\psi_{-\gamma}(\tau)} < 0,$$

and both functions are increasing, we get $\tau_{SN} > \tau_M$. Hence $\kappa'(\tau)$ does not change its sign for $\tau \in (0, \tau_M]$. Then $g'(u) > 0$ for $u \leqslant u_-(\tau_M)$ and the function g has at most one zero, so that system (3.1) has at most one symmetric periodic orbit. Since $g'(u) > 0$, the map U satisfies

$U'(u) > -1$. To determine the stability of the possible periodic orbit, we need to know $\operatorname{sign}(U'(u)-1) = \operatorname{sign}\eta'(\tau)$. From Lemma 3.14(c), we get $\eta'(\tau_P) = 0$ where τ_P satisfies the condition $\rho = \delta(\tau_P)$ being the function $\delta(\tau)$ defined in (3.11). From the inequality

$$\delta(\tau) - \beta(\tau) = \frac{(\gamma^2-1)\mathrm{sh}^2\tau}{-1+e^{\gamma\tau}\psi_{-\gamma}(\tau)} > 0,$$

having in mind that both functions are increasing, we conclude that $\tau_P < \tau_M$ and then, the function $\eta'(\tau)$ changes its sign at $\tau = \tau_P$. Again from Lemma 3.14(c), we have $U'(u_-(\tau_P)) = 1$, and

$$\begin{array}{rcll} -1 < & U'(u(\tau)) & < 1 & \text{for} \quad 0 < \tau < \tau_P, \\ 1 < & U'(u(\tau)) & & \text{for} \quad \tau_P < \tau < \tau_M. \end{array}$$

As functions $u_-(\tau)$ and $g(u)$ are increasing, we obtain

$$g(u_-(\tau_P)) = 2(y_E - y_P(\gamma)) < g(u_-(\tau_M)) = 2(y_E - y_{AG}(\gamma)),$$

and so $y_{AG}(\gamma) < y_P(\gamma)$. Now, different cases appear.

($b1$) If $y_E < y_{AG}(\gamma)$, then the function g does not vanish and system (3.1) has no periodic orbits.

($b2$) If $y_{AG}(\gamma) \leqslant y_E < y_P(\gamma)$, then $g(u_-(\tau_M)) \geqslant 0$ and so the function g has one zero and system (3.1) has one symmetric periodic orbit, which is unstable because $U'(u) > 1$ for $\tau_P < \tau < \tau_M$.

($b3$) If $y_E = y_P(\gamma)$, then $g(u_-(\tau_P)) = 0$ and system (3.1) has one symmetric periodic orbit, which is non-hyperbolic since $U'(u_-(\tau_P)) = 1$.

($b4$) If $y_E > y_P(\gamma)$, then there is one stable symmetric periodic orbit, as $g(u) \to -\infty$ when $u \to -\infty$, and $|U'(u)| < 1$ for $0 < \tau < \tau_P$.

Statement (b) is shown.

(c) If $x_E \geqslant 1$, (the virtual node case), then from Proposition 3.2 only symmetric periodic orbits are possible. The function $g(u)$ is defined for all $u \in \mathbb{R}$ and all $\tau > 0$. Moreover,

$$\lim_{u\to-\infty} g(u) = -\infty, \quad \lim_{u\to\infty} U(u) = y_E + (\gamma-1)(1-x_E),$$

and

$$\lim_{u\to\infty} g(u) = \infty.$$

From Lemma 3.10(a) and (c) we have $u'_-(\tau) > 0$ and the existence of $\varepsilon > 0$ such that $\kappa'(\tau) > 0$ for $\tau \in (0, \varepsilon)$. Furthermore, from Lemma 3.13(b) and (c) we get $\kappa'(\tau) \neq 0$, then, $\kappa'(\tau) > 0$ for all $\tau > 0$, and

$$g'(u) = U'(u) + 1 = \frac{\kappa'(\tau)}{u'_-(\tau)} > 0, \text{ for all } u \in \mathbb{R}. \tag{3.33}$$

Hence, the function g has only one zero, u_s, and the system has one periodic orbit. In addition, from Lemma 3.14(a) we obtain

$$U'(u) - 1 = \frac{\eta'(\tau)}{u'_-(\tau)} < 0. \tag{3.34}$$

From relations (3.33)-(3.34) we get $-1 < U'(u) < 1$ and the periodic orbit is stable. Moreover, from Lemma 3.12, there exists a value $\tau = \tau_{DG}$ such that $u_-(\tau_{DG}) = u^c_-$. Thus, if $y_E < y_{DG}(\gamma)$, then $g(u_-(\tau_{DG})) = g(u^c_-) < 0$, so that the existing periodic orbit satisfies $u_s > u^c_-$ and it is of cloud type. If $y_E \geqslant y_{DG}(\gamma)$, then $g(u^c_-) \geqslant 0$ and the periodic orbit is of lens type. Statement (c) is shown and the proof is complete.

3.2.2 Proof of Theorem 3.7

(a) If $x_E \leqslant -1$ then, from Proposition 3.2 only symmetric periodic orbits are possible. When $x_E < -1$, the proof for this statement is similar to the proof of statement (a) in Theorem 3.6. When $x_E = -1$, the flight time τ is not bounded and the point $(-1, \hat{u}_-)$ must be excluded from the set Σ^{ad}_- since $\hat{u}_- = y_E$; being the arguments similar to the case $x_E < -1$, we deal next with the remaining statements.

Note that in what follows, we have $x_E > -1$. Then the function g is defined in the interval $(-\infty, u^*_-)$, see (3.16), and parameter τ belongs to the interval $(0, \infty)$. Moreover,

$$\lim_{u \to -\infty} g(u) = \lim_{u \to u^*_-} g(u) = -\infty, \tag{3.35}$$

and

$$\lim_{u \to -\infty} g'(u) = 2, \quad \lim_{u \to u^*_-} g'(u) = -\infty. \tag{3.36}$$

(b) If $-1 < x_E < 0$ then, from Lemma 3.10(a) we get $u'_-(\tau) > 0$. According to Lemma 3.13(c) there exists a value $\tau = \tau_{SN}$ such that $\kappa'(\tau_{SN}) = 0$, and

$$\operatorname{sign} g'(u) = \operatorname{sign}(U'(u) + 1) = \operatorname{sign} \frac{\kappa'(\tau)}{u'_-(\tau)} = \operatorname{sign}(\tau_{SN} - \tau). \tag{3.37}$$

Then, $g(u_-(\tau_{SN}))$ is the maximum value of the function g. In addition, according to Lemma 3.14(c) there exists a value $\tau = \tau_P$ such that $\eta'(\tau_P) = 0$ and

$$\text{sign}(U'(u) - 1) = \text{sign}\frac{\eta'(\tau)}{u'_-(\tau)} = \text{sign}(\tau_P - \tau). \tag{3.38}$$

Since $U'(u) < -1$ for $\tau > \tau_{SN}$, while $U'(u) > 1$ for $\tau < \tau_P$, we must have $\tau_P < \tau_{SN}$. Furthermore, as $g(u_-(\tau_{SN}))$ is the maximum value of the function $g(u)$ we get

$$g(u_-(\tau_P)) = 2(y_E - y_P(\gamma)) < g(u_-(\tau_{SN})) = 2(y_E - y_{SN}(\gamma)),$$

and then $y_P(\gamma) > y_{SN}(\gamma)$. Now, different cases appear.

($b1$) If $y_E < y_{SN}(\gamma)$, then $g(u) < g(u_-(\tau_{SN})) < 0$, and there are no periodic orbits.

($b2$) If $y_E = y_{SN}(\gamma)$, then $g(u_-(\tau_{SN})) = 0$ and there exists one periodic orbit, which is non-hyperbolic because $U'(u_-(\tau_{SN})) = -1$.

($b3$) If $y_{SN}(\gamma) < y_E < y_P(\gamma)$, then $g(u_-(\tau_P)) < 0$ and $g(u_-(\tau_{SN})) > 0$. Using (3.37), we obtain that $g'(u) > 0$ for $0 < \tau < \tau_{SN}$, and so there exists a unique point u_s such that $g(u_s) = 0$, satisfying

$$u_-(\tau_P) < u_s < u_-(\tau_{SN}).$$

Then, from (3.38) we get $U'(u_s) < 1$. Moreover, as $g'(u_s) > 0$ we obtain from (3.37) that $U'(u_s) > -1$. Thus, such a zero, u_s, corresponds to a stable periodic orbit. Furthermore, from (3.35) and taking into account that $g'(u) < 0$ for $\tau > \tau_{SN}$, we get that there is another point u_u, such that $g(u_u) = 0$ and satisfying that

$$u_-(\tau_{SN}) < u_u < u^*_-.$$

From (3.37) we get $U'(u_u) < -1$ and such a zero represents an unstable periodic orbit. Regarding the shape of the existing periodic orbits, from Lemma 3.12 there exists a value τ_{DG} satisfying $u_-(\tau_{DG}) = u^c_-$. Recall that τ_{DG} and τ_{SN} satisfy the conditions $\rho = \omega(\tau_{DG})$ and $\rho = \alpha(\tau_{SN})$, see (3.29) and (3.31). Since

$$\omega(\tau) - \alpha(\tau) = \frac{(\gamma^2 - 1)\text{sh}^2\tau e^{-\gamma\tau}}{(\text{ch}\tau - \gamma\text{sh}\tau)[1 + e^{\gamma\tau}(\text{ch}\tau - \gamma\text{sh}\tau)]} > 0$$

and both functions are increasing, we get $\tau_{DG} < \tau_{SN}$. Moreover, as $g'(u^c_-) > 0$, we obtain $u^c_- < u_-(\tau_{DG})$. Different cases appear

depending on the value y_E. If $y_E < y_{DG}(\gamma)$, then $g(u_-^c) < 0$ and we get $u_-^c < u_s$. Thus, both periodic orbits are of cloud type. While for $y_E \geqslant y_{DG}(\gamma)$, we get $g(u_-^c) \geqslant 0$ satisfying

$$u_s \leqslant u_-^c < u_-(\tau_{SN}) < u_u < u_-^*$$

and we have one lens periodic orbit and one cloud periodic orbit.

($b4$) If $y_E = y_P(\gamma)$, then $g(u_-(\tau_P)) = 0$ and from (3.38), $U'(u_-(\tau_P)) = 1$, so that there exists a periodic orbit, which is non-hyperbolic, while the unstable periodic orbit of statement (b3) persists.

($b5$) If $y_E > y_P(\gamma)$, then $g(u_-(\tau_P)) > 0$, but from (3.35) we can assure that there exists a value $u_u^1 < u_-(\tau_P))$ such that $g(u_u^1) = 0$. From (3.38) we have $U'(u_(\tau)) > 1$ for $\tau < \tau_P$ and so, the zero u_u^1 corresponds to an unstable periodic orbit. As the unstable periodic orbit with flight time $\tau > \tau_{SN}$ of statement (b3) and (b4) still persists, we have in this case two unstable symmetric periodic orbits.

Statement (b) is complete.

(c) If $x_E \geqslant 0$, then from Proposition 3.2, only symmetric periodic orbits are possible. From Lemma 3.11(a), we obtain $g''(u) < 0$. Consequently, the derivative $g'(u)$ monotonically decreases and from (3.36) $g'(u) < 2$. Then, $U'(u) < 1$ and there exists a value τ_{SN} such that $g'(u_-(\tau_{SN})) = 0$. Thus, the function g is concave down and

$$g(u) \leqslant g(u_-(\tau_{SN})) = 2(y_E - y_{SN}(\gamma)).$$

We need to distinguish some different cases.

(c1) If $y_E < y_{SN}(\gamma)$, then $g(u_-(\tau_{SN})) < 0$, and there are no periodic orbits.

(c2) If $y_E = y_{SN}(\gamma)$, then $g(u_-(\tau_{SN})) = 0$, and we have $U'(u_-(\tau_{SN})) = -1$. Hence, the point $u_-(\tau_{SN})$ corresponds to the only periodic orbit, which is non-hyperbolic.

(c3) If $y_E > y_{SN}(\gamma)$, then $g(u_-(\tau_{SN})) > 0$ and we can assure from (3.35) the existence of two zeroes u_s and u_u, of the function g, which satisfy $u_s < u_-(\tau_{SN}) < u_u$. Using the concavity of g and (3.36), we have $|U'(u_s)| < 1$ and $U'(u_u) < -1$ so that the first zero corresponds to a stable periodic orbit and the second one to an unstable periodic orbit. Moreover from Lemma 3.12 there exists a value τ_{DG} satisfying $u_-(\tau_{DG}) = u_-^c$. The rest of the proof is similar to the one for statement (b3).

Statement (c) is shown and the proof of the theorem is done.

3.2.3 Proofs of theorems 3.8 and 3.9

We note that when $x_E \leqslant 1$, the admissible domain for the map T_U is the set

$$\Sigma_-^{\text{ad}} = \left\{(-1, u_-) : u_- < u_-^*\right\},$$

where the point $(-1, u_-^*)$ is defined in (3.16). Then, the map g is defined in the interval $(-\infty, u_-^*)$, and the parameter τ belongs to the interval $(0, \infty)$. Moreover, in addition to the properties stated in Lemma 3.4, we have

$$g(u_-^*) = \lim_{u \to u_-^*} g(u) = u_+^* + u_-^* = 2(y_E - y_{HT}(\gamma)).$$

If $x_E = 1$, then $\lim_{u\to u^*_-} g'(u) = +\infty$, if $x_E = -1$, $\lim_{u\to u^*_-} g'(u) = 1$, otherwise

$$\lim_{u \to u_-^*} g'(u) = \begin{cases} 1, & \text{if } -1 < \gamma < 0, \\ 1-\rho, & \text{if } \gamma = 0, \\ \text{sign}(-\rho)\infty, & \text{if } 0 < \gamma < 1. \end{cases}$$

Proof of Theorem 3.8

First, from Proposition 3.2 non-symmetric periodic orbits are impossible and the following cases arise.

(a1) If $x_E < -1$ and $-1 < \gamma \leqslant 0$ then from lemmas 3.10(a) and 3.13(a) we get $g'(u) > 0$ and so $U'(u) > -1$. Then, the function g is increasing, its maximum value is given by $g(u_-^*) = 2(y_E - y_{HT}(\gamma))$ and it has at most one zero. Depending on the value $g(u_-^*)$, different sub-cases appear.

(i) If $y_E = y_{HT}(\gamma)$, then $g(u_-^*) = 0$ and it directly follows the existence of a double heteroclinic connection.

(ii) If $y_E < y_{HT}(\gamma)$, then the function g does not vanish and so, system (3.1) has no periodic orbits.

(iii) If $y_E > y_{HT}(\gamma)$, then $g(u_-^*) > 0$ and so, since from Lemma 3.4 the function g takes negative values, it has one zero and system (3.1) has only one periodic orbit. Moreover, since $U'(u) > -1$ and from Lemma 3.14(a) the inequality $U'(u) < 1$ follows, the periodic orbit is stable. Furthermore, from Lemma 3.12 there exists a value τ_{DG} such that $g(u_-(\tau_{DG})) = g(u_-^c)$. Since $g(u_-^*)$ is the maximum value of the function g, we get

$$g(u_-^c) = 2(y_E - y_{DG}(\gamma)) < g(u_-^*) = 2(y_E - y_{HT}(\gamma)).$$

Then, if $y_E < y_{DG}(\gamma)$ we obtain $g(u_-^c) < 0$ and the existing periodic orbit is of cloud type. In the case where $y_E \geqslant y_{DG}(\gamma)$, we have $g(u_-^c) \geqslant 0$ and such a periodic orbit is a lens.

(a2) If $x_E < -1$ and $0 < \gamma < 1$, then from Lemma 3.11(b) we know that $g''(u) < 0$. Thus, the function g is concave down and there exists $\tau = \tau_{SN}$ such that its maximum value is $g(u_-(\tau_{SN}))$, that is

$$g(u_-^*) = 2(y_E - y_{HT}(\gamma)) \leqslant g(u_-(\tau_{SN})) = 2(y_E - y_{SN}(\gamma)),$$

and so $y_{SN}(\gamma) < y_{HT}(\gamma)$. Now, different sub-cases arise.

(a2.1) If $y_E < y_{SN}(\gamma)$, then $g(u_-(\tau_{SN})) < 0$ and the function g does not vanish, so that there are no periodic orbits.

(a2.2) If $y_E = y_{SN}(\gamma)$, then $g(u_-(\tau_{SN})) = 0$, and we have $U'(u_-(\tau_{SN})) = -1$. Hence, the point $u_-(\tau_{SN})$ corresponds to the only periodic orbit, which is non-hyperbolic.

(a2.3) If $y_{SN}(\gamma) < y_E < y_{HT}(\gamma)$, then $g(u_-(\tau_{SN})) > 0$. From Lemma 3.4, we get that $g(u) \to -\infty$ when $u \to -\infty$. Thus, since $g'(u) > 0$ for $0 < \tau < \tau_{SN}$ there exists a unique point $u_s < u_-(\tau_{SN})$ such that $g(u_s) = 0$ and $U'(u_s) > -1$. Using Lemma 3.4 again, we get $U'(u_s) < 1$ and so, such a zero u_s corresponds to a stable periodic orbit. Furthermore, $g(u_-^*) < 0$ and $g'(u) < 0$ for $\tau > \tau_{SN}$ and so, there exists another point u_u such that $g(u_u) = 0$ with $u_-(\tau_{SN}) < u_u < u_-^*$ and $U'(u_u) < -1$. So that, the point u_u represents an unstable periodic orbit. Regarding the shape of the existing periodic orbits, from Lemma 3.12 there exists a value τ_{DG} satisfying $u_-(\tau_{DG}) = u_-^c$, where $\tau_{DG} < \tau_{SN}$ as in the node case. Since $g'(u_-^c) > 0$, we obtain $u_-^c < u_-(\tau_{DG})$. Different cases appear depending on the value y_E. If $y_E < y_{DG}(\gamma)$, then $g(u_-^c) < 0$ and we get $u_-^c < u_s$. Thus, both periodic orbits are of cloud type. If $y_E \geqslant y_{DG}(\gamma)$, we get $g(u_-^c) \geqslant 0$ satisfying

$$u_s \leqslant u_-^c < u_-(\tau_{SN}) < u_u < u_-^*$$

and we have one lens periodic orbit and one cloud periodic orbit.

(a2.4) If $y_E = y_{HT}(\gamma)$, then $g(u_-^*) = 0$ and there appears a double heteroclinic connection which coexists with the stable periodic orbit of statement (a2.3).

(a2.5) If $y_E > y_{HT}(\gamma)$ then $g(u_-^*) > 0$ and there is only one periodic orbit which is stable because $|U'(u)| < 1$ for $0 < \tau < \tau_{SN}$.

Statement (a) is shown. The proof of statement (b) in Theorem 3.8 is similar to the proof of statement (a) in Theorem 3.6.

Finally, by considering $|x_E| = 1$, from Lemma 3.10(a) we have $u'_-(\tau) > 0$. Thus, using Lemma 3.13(a) or Lemma 3.14(a), we get $g'(u) > 0$. Then, the

function g is increasing and its maximum value is $g(u_-^*) = 2(y_E - y_{HT}(\gamma))$. Since the function g takes also negative values, the conclusion follow.

Proof of Theorem 3.9

(a) If $\gamma = x_E = 0$, then from Lemma 3.10 the map U is the identity in its domain $u < u_-^* = y_E - 1$ so that $g(u) = 2u$. Furthermore, the above domain coincides with the image of U. Since the domain of the map $L(l)$ is, by the symmetry, $l > 1 - y_E$, the global transition map $L \circ U$ only exists when $1 - y_E < y_E - 1$ that is, for $y_E > 1$. Clearly, if $y_E = 1$ then $g(u_-^*) = 0$ and there is a double heteroclinic connection as the unique invariant closed curve. If $y_E > 1$ then, the map $L \circ U$ is the identity defined in the interval $(1 - y_E, y_E - 1)$ leading to periodic orbits in any value in such a interval, being only symmetric the corresponding to $u = 0$. In the two limit values $u = \pm(1 - y_E)$, we have homoclinic connections.

(b) If $|\gamma| + |x_E| \neq 0$, from lemmas 3.10(a) and 3.13(a) we get $u'_-(\tau) > 0$ and $g'(u) > 0$. Hence, the function g is increasing and satisfies

$$g(u) < g(u_-^*) = 2(y_E - y_{HT}(\gamma)).$$

Depending on the value $g(u_-^*)$, different cases appear.

(b1) If $y_E < y_{HT}(\gamma)$, then the function g does not vanish and system (3.1) has no symmetric periodic orbits.

(b2) If $y_E = y_{HT}(\gamma)$, then $g(u_-^*) = 0$ and it directly follows the existence of a double heteroclinic connection.

(b3) If $y_E > y_{HT}(\gamma)$, then $g(u_-^*) > 0$ and so the function g has one zero and system (3.1) has only one periodic orbit. Next, we study the stability of such an orbit. If $\gamma x_E \geqslant 0$, then from Lemma 3.14(a) and (b) we deduce that

$$\operatorname{sign} \eta'(\tau) = \operatorname{sign}(U'(u) - 1)) = \begin{cases} \operatorname{sign} x_E & \text{if} \quad x_E \neq 0 \\ \operatorname{sign} \gamma & \text{if} \quad x_E = 0 \end{cases}$$

Since $g'(u) > 0$, we get $U'(u) > -1$ and so the periodic orbit is stable when $x_E < 0$ and unstable when $x_E > 0$. If $x_E = 0$ the periodic orbit is stable for $\gamma < 0$ and unstable for $\gamma > 0$.

If $\gamma x_E < 0$, then from Lemma 3.14(c) there exists a value $\tau = \tau_P$ such that

$$\operatorname{sign}(U'(u) - 1) = \operatorname{sign}[(\tau_P - \tau)x_E].$$

Thus, for $y_E < y_P(\gamma)$ the existing periodic orbit has a flight time $\tau > \tau_P$ and so $\operatorname{sign}(U'(u) - 1) = -\operatorname{sign} x_E$. If $y_E = y_P(\gamma)$, the periodic orbit is non-hyperbolic because $U'(u) = 1$. When $y_E > y_P(\gamma)$, such a periodic orbit has a flight time $\tau < \tau_P$ and so $\operatorname{sign}(U'(u) - 1) = \operatorname{sign} x_E$. As $g'(u) > 0$, then $U'(u) > -1$, and the conclusion follows.

(c) Consider $|\gamma| + |x_E| \neq 0$. Let us show first the existence of homoclinic connections when $|x_E| < 1$ and $\gamma x_E < 0$. That is, we study the possible solutions of the following equations

$$u_L = u_+(\tau), \quad u_R = u_-(\tau). \tag{3.39}$$

where u_L and u_R are defined in (3.20). Equations (3.39) are equivalent to,

$$y_E = \frac{(x_E + 1)\psi_\gamma(\tau) - (x_E - 1)(e^{-\gamma\tau} - (\gamma - 1)\mathrm{sh}\tau)}{2\mathrm{sh}\tau},$$

$$y_E = \frac{(x_E + 1)(e^{\gamma\tau} + (\gamma + 1)\mathrm{sh}\tau) - (x_E - 1)\psi_{-\gamma}(\tau)}{2\mathrm{sh}\tau}.$$

By eliminating y_E, we get the implicit expression of τ_H as the positive solution of equation $\rho = \mu(\tau)$, see (3.21). Then, we must prove that equation (3.21) has a positive solution $\tau = \tau_H$ for some values of parameter $|\gamma| < 1$. Elementary computations give

$$\lim_{\tau \to 0^+} \mu(\tau) = \frac{\gamma - 1}{\gamma + 1} < 0,$$

and

$$\lim_{\tau \to \infty} \mu(\tau) = \begin{cases} 0, & \text{if } \gamma > 0, \\ -\infty, & \text{if } \gamma < 0, \end{cases}$$

and its derivative satisfies $\operatorname{sign} \mu'(\tau) = \operatorname{sign} \gamma$.

On the one hand, if $\gamma < 0$, then the function $\mu(\tau)$ decreases, and so equation $\rho = \mu(\tau)$ has a solution only if

$$\rho < \frac{\gamma - 1}{\gamma + 1},$$

that is, if $-x_E < \gamma < 0$.

On the other hand, for $\gamma > 0$, the function $\mu(\tau)$ is increasing. Thus, equation $\rho = \mu(\tau)$ will have a solution only if

$$\frac{\gamma - 1}{\gamma + 1} < \rho < 0,$$

so that we need $0 < \gamma < -x_E$.

Then, for $\gamma x_E < 0$ the equation $\rho = \mu(\tau)$ has a unique positive solution $\tau = \tau_H$, such that $y_H(\gamma) = y_{\text{ref}}(\gamma, \tau_H)$, defined for all values of γ between 0 and $-x_E$. We conclude the existence of a symmetric pair of non-symmetric homoclinic connections when $y_E = y_H(\gamma)$.

For the sake of brevity, we indicate without proof that when $\tau \to 0^+$, then $\gamma \to -x_E$ and so $y_H(\gamma) \to \infty$. Also, if $\tau \to \infty$, then $\gamma \to 0$ and so $y_H(\gamma) \to 1$.

Statement (c) is shown and the proof is complete.

Chapter 4

Systems with non-zero double eigenvalue

In this chapter, we consider a degenerate case of the hysteretic system (1.12) corresponding to the intermediate situation between node and focus dynamics, namely the case where the matrix A has a non-vanishing double eigenvalue whose geometric multiplicity is one.

As before, we study the properties of the transition map U to detect periodic orbits and bifurcations. Here, we will have always equilibria, being real or virtual. We deal with system (1.12) with $\mu = 0$, and $\gamma \neq 0$. So that, system (1.12) leads to the systems S_U and S_L,

$$\left\{ \begin{array}{rcl} x' & = & 2\gamma(x \mp x_E) - (y \mp y_E), \\ y' & = & \gamma^2(x \mp x_E), \end{array} \right. \qquad \mp x \geqslant -1. \tag{4.1}$$

The solution of the upper system S_U

$$\left(\begin{array}{c} x(\tau) - x_E \\ y(\tau) - y_E \end{array} \right) = e^{A\tau} \left(\begin{array}{c} x(0) - x_E \\ y(0) - y_E \end{array} \right). \tag{4.2}$$

Here, since the matrix A of the linear part of the upper system in (4.1) is not diagonalizable. By means of the associated Jordan matrix J and a transition matrix P we obtain

$$e^{A\tau} = Pe^{J\tau}P^{-1} = e^{\gamma\tau} \left(\begin{array}{cc} 1 + \gamma\tau & -\tau \\ \gamma^2\tau & 1 - \gamma\tau \end{array} \right). \tag{4.3}$$

From (4.2)-(4.3), we get the following parametric representation for the map $u_+ = U(u_-)$

$$\begin{array}{l} u_-(\tau) = y_E + \dfrac{(x_E - 1)e^{-\gamma\tau} - (x_E + 1)(1 + \gamma\tau)}{\tau}, \\ \\ u_+(\tau) = y_E - \dfrac{(x_E + 1)e^{\gamma\tau} - (x_E - 1)(1 - \gamma\tau)}{\tau}, \end{array} \tag{4.4}$$

where the flight time τ belongs to some interval $\mathcal{I} = (0, \tau_M]$ to be specified in Lemma 4.4.

4.1 Main results of the chapter

In the non-generic case $\gamma = 0$ the condition that allowed us to obtain the canonical form (1.12) is not satisfied. This case is studied in the next result, which is included for the sake of completeness.

Proposition 4.1. *When $\gamma = 0$ there are periodic orbits only if $y_E > 0$. In such a case, there exists a bounded continuum of invariant closed curves.*

Proof. If $\gamma = 0$, then $U(u_-) = u_-$ and $L(u_+) = u_+$ within their respective domains and all the trajectories are horizontal straight lines.

When $\gamma = 0$, the straight line $(y - y_E) = 0$ is full of equilibria. The map U is defined for $u_- < y_E$ and the map L is defined for $u_+ > -y_E$, so we have $L(U(u_-)) = u_-$ for

$$-y_E < u_- < y_E,$$

which is only possible if $y_E > 0$.

□

This result is very similar to the one described in Chapter 3 when considering $\gamma^2 = 1$. Next, we give a first result about existence of symmetric periodic orbits in system (4.1).

Proposition 4.2. *Assume that $\gamma \neq 0$ in system 4.1. If either $|x_E| \geqslant 1$ or $\gamma x_E \geqslant 0$ with $|\gamma| + |x_E| \neq 0$, then the following statements hold.*

(a) System (4.1) only can have symmetric periodic orbits.

(b) When $u'_-(\tau) \neq 0$ for all $\tau \in \mathcal{I}$, we have

$$\frac{dU}{du} = \frac{u'_+(\tau)}{u'_-(\tau)} \neq 1.$$

Proof. From statements (a) and (b) of Lemma 4.11 in Section 4.2 the derivative of the function $\eta(\tau) = u_+(\tau) - u_-(\tau)$ does not vanish for all $\tau \in \mathcal{I}$, and so the function $\eta(\tau)$ is injective. According to Proposition 1.7, the existence of non-symmetric periodic orbits is precluded and statement (a) is shown. Statement (b) follows from the inequality $\eta'(\tau) \neq 0$, and the proof is done.

□

Next, we show, without proof, the behaviour of the functions $u_-(\tau)$ and $u_+(\tau)$ when $\tau \to 0^+$.

Lemma 4.3. *The functions $u_-(\tau)$, $u_+(\tau)$ given in (4.4) and the corresponding function $U(u)$ satisfy the following properties*

$$\lim_{\tau\to 0^+} u_-(\tau) = \lim_{\tau\to 0^+} u_+(\tau) = -\infty, \quad \lim_{u\to-\infty} U(u) = -\infty,$$

$$\lim_{u\to-\infty} \frac{dU}{du} = \lim_{\tau\to 0^+} \frac{u'_+(\tau)}{u'_-(\tau)} = 1.$$

According to Definition 1.10, the contact point at the falling line, $(1, u_+^c)$, is characterized by the condition $x'(\tau) = 0$, so that

$$u_+^c = y_E + 2\gamma(1 - x_E). \tag{4.5}$$

As remarked in Chapter 1, the parameter τ belongs to a bounded interval $\mathcal{I} = (0, \tau_M]$ in the cases specified in the following lemma. In addition, we give the condition satisfied by such a maximum value τ_M.

Lemma 4.4. *Consider system (4.1) with either $x_E < -1$ or $|x_E| < 1$ with $\gamma < 0$. Then, there exists a value τ_M for the flight time such that $\tau \in \mathcal{I} = (0, \tau_M]$. Furthermore, the derivative $u'_-(\tau_M) = 0$ and the value τ_M is the only solution of equation*

$$\rho = \beta(\tau) := e^{-\gamma\tau}(1 + \gamma\tau), \tag{4.6}$$

where the parameter ρ is defined in (1.24).

Proof. Let us study when the contact point at the line Σ_+ has a visible character. Following Lemma 1.12 and relations in (1.13) it is necessary to have

$$x'' \,|_{(1,u_+^c)} = \gamma^2(x_E - 1) < 0,$$

and so the condition $x_E < 1$ follows. Furthermore, the case where $x_E \in [-1, 1)$ with $\gamma > 0$ must be excluded because there is not an orbit of the upper system starting at a point $(-1, u_-)$, which arrives at the contact point $(1, u_+^c)$. In conclusion, such a maximum flight time τ_M exists only if either $x_E < -1$ or $|x_E| < 1$ and $\gamma < 0$. By definition, $u_-(\tau_M)$ corresponds to the maximum value of the transition map U, so that $u'_-(\tau_M) = 0$. Finally, to get equation (4.6), it suffices to impose that $u_+(\tau) = u_+^c$, namely

$$y_E - \frac{(x_E + 1)e^{\gamma\tau} - (x_E - 1)(1 - \gamma\tau)}{\tau} = y_E + 2\gamma(1 - x_E).$$

Taking into account the parameter ρ given in (1.24), we get (4.6).

□

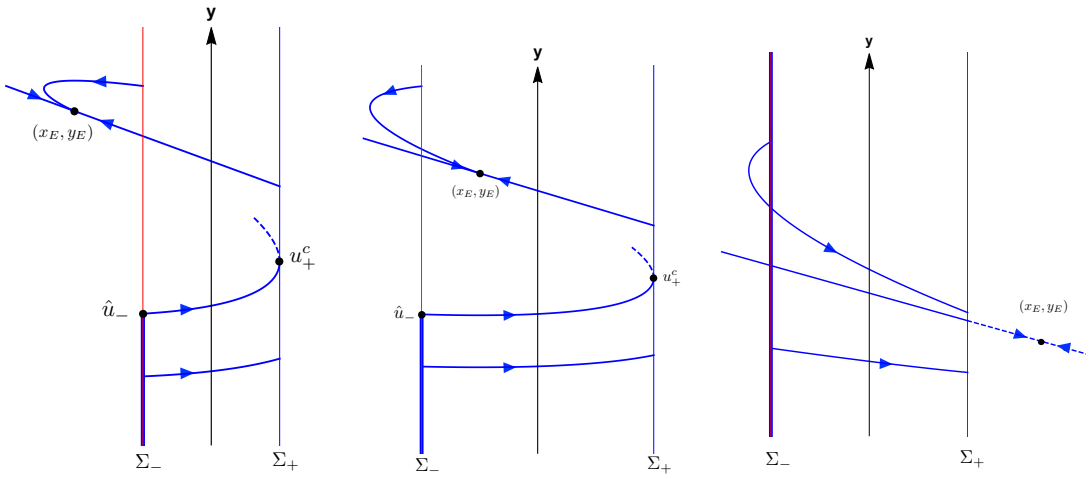

Figure 4.1: The stable improper node cases. (a) The real stable improper node outside the hysteresis band. (b) The real stable improper node inside the hysteresis band. (c) The virtual stable improper node. The thick part of the line Σ_- corresponds to the set Σ_-^{ad}.

Due to the fact that symmetric periodic orbits are determined by equation (1.18), in the following we establish the existence of symmetric periodic orbits by studying the zeroes of the function

$$g(u) = U(u) + u = 2[y_E - y_{\text{ref}}(\tau, \gamma)], \tag{4.7}$$

where we have introduced the reference function

$$y_{\text{ref}}(\tau, \gamma) = \gamma x_E + \frac{x_E \text{sh}(\gamma\tau) + \text{ch}(\gamma\tau) + 1}{\tau}. \tag{4.8}$$

Next, we will analyze different cases taking into account the value of x_E and the stability of the equilibrium. The parameters γ and y_E will be chosen as main bifurcation parameters.

4.1.1 The stable improper node case

Here, we assume that the equilibria of both sub-systems S_U and S_L are either real or virtual stable improper nodes, see Fig 4.1. Next, we consider some distinguished values for the flight time which are significant to study bifurcations in our system.

In the cases where the value τ_M is defined, see Lemma 4.4, by using (4.8) we define the function

$$y_{AG}(\gamma) = y_{\text{ref}}(\tau_M, \gamma). \tag{4.9}$$

If there exists a value $\tau_P \in \mathcal{I}$ such that the derivative of the function $\eta(\tau) = u_+(\tau) - u_-(\tau)$ vanishes, see Lemma 4.11, we get that τ_P is the only solution of equation

$$\rho = \frac{1 - e^{-\gamma\tau}(1 + \gamma\tau)}{-1 + e^{\gamma\tau}(1 - \gamma\tau)}, \tag{4.10}$$

and using (4.8) again, we introduce the function

$$y_P(\gamma) = y_{\text{ref}}(\tau_P, \gamma). \tag{4.11}$$

According to Definition 1.10, the contact point at the rising line, $(-1, u_-^c)$, is characterized by the condition $x'(\tau) = 0$, so that

$$u_-^c = y_E - 2\gamma(1 + x_E). \tag{4.12}$$

If there exists a value $\tau_{DG} \in \mathcal{I}$ such that $u_-(\tau_{DG}) = u_-^c$ with $x'' > 0$ at the point $(-1, u_-^c)$, see Lemma 4.9, we get that τ_{DG} is the only solution of the equation

$$\rho = \frac{-e^{-\gamma\tau}}{(1 - \gamma\tau)}, \tag{4.13}$$

and using again (4.8) we introduce the function

$$y_{DG}(\gamma) = y_{\text{ref}}(\tau_{DG}, \gamma). \tag{4.14}$$

The three functions y_{AG}, y_P and y_{DG} are crucial in stating main findings for the stable improper node case.

Theorem 4.5 (**Stable improper node case**). *Assume that $\gamma < 0$ in system* (4.1) *and consider functions $y_{AG}(\gamma)$, $y_P(\gamma)$ and $y_{DG}(\gamma)$ defined in* (4.9), (4.11) *and* (4.14) *respectively. Then, the following statements hold.*

(a) If $x_E \leqslant 0$, then non-symmetric periodic orbits are impossible. Furthermore, for $y_E < y_{AG}(\gamma)$ there are no periodic orbits while for $y_E \geqslant y_{AG}(\gamma)$ there is one symmetric periodic orbit which is unstable.

(b) If $0 < x_E < 1$, then the following cases arise.

(b1) If $y_E < y_{AG}(\gamma)$, then there are no periodic orbits.

(b2) If $y_{AG}(\gamma) \leqslant y_E < y_P(\gamma)$, then there is only one periodic orbit, which is unstable and symmetric.

(b3) If $y_E = y_P(\gamma)$, then there is only one periodic orbit, which is non hyperbolic and symmetric.

(b4) If $y_E > y_P(\gamma)$, then there is one symmetric periodic orbit, which is stable.

(c) If $x_E \geqslant 1$, then non-symmetric periodic orbits are impossible and there exists one symmetric periodic orbit which is stable. If $y_E < y_{DG}(\gamma)$, then such a symmetric periodic orbit is of cloud type while for $y_E \geqslant y_{DG}(\gamma)$ it is of lens type.

As expected, the dynamical behaviour for the stable improper node is similar to the stable node case described in Chapter 3. We detect for $y_E = y_{AG}(\gamma)$ an arrival-grazing bifurcation of periodic orbits, for $y_E = y_P(\gamma)$ a pitchfork bifurcation of periodic orbits, and for $y_E = y_{DG}(\gamma)$ a departure-grazing periodic orbit bifurcation.

These above bifurcation curves are plotted in figures 4.3, 4.4, 4.5 and 4.6 labelled with AG, P and DG respectively. In the open regions between bifurcation curves, we label with $C^{\{l,c\}}_{\{s,u\}}$ when a periodic orbit exists. The subscript stands for its stability character (s =stable, u =unstable) and the superscript does for its shape (l =lens, c =cloud). If the periodic orbit is non-symmetric, it has a companion, so that we add an upper bar to indicate such a pair.

4.1.2 The unstable improper node case

Next, we assume that both sub-systems S_U and S_L have an unstable improper node either real or virtual that is, we assume $\gamma > 0$, see Fig. 4.2. Before giving our next result, let us recall the distinguished point $(-1, u^*_-)$, introduced in Definition 1.10, where the invariant manifold of the S_U-system intersects the line Σ_-. A direct computation shows that

$$u^*_- = y_E - \gamma(x_E + 1). \tag{4.15}$$

If there exists a value $\tau_{SN} \in \mathcal{I}$ such that the derivative of the function $\kappa(\tau) = u_+(\tau) + u_-(\tau)$ vanishes, see Lemma 4.10, we get that τ_{SN} is the only solution of equation

$$\rho = \frac{1 + e^{-\gamma\tau}(1 + \gamma\tau)}{1 + e^{\gamma\tau}(1 - \gamma\tau)}. \tag{4.16}$$

Using again (4.8), we introduce the function

$$y_{SN}(\gamma) = y_{\text{ref}}(\tau_{SN}, \gamma), \tag{4.17}$$

which is needed in the next result.

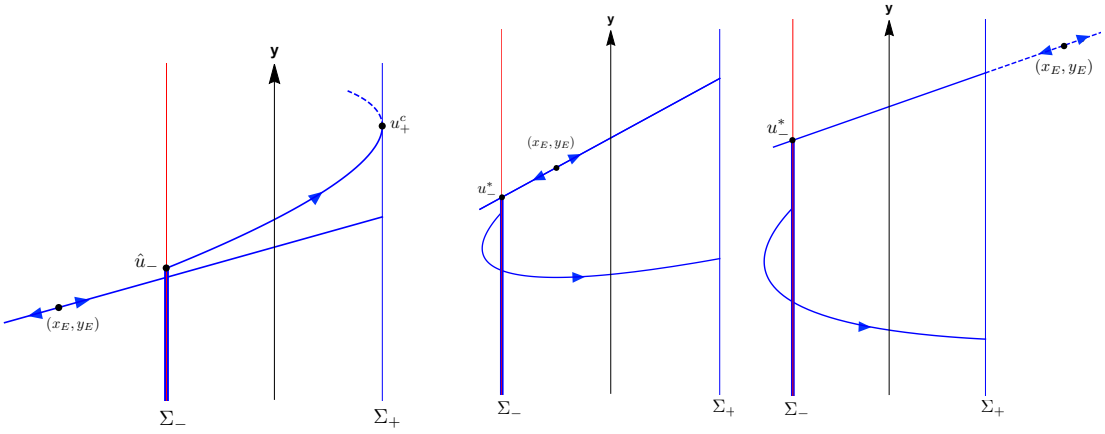

(a) (b) (c)

Figure 4.2: The unstable improper node cases. (a) The real unstable improper node outside the hysteresis band. (b) The real unstable improper node inside the hysteresis band. (c) The virtual unstable improper node. The thicker part of Σ_- corresponds to Σ_-^{ad}.

Theorem 4.6 (**Unstable improper node case**). *Assume that* $\gamma > 0$ *in system* (4.1) *and consider functions* $y_{AG}(\gamma)$, $y_P(\gamma)$, $y_{DG}(\gamma)$ *and* $y_{SN}(\gamma)$ *defined in* (4.9),(4.11), (4.14) *and* (4.17) *respectively. Then, the following statements hold.*

(a) If $x_E \leqslant -1$, *then non-symmetric periodic orbits are impossible. Furthermore, for* $y_E < y_{AG}(\gamma)$ *there are no periodic orbits while for* $y_E \geqslant y_{AG}(\gamma)$ *there is one symmetric periodic orbit which is unstable.*

(b) If $-1 < x_E < 0$, *then the following cases arise.*

(b1) If $y_E < y_{SN}(\gamma)$, *then there are no periodic orbits.*

(b2) If $y_E = y_{SN}(\gamma)$, *then there is one symmetric periodic orbit which is non hyperbolic.*

(b3) If $y_{SN}(\gamma) < y_E < y_P(\gamma)$, *then there are two symmetric periodic orbits with opposite stabilities. If* $y_E < y_{DG}(\gamma)$, *then such periodic orbits are clouds, while* $y_{DG}(\gamma) \leqslant y_E$ *one of the periodic orbits changes to a lens type.*

(b4) If $y_E = y_P(\gamma)$, *then there are two symmetric periodic orbit, one is unstable and the other one is non-hyperbolic.*

(b5) If $y_E > y_P(\gamma)$, *then there are two unstable symmetric periodic orbits.*

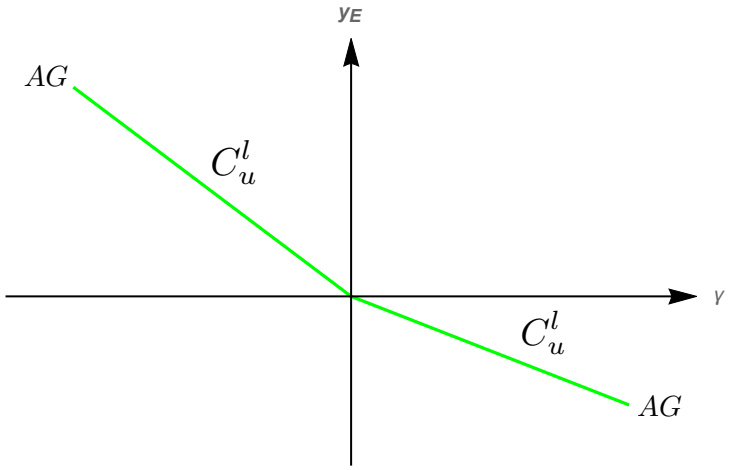

Figure 4.3: The bifurcation set for $x_E \leqslant -1$. We label the bifurcation curves and the open regions with different number of periodic orbits as explained in the text.

(c) If $x_E \geqslant 0$, then non-symmetric periodic orbits are impossible. Furthermore, if $y_E < y_{SN}(\gamma)$, then there are no periodic orbits; if $y_E = y_{SN}(\gamma)$, then there is one periodic orbit which is non hyperbolic; finally, if $y_E > y_{SN}(\gamma)$, then there are two periodic orbits with opposite stabilities being both of cloud type if $y_E < y_{DG}(\gamma)$ and of different shape if $y_E \geqslant y_{DG}(\gamma)$.

The above result are in concordance with the obtained ones for the unstable node case in Theorem 3.7. We get for $y_E = y_{AG}(\gamma)$ an arrival-grazing bifurcation of periodic orbits, for $y_E = y_{SN}(\gamma)$ a saddle-node bifurcation of periodic orbits, for $y_E = y_P(\gamma)$ we have a pitchfork bifurcation of periodic orbits, and finally for $y_E = y_{DG}(\gamma)$ a departure-grazing bifurcation of periodic orbits. Accordingly, the different bifurcation curves appear in the bifurcation sets of Figure 4.3, 4.4, 4.5 and 4.6, labelled with AG, SN, P and DG.

4.2 Proof of the main results

We give in this section some previous results regarding the properties of the functions $U(u)$, $g(u)$, $\kappa(\tau)$ and $\eta(\tau)$ defined in Chapter 1. Next, we include the proofs of the two theorems 4.5 and 4.6 following the same ideas that in Section 3.2.

Direct computations show that the two first derivatives of functions $u_-(\tau)$

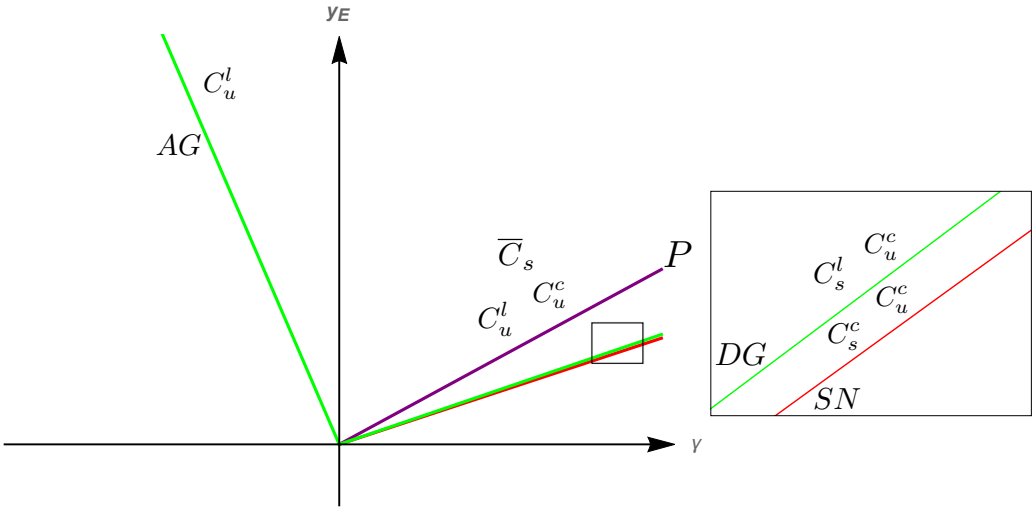

Figure 4.4: The bifurcation set for $-1 < x_E < 0$. We label the bifurcation curves and the open regions with different number periodic orbits as explained in the text. In the right panel, we show a magnification of the square in the left panel.

and $u_+(\tau)$ defined in (4.4) are

$$\begin{aligned} u'_-(\tau) &= \frac{(x_E+1)-(x_E-1)e^{-\gamma\tau}(1+\gamma\tau)}{\tau^2}, \\ u'_+(\tau) &= -\frac{(x_E-1)-(x_E+1)e^{\gamma\tau}(1-\gamma\tau)}{\tau^2}, \end{aligned} \tag{4.18}$$

and

$$\begin{aligned} u''_-(\tau) &= \frac{(x_E-1)e^{-\gamma\tau}[1+(1+\gamma\tau)^2]-2(x_E+1)}{\tau^3}, \\ u''_+(\tau) &= \frac{2(x_E-1)-(x_E+1)e^{\gamma\tau}[1+(1-\gamma\tau)^2]}{\tau^3}. \end{aligned} \tag{4.19}$$

In the next lemma, we study some properties of the derivative $u'_-(\tau)$ and $\kappa'(\tau)$.

Lemma 4.7. *If $\gamma = 0$ in system (4.1), then the functions $u_\pm$ satisfy the equality $u_+(\tau) = u_-(\tau)$.*

If $\gamma \neq 0$, then the following properties hold for $\tau > 0$.

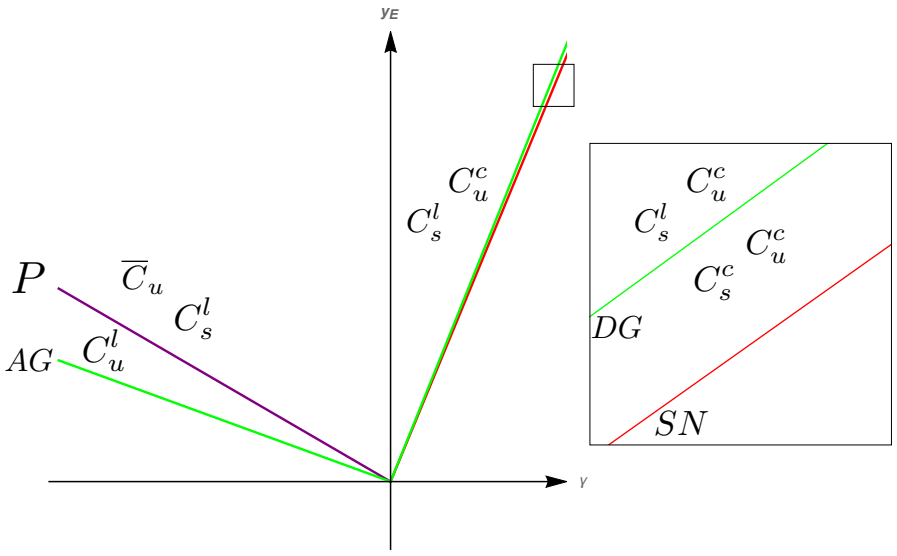

Figure 4.5: The bifurcation set for $0 < x_E < 1$. In the right panel, an enlarged region for $\gamma > 0$ is shown. The different labels are explained in the text.

(a) If $|x_E| \leqslant 1$ *and* $\gamma > 0$ *or* $x_E \geqslant 1$, *then* $u'_-(\tau) > 0$, *for* $\tau > 0$.

(b) If $x_E < 1$ *and there exists a value* τ_M *such that* $u'_-(\tau_M) = 0$, *then* $u'_-(\tau) > 0$ *for all* $\tau \in (0, \tau_M)$.

(c) Under hypotheses of statements (a) *or* (b), *there exists* $\varepsilon > 0$ *such that* $\kappa'(\tau) > 0$ *for* $\tau \in (0, \varepsilon)$.

Proof. The assertion about the case $\gamma = 0$ is direct from (4.18).

If $\gamma \neq 0$, from (4.18), we get

$$\operatorname{sign} u'_-(\tau) = \operatorname{sign} f(\tau),$$

where

$$f(\tau) = (x_E + 1) - (x_E - 1)e^{-\gamma\tau}(1 + \gamma\tau),$$

and

$$f(0) = 2, \quad f'(\tau) = (1 - x_E)\gamma^2\tau e^{-\gamma\tau}.$$

Regarding statement (a), if $|x_E| \leqslant 1$ and $\gamma > 0$, the conclusion directly follows. If $x_E = 1$ so that $u'_-(\tau) > 0$ always. If $x_E > 1$, then $f'(\tau) > 0$, which implies $f(\tau) > 0$, and so $u'_-(\tau) > 0$ and statement (a) is shown.

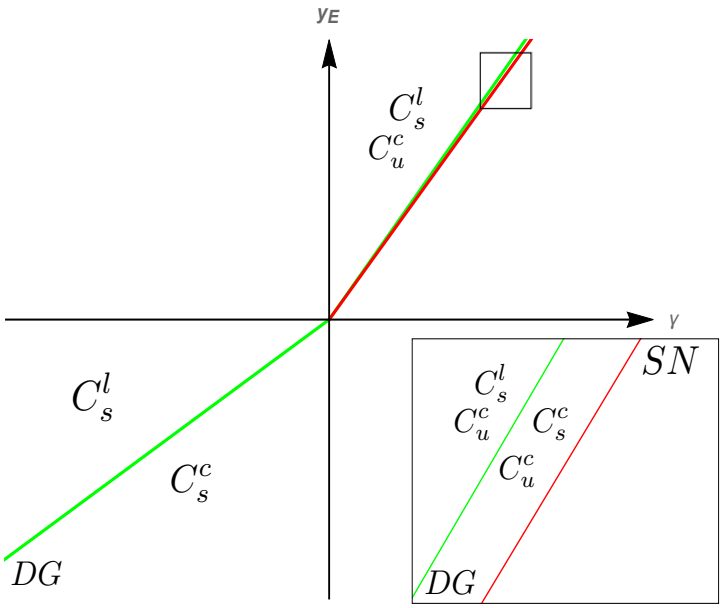

Figure 4.6: The bifurcation set for $x_E \geqslant 1$. In the right panel an enlarged region for $\gamma > 0$ is shown. The different labels are explained in the text.

Considering now statement (b), if $x_E < 1$ then $f'(\tau) < 0$. Taking into account that $f(0) = 2$ and $f(\tau_M) = 0$, we conclude that $f(\tau) > 0$ and consequently $u'_-(\tau) > 0$ for $0 < \tau < \tau_M$. Statement (b) follows.

To prove statement (c), from Lemma 4.3 we obtain

$$\lim_{u\to-\infty} U'(u) = \lim_{u\to-\infty} \frac{dU}{du} = \lim_{\tau\to 0^+} \frac{u'_+(\tau)}{u'_-(\tau)} = 1,$$

so that under the hypotheses of statements (a) or (b), there exists a value $\varepsilon > 0$ such that for $\tau \in (0, \varepsilon)$, we have $u'_-(\tau) > 0$ and $\operatorname{sign} u'_+(\tau) = \operatorname{sign} u'_-(\tau)$. Then, statement (c) follows and the proof is complete.

□

Lemma 4.8. *Consider the function $g(u)$ given in (4.7). If $\gamma > 0$ and $x_E \geqslant 0$, then $g''(u) < 0$ for all u belonging to its domain.*

Proof. From Lemma 4.7, $u'_-(\tau) > 0$ and by computing the derivative

$$\frac{d}{d\tau}\left(\frac{dU}{du_-}\right) = \frac{d^2U}{du_-^2}\frac{du_-}{d\tau} = \frac{d}{d\tau}\left(\frac{u'_+(\tau)}{u'_-(\tau)}\right)$$

we get

$$\operatorname{sign}\frac{d^2g}{du_-^2} = \operatorname{sign}\frac{d^2U}{du_-^2} = \operatorname{sign}\left(\frac{d}{d\tau}\left(\frac{u'_+(\tau)}{u'_-(\tau)}\right)\right).$$

In the specific case $x_E = 1$ we get directly $g''(u) < 0$. For $x_E \neq 1$ using (4.19), we obtain

$$\frac{d}{d\tau}\left(\frac{u'_+(\tau)}{u'_-(\tau)}\right) = \frac{-\gamma^2\tau e^{\gamma\tau}h(\rho)}{[\rho e^{\gamma\tau} - \psi_\gamma(\tau)]^2},$$

and then

$$\operatorname{sign}\frac{d^2g}{du_-^2} = -\operatorname{sign} h(\rho) \tag{4.20}$$

where $h(\rho) = \rho^2 e^{2\gamma\tau} - 2\gamma\tau\rho e^{\gamma\tau} - 1$ is a quadratic function in the variable ρ. Since $h(0) = -1$, the function h vanishes at two values $\rho^- < 0 < \rho^+$ such that $h(\rho) < 0$ for $\rho \in (\rho^-, \rho^+)$ and $h(\rho) \geqslant 0$ otherwise. In addition,

$$\begin{aligned} &\operatorname{sign} h(-1) = \operatorname{sign}[\operatorname{sh}(\gamma\tau) + \gamma\tau] = \operatorname{sign}\gamma, \\ &\operatorname{sign} h(1) = \operatorname{sign}[\operatorname{sh}(\gamma\tau) - \gamma\tau] = \operatorname{sign}\gamma. \end{aligned} \tag{4.21}$$

When $x_E \neq 1$ and $\gamma > 0$, from (4.21) we obtain

$$-1 < \rho^- < \rho^+ < 1,$$

and then $h(\rho) > 0$ for $\rho \in (-\infty, -1) \cup (1, \infty)$ or, according to the definition of ρ in (1.24), $h(\rho) > 0$ for $x_E \in (0, 1) \cup (1, \infty)$. Thus, from (4.20) we get $g''(u) < 0$ and we are done.

□

Lemma 4.9. *Consider system* (4.1) *with* $\gamma \neq 0$. *Then, there exists a value* τ_{DG} *for the flight time such that* $u_-(\tau_{DG}) = u_-^c$ *with* $x'' > 0$ *at the point* $(-1, u_-^c)$ *and* $u'_+(\tau_{DG}) = 0$ *when one of the following condition holds.*

(a) If $x_E = 1$ *and* $\gamma > 0$. *Furthermore, the value* $\tau_{DG} = 1/\gamma$.

(b) If either $x_E > 1$ *or* $|x_E| < 1$ *along with* $\gamma > 0$. *Furthermore, the value* τ_{DG} *is the only solution of the equation*

$$\rho = \omega(\tau) := \frac{-e^{-\gamma\tau}}{1 - \gamma\tau}, \tag{4.22}$$

where the parameter ρ *is defined in* (1.24).

Proof. Let us study when the derivative x'' at the contact point $(-1, u_-^c)$ is positive. The quoted derivative x'' is given by

$$x''|_{(-1,u_-^c)} = \gamma^2(1 + x_E),$$

which is positive only if $x_E > -1$. The case where $-1 < x_E \leqslant 1$ with $\gamma < 0$ must be excluded because the orbit starting at the point $(-1, u_-^c)$ does not arrive at the falling line Σ_+. Thus, the existence of the value τ_{DG} is guaranteed

in the stated cases. By definition, $u_+(\tau_{DG})$ is the maximum value of the image of the transition map U, so that any orbit of the upper system arrives at a point of the line Σ_+ satisfying $u_+ \leqslant u_+(\tau_{DG})$, then $u'_+(\tau_{DG}) = 0$.

If $x_E = 1$, then the condition $u_-(\tau) = u_-^c$ implies $\tau_{DG} = 1/\gamma$. If $x_E \neq 1$, imposing the condition $u_-(\tau) = u_-^c$ we get

$$y_E + \frac{(x_E - 1)e^{-\gamma\tau} - (x_E + 1)(1 + \gamma\tau)}{\tau} = y_E - 2\gamma(1 + x_E).$$

Taking into account the definition of the parameter ρ in (1.24), equation (4.22) follows.

□

Lemma 4.10. *Assuming $\gamma \neq 0$, the following statements hold for the function $\kappa'(\tau) = u'_+(\tau) + u'_-(\tau)$.*

(a) If either $x_E = -1$ and $\gamma > 0$ or $|x_E| > 1$ and $\gamma x_E < 0$, then $\kappa'(\tau) > 0$ for all $\tau \in \mathcal{I}$.

(b) If $x_E = 1$, then the condition $\kappa'(\tau) = 0$ is equivalent to the equation

$$\nu(\tau) := 1 + e^{\gamma\tau}(1 - \gamma\tau) = 0, \tag{4.23}$$

and it has a (unique) solution $\tau = \tau_{SN}$ only if $\gamma > 0$. Furthermore, $\operatorname{sign}\kappa'(\tau) = \operatorname{sign}(\tau_{SN} - \tau)$.

(c) If $x_E \neq 1$, then the condition $\kappa'(\tau) = 0$ is equivalent to the equation

$$\rho = \alpha(\tau) := \frac{1 + e^{-\gamma\tau}(1 + \gamma\tau)}{1 + e^{\gamma\tau}(1 - \gamma\tau)}. \tag{4.24}$$

The equation $\kappa'(\tau) = 0$ has a (unique) solution $\tau = \tau_{SN}$ only in the following two cases.

(i) If $\gamma > 0$ and $x_E > -1$.

(ii) If $\gamma < 0$ and $x_E < 1$.

Furthermore, $\operatorname{sign}\kappa'(\tau) = \operatorname{sign}(\tau_{SN} - \tau)$.

Proof. Introducing the functions

$$h_1(\tau) = (x_E + 1)[1 + e^{\gamma\tau}(1 - \gamma\tau)], \quad h_2(\tau) = (x_E - 1)[1 + e^{-\gamma\tau}(1 + \gamma\tau)],$$

from the derivatives (4.18) we get

$$\kappa'(\tau) = \frac{h_1(\tau) - h_2(\tau)}{\tau^2} = \frac{h(\tau)}{\tau^2}.$$

If $x_E = -1$, then $h(\tau) > 0$ for $\gamma > 0$. Next, we study the sign of the derivative

$$h'(\tau) = -2\gamma^2\tau[\mathrm{ch}(\gamma\tau) + x_E\mathrm{sh}(\gamma\tau)].$$

For $|x_E| > 1$, with $\gamma x_E < 0$ we have $h'(\tau) > 0$. Then, since $h(0) = 4$, statement (a) follows.

Regarding the remaining statements, it is easy to see that the condition $\kappa'(\tau) = 0$ is equivalent to equation (4.23) if $x_E = 1$ and to equation (4.24) otherwise.

If $x_E = 1$, we study the solutions of equation (4.23). When $\gamma < 0$, then $\nu(\tau) > 0$ for all τ. Since $\nu'(\tau) = -\gamma^2\tau e^{\gamma\tau}$, $\nu(0) = 2$, and for $\gamma > 0$ we have $\nu(\tau) \to -\infty$ when $\tau \to \infty$, we conclude that $\nu(\tau)$ only vanishes at some value $\tau = \tau_{SN}$ when $\gamma > 0$. Statement (b) is shown.

If $x_E \neq 1$, we study the existence of solutions for equation (4.24) by analyzing the properties of function α. First, note that $\alpha(0) = 1$ for all γ. When $\gamma = 0$, the function α satisfies $\alpha(\tau) \equiv 1$.

Observe also that the function $\alpha(\tau)$ is not defined when its denominator

$$\nu(\tau) = 1 + e^{\gamma\tau}(1 - \gamma\tau)$$

vanishes. From the proof of statement (b), we know that the denominator of $\alpha(\tau)$ only vanishes if $\gamma > 0$ at some point, say $\tau = \hat{\tau}$.

The derivative of function $\alpha(\tau)$ is

$$\alpha'(\tau) = \frac{2\gamma^2\tau[\mathrm{sh}(\gamma\tau) + \gamma\tau]}{[1 + e^{\gamma\tau}(1 - \gamma\tau)]^2},$$

and so $\operatorname{sign}\alpha'(\tau) = \operatorname{sign}\gamma$.

When $\gamma > 0$, we have

$$\lim_{\tau\to\widehat{\tau}^-} \alpha(\tau) = \infty, \quad \lim_{\tau\to\widehat{\tau}^+} \alpha(\tau) = -\infty, \quad \lim_{\tau\to\infty} \alpha(\tau) = 0.$$

For $\gamma < 0$, we have

$$\lim_{\tau\to\infty} \alpha(\tau) = -\infty$$

To conclude the proof, we take into account the definition of ρ in (1.24) and analyze the two cases of statement (c), once we know the sign of the derivative $\alpha'(\tau)$.

(i) If $\gamma > 0$, then the function α is increasing and takes values in the set $(1, \infty) \cup (-\infty, 0)$. Hence equation (4.24) only has solutions when the parameter $\rho \in (1, \infty) \cup (-\infty, 0)$ that is, when $x_E > -1$.

(ii) If $\gamma < 0$, then the function α is decreasing and satisfies $-\infty < \alpha(\tau) < 1$. Hence equation (4.24) has solutions only when $-\infty < \rho < 1$ that is, when $x_E < 1$.

Statement (c) is shown and the proof is complete.

□

Lemma 4.11. *Assuming $\gamma \neq 0$, the following statements hold for the function $\eta'(\tau) = u'_+(\tau) - u'_-(\tau)$.*

(a) If either $|x_E| \geqslant 1$ or $\gamma x_E > 0$, then $\operatorname{sign} \eta'(\tau) = -\operatorname{sign} x_E$.

(b) If $x_E = 0$, then $\operatorname{sign} \eta'(\tau) = \operatorname{sign} \gamma$.

(c) If $x_E \neq 1$, then the condition $\eta'(\tau) = 0$ is equivalent to the equation

$$\rho = \delta(\tau) := \frac{1 - e^{-\gamma\tau}(1 + \gamma\tau)}{-1 + e^{\gamma\tau}(1 - \gamma\tau)}, \tag{4.25}$$

which has a (unique) solution $\tau = \tau_P$ if the two conditions $|x_E| < 1$ and $\gamma x_E < 0$ hold. Furthermore,

$$\operatorname{sign} \eta'(\tau) = \operatorname{sign}[(\tau - \tau_P)x_E].$$

Proof. Introducing the new functions

$$h_1(\tau) = (x_E - 1)[-1 + e^{-\gamma\tau}(1 + \gamma\tau)], \quad h_2(\tau) = (x_E + 1)[-1 + e^{\gamma\tau}(1 - \gamma\tau)],$$

from the derivatives (4.18) we get

$$\eta'(\tau) = \frac{h_1(\tau) + h_2(\tau)}{\tau^2}.$$

Next, we study the sign of the derivative of the function $h(\tau) = h_1(\tau) + h_2(\tau)$, obtaining

$$h'(\tau) = -2\gamma^2\tau[x_E \operatorname{ch}(\gamma\tau) + \operatorname{sh}(\gamma\tau)].$$

If $|x_E| \geqslant 1$, or $\gamma x_E > 0$, we get $\operatorname{sign} h'(\tau) = -\operatorname{sign} x_E$, and statement (a) follows.

If $x_E = 0$, then $\operatorname{sign} h'(\tau) = \operatorname{sign} \gamma$. Since $h(0) = 0$, statement (b) is shown.

Regarding statement (c), it is direct to see that the condition $\eta'(\tau) = 0$ is equivalent to equation (4.25). Next, we study the existence of solutions for equation (4.25), under the assumptions $|x_E| < 1$ and $\gamma x_E < 0$.

First, note that the denominator of the function $\delta(\tau)$ only vanishes at $\tau = 0$. Since the function δ satisfies

$$\lim_{\tau\to 0} \delta(\tau) = -1, \quad \lim_{\tau\to\infty} \delta(\tau) = \begin{cases} -\infty, & \text{if} \quad \gamma < 0, \\ 0, & \text{if} \quad \gamma > 0, \end{cases}$$

and its derivative

$$\delta'(\tau) = \frac{2\gamma^2\tau(\mathrm{sh}\gamma\tau - \gamma\tau)}{[-1 + e^{\gamma\tau}(1-\gamma\tau)]^2}$$

does not vanishes, we get $\operatorname{sign}\delta'(\tau) = \operatorname{sign}\gamma$. To conclude the proof, we take into account the definition of ρ given in (1.24) and use the sign of $\delta'(\tau)$ to analyze the following cases.

(i) If $\gamma > 0$ then the function δ is monotone increasing with $-1 < \delta(\tau) < 0$. Hence equation (4.25) has solutions only when $-1 < \rho < 0$, that is when $-1 < x_E < 0$.

(ii) If $\gamma < 0$ then the function δ is monotone decreasing with $-\infty < \delta(\tau) < -1$. Hence equation (4.25) has only solutions when $-\infty < \rho < -1$, that is $0 < x_E < 1$.

In these cases, equation (4.25) has a unique positive solution τ_P. Furthermore, the function $h(\tau) = h_1(\tau) + h_2(\tau)$, satisfies $h(0) = h'(0) = 0$ and $h''(0) = -2\gamma^2 x_E$, so we can conclude that $\eta'(\tau_P) = 0$ and

$$\operatorname{sign}\eta'(\tau) = \begin{cases} -\operatorname{sign} x_E \text{ for } 0 < \tau < \tau_P, \\ \\ \operatorname{sign} x_E \text{ for } \tau_P < \tau. \end{cases}$$

Statement (c) is shown and the proof is complete. □

4.2.1 Proof of Theorem 4.5

When $x_E < 1$, , the admissible domain for the map T_U is the set

$$\Sigma_-^{\mathrm{ad}} = \left\{(-1, u_-) : u_- \leqslant U^{-1}(u_+^c) = \hat{u}_-\right\},$$

where the point $(1, u_+^c)$ is introduced in (4.5). Then, the map $g(u)$ is defined for $u \leqslant \hat{u}_- = u_-(\tau_M)$ and the parameter τ belongs to the interval $(0, \tau_M]$, see Lemma 3.5.

(a) If $x_E \leqslant 0$, then $\gamma x_E \geqslant 0$ and from Proposition 4.2, only symmetric periodic orbits are possible. From lemmas 4.4 and 4.7(b), there exists $\tau_M > 0$ such that $u'_-(\tau) > 0$ for $\tau \in (0, \tau_M)$. Thus, from Lemma 4.11(a) or (b) we get $\eta'(\tau) > 0$ and consequently $U'(u) > 1$. Then the derivative $g'(u) = U'(u) + 1 > 2$, and so the function g is increasing and it has at most one zero. Note that

$$\lim_{u\to-\infty} g(u) = -\infty, \quad g(u) \leqslant g(\hat{u}_-) = 2(y_E - y_{AG}(\gamma)),$$

where we have used (4.7) and (4.9). According to the value of y_E, different cases arise.

(*i*) If $y_E < y_{AG}(\gamma)$, then the function g does not vanish and system (4.1) has no periodic orbits.

(*ii*) If $y_E \geqslant y_{AG}(\gamma)$, then $g(\hat{u}_-) \geqslant 0$, and so the function g has one zero and system (4.1) has one symmetric periodic orbit which is unstable because $U'(u) > 1$.

Statement (a) is shown.

(b) If $0 < x_E < 1$, from lemmas 4.4 and 4.7(b), we obtain $u'_-(\tau) > 0$ for $\tau \in (0, \tau_M)$. From Lemma 4.7(c), there exists $\varepsilon > 0$ such that $g'(u) = \kappa'(\tau)/u'_-(\tau) > 0$ for $\tau \in (0, \varepsilon)$. Next, we study $\operatorname{sign} \kappa'(\tau)$ for $\tau \in (0, \tau_M)$. From Lemma 4.10(c), we obtain $\kappa'(\tau_{SN}) = 0$ where τ_{SN} satisfies the condition $\rho = \alpha(\tau_{SN})$, see (4.16). Recall that τ_M satisfies the condition $\rho = \beta(\tau_M)$, see (4.4). Since,

$$\alpha(\tau) - \beta(\tau) = \frac{\gamma^2\tau^2}{1 + e^{\gamma\tau}(1 - \gamma\tau)} > 0,$$

and both functions are decreasing, we get $\tau_{SN} > \tau_M$. Hence $\kappa'(\tau)$ does not change its sign for $\tau \in (0, \tau_M]$. Then $g'(u) > 0$ for $u \leqslant u_-(\tau_M)$ and the function g has at most one zero, so that system (4.1) has at most one symmetric periodic orbit. Since $g'(u) > 0$, the map U satisfies $U'(u) > -1$. To determine the stability of the possible periodic orbit, we need to know $\operatorname{sign}(U'(u) - 1) = \operatorname{sign} \eta'(\tau)$. From Lemma 4.11(c), we get $\eta'(\tau_P) = 0$ where τ_P satisfies the condition $\rho = \delta(\tau_P)$ being the function $\delta(\tau)$ defined in (3.11). From the inequality

$$\delta(\tau) - \beta(\tau) = \frac{\gamma^2\tau^2}{-1 + e^{\gamma\tau}(1 - \gamma\tau)} > 0,$$

having in mind that both functions are decreasing, we conclude that $\tau_P < \tau_M$ and then, the function $\eta'(\tau)$ changes its sign at $\tau = \tau_P$. Again from Lemma 4.11(c), we have $U'(u_-(\tau_P)) = 1$, and

$$\begin{array}{rlll} -1 < & U'(u(\tau)) < 1 & \text{for} & 0 < \tau < \tau_P, \\ 1 < & U'(u(\tau)) & \text{for} & \tau_P < \tau < \tau_M. \end{array}$$

As functions $u_-(\tau)$ and $g(u)$ are increasing, we obtain

$$g(u_-(\tau_P)) = 2(y_E - y_P(\gamma)) < g(u_-(\tau_M)) = 2(y_E - y_{AG}(\gamma)),$$

and so $y_{AG}(\gamma) < y_P(\gamma)$. Now, different cases appear.

(*b*1) If $y_E < y_{AG}(\gamma)$, then the function g does not vanish and system (4.1) has no periodic orbits.

($b2$) If $y_{AG}(\gamma) \leqslant y_E < y_P(\gamma)$, then $g(u_-(\tau_M)) \geqslant 0$ and so the function g has one zero and system (4.1) has one symmetric periodic orbit, which is unstable because $U'(u) > 1$ for $\tau_P < \tau < \tau_M$.

($b3$) If $y_E = y_P(\gamma)$, then $g(u_-(\tau_P)) = 0$ and system (4.1) has one symmetric periodic orbit, which is non-hyperbolic since $U'(u_-(\tau_P)) = 1$.

($b4$) If $y_E > y_P(\gamma)$, then there is one stable symmetric periodic orbit, as $g(u) \to -\infty$ when $u \to -\infty$, and $|U'(u)| < 1$ for $0 < \tau < \tau_P$.

Statement (b) is shown.

(c) If $x_E \geqslant 1$, then from Proposition 4.2 only symmetric periodic orbits are possible. The function $g(u)$ is defined for all $u \in \mathbb{R}$ and all $\tau > 0$. Moreover,

$$\lim_{u\to-\infty} g(u) = -\infty, \quad \lim_{u\to\infty} U(u) = y_E + \gamma(1 - x_E),$$

and

$$\lim_{u\to\infty} g(u) = \infty.$$

From Lemma 4.7(a) and (c) we have $u'_-(\tau) > 0$ and the existence of $\varepsilon > 0$ such that $\kappa'(\tau) > 0$ for $\tau \in (0, \varepsilon)$. Furthermore, from Lemma 4.10(b) and (c) we get $\kappa'(\tau) \neq 0$, then, $\kappa'(\tau) > 0$ for all $\tau > 0$, and

$$g'(u) = U'(u) + 1 = \frac{\kappa'(\tau)}{u'_-(\tau)} > 0, \text{ for all } u \in \mathbb{R}. \tag{4.26}$$

Hence, the function g has only one zero u_s, and the system has one periodic orbit. In addition, from Lemma 3.14(a) we obtain

$$U'(u) - 1 = \frac{\eta'(\tau)}{u'_-(\tau)} < 0. \tag{4.27}$$

From relations (4.26)-(4.27) we get $-1 < U'(u) < 1$ and the periodic orbit is stable. Moreover, from Lemma 4.9, there exists a value $\tau = \tau_{DG}$ such that $u_-(\tau_{DG}) = u^c_-$. Thus, if $y_E < y_{DG}(\gamma)$, then $g(u_-(\tau_{DG})) = g(u^c_-) < 0$, so that the existing periodic orbit satisfies $u_s > u^c_-$ and it is of cloud type. If $y_E \geqslant y_{DG}(\gamma)$, then $g(u^c_-) \geqslant 0$ and the stable periodic orbit is of lens type.

Statement (c) is shown and the proof is complete.

4.2.2 Proof of Theorem 4.6

(a) If $x_E \leqslant -1$ then, from Proposition 4.2 only symmetric periodic orbits are possible. When $x_E < -1$, the proof for this statement is similar to

the proof of statement (a) in Theorem 4.5. When $x_E = -1$, the flight time τ is not bounded and the point $(-1, \hat{u}_-)$ must be excluded from the set Σ_-^{ad} since $\hat{u}_- = y_E$; being the arguments similar to the case $x_E < -1$, we deal next with the remaining statements.

Note that in what follows, we have $x_E > -1$. Then the function g is defined in the interval $(-\infty, u_-^*)$, see (4.15), and parameter τ belongs to the interval $(0, \infty)$. Moreover,

$$\lim_{u\to-\infty} g(u) = \lim_{u\to u_-^*} g(u) = -\infty, \tag{4.28}$$

and

$$\lim_{u\to-\infty} g'(u) = 2, \quad \lim_{u\to u_-^*} g'(u) = -\infty. \tag{4.29}$$

(b) If $-1 < x_E < 0$ then, from Lemma 4.7(a) we get $u'_-(\tau) > 0$. According to Lemma 4.10(c) there exists a value $\tau = \tau_{SN}$ such that $\kappa'(\tau_{SN}) = 0$, and

$$\operatorname{sign} g'(u) = \operatorname{sign}(U'(u) + 1) = \operatorname{sign}\frac{\kappa'(\tau)}{u'_-(\tau)} = \operatorname{sign}(\tau_{SN} - \tau). \tag{4.30}$$

Then, $g(u_-(\tau_{SN}))$ is the maximum value of the function g. In addition, according to Lemma 4.11(c) there exists a value $\tau = \tau_P$ such that $\eta'(\tau_P) = 0$ and

$$\operatorname{sign}(U'(u) - 1) = \operatorname{sign}\frac{\eta'(\tau)}{u'_-(\tau)} = \operatorname{sign}(\tau_P - \tau). \tag{4.31}$$

Since $U'(u) < -1$ for $\tau > \tau_{SN}$, while $U'(u) > 1$ for $\tau < \tau_P$, we must have $\tau_P < \tau_{SN}$. Furthermore, as $g(u_-(\tau_{SN}))$ is the maximum value of the function $g(u)$ we get

$$g(u_-(\tau_P)) = 2(y_E - y_P(\gamma)) < g(u_-(\tau_{SN})) = 2(y_E - y_{SN}(\gamma)),$$

and then $y_P(\gamma) > y_{SN}(\gamma)$. Now, different cases appear.

($b1$) If $y_E < y_{SN}(\gamma)$, then $g(u) < g(u_-(\tau_{SN})) < 0$, and there are no periodic orbits.

($b2$) If $y_E = y_{SN}(\gamma)$, then $g(u_-(\tau_{SN})) = 0$ and there exists one periodic orbit, which is non-hyperbolic because $U'(u_-(\tau_{SN})) = -1$.

($b3$) If $y_{SN}(\gamma) < y_E < y_P(\gamma)$, then $g(u_-(\tau_P)) < 0$ and $g(u_-(\tau_{SN})) > 0$. Using (4.30), we obtain that $g'(u) > 0$ for $0 < \tau < \tau_{SN}$, and so there exists a unique point u_s such that $g(u_s) = 0$, satisfying

$$u_-(\tau_P) < u_s < u_-(\tau_{SN}).$$

Then, from (4.31) we get $U'(u_s) < 1$. Moreover, as $g'(u_s) > 0$ we obtain from (4.30) that $U'(u_s) > -1$. Thus, such a zero, u_s, corresponds to a stable periodic orbit. Furthermore, from (4.28) and taking into account that $g'(u) < 0$ for $\tau > \tau_{SN}$, we get that there is another point u_u, such that $g(u_u) = 0$ and satisfying that

$$u_-(\tau_{SN}) < u_u < u_-^*.$$

From (3.37) we get $U'(u_u) < -1$ and such a zero represents an unstable periodic orbit. Regarding the shape of the existing periodic orbits, from Lemma 4.9 there exists a value τ_{DG} satisfying $u_-(\tau_{DG}) = u_-^c$. Recall that τ_{DG} and τ_{SN} satisfy the conditions $\rho = \omega(\tau_{DG})$ and $\rho = \alpha(\tau_{SN})$, see (4.22) and (4.24). Since

$$\omega(\tau) - \alpha(\tau) = \frac{\gamma^2\tau^2 e^{-\gamma\tau}}{(1-\gamma\tau)[1+e^{\gamma\tau}(1-\gamma\tau)]} > 0$$

and both functions are increasing, we get $\tau_{DG} < \tau_{SN}$. Moreover, as $g'(u_-^c) > 0$, we obtain $u_-^c < u_-(\tau_{DG})$. Different cases appear depending on the value y_E. If $y_E < y_{DG}(\gamma)$, then $g(u_-^c) < 0$ and we get $u_-^c < u_s$. Thus, both periodic orbits are of cloud type. While $y_E \geqslant y_{DG}(\gamma)$, we get $g(u_-^c) \geqslant 0$ satisfying

$$u_s \leqslant u_-^c < u_-(\tau_{SN}) < u_u < u_-^*$$

and we have one lens periodic orbit and one cloud periodic orbit.

($b4$) If $y_E = y_P(\gamma)$, then $g(u_-(\tau_P)) = 0$ and from (4.31), $U'(u_-(\tau_P)) = 1$, so that there exists a periodic orbit, which is non-hyperbolic, while the unstable periodic orbit of statement (b3) persists.

($b5$) If $y_E > y_P(\gamma)$, then $g(u_-(\tau_P)) > 0$, but from (4.28) we can assure that there exists a value $u_u^1 < u_-(\tau_P))$ such that $g(u_u^1) = 0$. From (4.31) we have $U'(u_-(\tau)) > 1$ for $\tau < \tau_P$ and so, the zero u_u^1 corresponds to an unstable periodic orbit. As the unstable periodic orbit with flight time $\tau > \tau_{SN}$ of statement (b3) and (b4) still persists, we have in this case two unstable symmetric periodic orbits.

Statement (b) is complete.

(c) If $x_E \geqslant 0$, then from Proposition 4.2, only symmetric periodic orbits are possible. From Lemma 4.8, we obtain $g''(u) < 0$. Consequently, the derivative $g'(u)$ monotonically decreases and from (4.29) $g'(u) < 2$. Then, $U'(u) < 1$ and there exists a value τ_{SN} such that $g'(u_-(\tau_{SN})) = 0$. Thus, the function g is concave down and

$$g(u) \leqslant g(u_-(\tau_{SN})) = 2(y_E - y_{SN}(\gamma)).$$

We need to distinguish some different cases.

(c1) If $y_E < y_{SN}(\gamma)$, then $g(u_-(\tau_{SN})) < 0$, and there are no periodic orbits.

(c2) If $y_E = y_{SN}(\gamma)$, then $g(u_-(\tau_{SN})) = 0$, and we have $U'(u_-(\tau_{SN})) = -1$. Hence, the point $u_-(\tau_{SN})$ corresponds to the only periodic orbit, which is non-hyperbolic.

(c3) If $y_E > y_{SN}(\gamma)$, then $g(u_-(\tau_{SN})) > 0$ and we can assure from (4.28) the existence of two zeroes u_s and u_u, of the function g, which satisfy $u_s < u_-(\tau_{SN}) < u_u$. By using that the function g is concave down and relation (4.29), we have $|U'(u_s)| < 1$ and $U'(u_u) < -1$ so that the first zero corresponds to a stable periodic orbit and the second one to an unstable periodic orbit.

Moreover from Lemma 4.9 there exists a flight time $\tau = \tau_{DG}$ satisfying $u_-(\tau_{DG}) = u_-^c$. The rest of the proof is similar to the discussion for statement (b3).

Statement (c) is shown and the proof is done.

Chapter 5

Complex eigenvalues: a chaos boundary crisis

In this chapter, we deal with in the complex eigenvalues case, adopting a different point of view with respect to previous chapters. On the one hand, this case has been the most studied in the literature, mainly due to its potential capacity of generating chaotic solutions, see [33, 35–38, 43, 45, 46, 48, 55]. The features of focus dynamics make it rather difficult to do a systematic covering of all possible cases. In particular, the corresponding transition map can be discontinuous, see [47], and there can appear periodic orbits with many jumps, so that the study of such periodic orbits should require a specific treatment which is out of the scope of this work. On the other hand, the analytical expressions of transition maps are more involved than in the real eigenvalues case. Therefore, we have decided to limit our analysis to some specific cases, putting our goal in a first study of the concrete situation that corresponds to the separating barrier between smooth transition maps and discontinuous ones.

We deal always with the normalized canonical form (1.12) with the corresponding value of the modal parameter ($\mu = i$). First we consider the simplest case where the real part of the eigenvalues is zero, that is, the upper and lower systems have an equilibrium of centre type, where a complete analysis is straightforward. Section 5.2 is devoted to focus type equilibria, so that the eigenvalues have a non-vanishing real part.

While for the centre case we will provide the complete bifurcation set, this set will not be given for the non-zero real part case as already mentioned. In particular, in both cases the domain of the transition map U can be disconnected, and in the focus case we can also have discontinuities even when there exists a connected domain. Our main contribution is to prove the existence of a specific phenomenon leading to chaos, to be referred as *chaos boundary*

crisis bifurcation.

5.1 The complex eigenvalues case with zero real part

In this Section, we shall consider system (1.12) where the equilibria are centre type, that is, we take the modal parameter $\mu = i$ and $\gamma = 0$, namely

$$\left\{ \begin{array}{rcl} \dot{x} & = & -(y \mp y_E) \\ \dot{y} & = & x \mp x_E \end{array} \right. \qquad \mp x \geqslant -1 \tag{5.1}$$

We start by computing the transition map U. First, note that at the line $x = 1$, we have $x' \geqslant 0$ only if $y \leqslant y_E$, so that necessarily $u_+ \leqslant y_E$. The upper system in (5.1) can be integrated to obtain as general solution

$$(x - x_E)^2 + (y - y_E)^2 = C. \tag{5.2}$$

Thus, to get the transition map U, we consider that an orbit with initial point $(-1, u_-)$, arrives to the point $(1, u_+)$ and we obtain

$$(1 - x_E)^2 + (u_+ - y_E)^2 = (1 + x_E)^2 + (u_- - y_E)^2. \tag{5.3}$$

Then,

$$u_+ = U(u_-) = y_E - \sqrt{(u_- - y_E)^2 + 4x_E} \tag{5.4}$$

since the other root cannot satisfy the condition $u_+ \leqslant y_E$, and so the set Σ_-^{ad} is not always a connected set. In fact, the domain of the transition map U is

$$\mathrm{Dom}(U) = \left\{ \begin{array}{ll} \{u_- \in \mathbb{R} : |u_- - y_E| \geqslant 2\sqrt{-x_E}\}, & \text{if} \quad x_E < 0, \\ \mathbb{R}, & \text{if} \quad x_E \geqslant 0. \end{array} \right.$$

Furthermore, the derivative of the transition map U in its domain, is

$$U'(u_-) = -\frac{u_- - y_E}{\sqrt{(u_- - y_E)^2 + 4x_E}}. \tag{5.5}$$

Here, we can obtain all the periodic orbits, by writing equations (1.20), namely

$$\begin{array}{rcl} u_+ & = & y_E - \sqrt{(u_- - y_E)^2 + 4x_E}, \\ -u_- & = & y_E - \sqrt{(-u_+ - y_E)^2 + 4x_E}. \end{array} \tag{5.6}$$

We can write so

$$\begin{array}{rcl} \sqrt{(u_- - y_E)^2 + 4x_E} & = & y_E - u_+, \\ \sqrt{(u_+ + y_E)^2 + 4x_E} & = & y_E + u_-, \end{array}$$

leading to

$$\begin{aligned}(u_- - y_E)^2 + 4x_E - (y_E - u_+)^2 &= 0,\\ (u_+ + y_E)^2 + 4x_E - (y_E + u_-)^2 &= 0.\end{aligned}$$

Therefore, by adding and subtracting both equations, we arrive at the two conditions

$$\begin{aligned}u_+ y_E - u_- y_E + 2x_E &= 0,\\ u_-^2 - u_+^2 &= 0,\end{aligned} \tag{5.7}$$

so that we have two possibilities: (i) $u_+ = u_-$ and then $x_E = 0$, (ii) $u_+ = -u_-$ and then $u_- = x_E/y_E$ with $y_E \neq 0$. We study those cases separately in theorems 5.1 and 5.2.

Theorem 5.1. *When $x_E = 0$, the hysteretic system (5.1) undergoes a rather degenerate bifurcation at $y_E = 0$, so that there are no periodic orbits for $y_E < 0$, an unbounded continuum of symmetric periodic orbits for $y_E = 0$, and a bounded continuum of non-symmetric periodic orbits for $y_E > 0$.*

Proof. For $x_E = 0$, the first condition in (5.7) leads to

$$y_E(u_+ - u_-) = 0.$$

Therefore, if $x_E = y_E = 0$ then the transition map $U(u) = -|u|$, and so we get that all the points $(u_-, -u_-)$ with $u_- \geqslant 0$ represent symmetric periodic orbits. Then, there is an unbounded continuum of symmetric periodic orbits.

However, if $y_E \neq 0$ we obtain that $u_+ = u_-$, but coming back to (5.6) we see that

$$\begin{cases} u_+ &= y_E - \sqrt{(u_- - y_E)^2},\\ u_- &= -y_E + \sqrt{(u_+ + y_E)^2}, \end{cases}$$

and so

$$2y_E = |u_- - y_E| + |u_- + y_E|,$$

which implies that $y_E > 0$ and all the points (u_-, u_+) such that $u_+ = u_-$ with $u_- \in [-y_E, y_E]$ represent periodic orbits. Then, there exists a bounded continuum of periodic orbits. In fact, all of the periodic orbits are non-symmetric except the one corresponding to the origin, which is symmetric. □

Theorem 5.2. *Considering system (5.1) for $x_E \neq 0$, the following statements hold.*

(a) The maximum number of periodic orbit is one, and it is symmetric.

(b) There exists a periodic orbit if and only if either $x_E \geqslant -y_E^2$ and $y_E > 0$, or $x_E \leqslant -y_E^2$ for $y_E < 0$.

(c) The system undergoes a periodic orbit bifurcation from infinity at $y_E = 0$, so that for small $|y_E|$ and $x_E y_E > 0$ there appears a symmetric periodic orbit of great size and cloud type, being stable for $x_E > 0$ and $y_E > 0$ and unstable for $x_E < 0$ and $y_E < 0$.

(d) For $y_E > 0$, at $x_E = -y_E^2$ the system undergoes an arrival-grazing periodic orbit bifurcation, so that for $x_E < -y_E^2$ there are no periodic orbits, while for small $y_E^2 + x_E > 0$, there exists a symmetric unstable periodic orbit of lens type. This periodic orbit comes from a critical periodic orbit existing for $x_E = -y_E^2$, which is tangent to both lines $\Sigma_\pm$ at the points $(\pm 1, \pm y_E)$.

(e) For $y_E > 0$, at $x_E = y_E^2$ the system undergoes an departure-grazing periodic orbit bifurcation, so that for $x_E > y_E^2$ there exists a symmetric stable periodic orbit of cloud type, while for small $y_E^2 - x_E > 0$ such periodic orbit becomes of lens type keeping its symmetry and stability properties.

(f) For $y_E < 0$, at $x_E = -y_E^2$ the system undergoes an arrival-grazing periodic orbit bifurcation, so that for $x_E > -y_E^2$ there are no periodic orbits, while for small $y_E^2 + x_E < 0$, there exists a symmetric unstable periodic orbit of cloud type. This periodic orbit comes from a critical periodic orbit existing for $x_E = -y_E^2$, which is tangent to both lines $\Sigma_\pm$ at the points $(\pm 1, \pm y_E)$.

Proof. If $x_E \neq 0$, the condition for having a symmetric periodic orbit is, see (5.6), leads to

$$u_- = \frac{x_E}{y_E}, \text{ with } y_E \neq 0. \tag{5.8}$$

Such a solution represents a symmetric periodic orbit, because otherwise, there would be another solution of (5.6), see Proposition 1.4. So that there is a symmetric periodic orbit corresponding to the point $(u_-, u_+) = (x_E/y_E, -x_E/y_E)$. Statement (a) is shown.

Condition $u_+ \leqslant y_E$ gives now $\frac{-x_E}{y_E} \leqslant y_E$, that is $x_E \geqslant -y_E^2$ for $y_E > 0$, and $x_E \leqslant -y_E^2$ for $y_E < 0$. Clearly, if $x_E > 0$ and $y_E < 0$, symmetric periodic orbits are not possible. However, for $x_E > 0$ and $y_E > 0$ there is always a symmetric periodic orbit, being a cloud orbit if $u_- \geqslant y_E$, that is when $x_E > y_E^2$, and a lens orbit if $x_E \leqslant y_E^2$. Statement (b) follows.

Regarding statement (c), consider expression (5.8) and $x_E < 0$ then taking limits when y_E tends to zero from below, and noting that $x' < 0$ at $(-1, u_-)$ assures the cloud type for the periodic orbit. The stability comes from (5.5). Analogously for $x_E > 0$ and $y_E \to 0^+$.

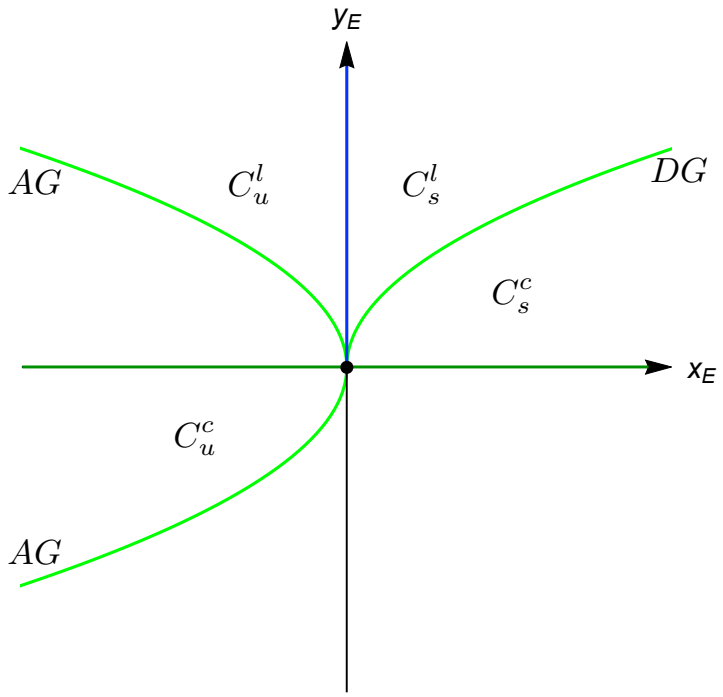

Figure 5.1: Bifurcation set in the parameter plane (x_E, y_E). The curves in light green represent the grazing bifurcations. The dark green and blue lines represent more degenerated bifurcations; in particular, the dark green line represent a bifurcation from infinity at $y_E = 0$, while for $x_E = 0$ and $y_E \geqslant 0$ the global system has a continuum of periodic orbits.

The limit situations of statements (d) and (f) correspond to the case $u_+ = u_+^c = y_E$. This case agree with the previous definition of arrival-grazing periodic orbit bifurcation, see Definition 1.14. The involved periodic orbits are unstable as $x_E < 0$ in (5.5). Statement (e) is analogous, and the proof is complete. □

Remark 5.3. *Taking into account theorems 5.1 and 5.2, we conclude that for $y_E > 0$ there appears a kind of unstable limit cycle-centre-stable limit cycle bifurcation at $x_E = 0$, since we pass from a situation with an unstable periodic orbit of lens type for $x_E < 0$ to a bounded continuum of periodic orbits at $x_E = 0$, finally having a configuration with a stable periodic orbits of lens type for $x_E > 0$.*

Regarding theorems 5.1 and 5.2, we detect some bifurcation curves. First, when $x_E = 0$, a continuum of periodic orbits appears. In the more general case when $x_E \neq 0$, we obtain the two types of grazing bifurcation of periodic orbits, that is, a departure-grazing bifurcation of periodic orbits and two arrival-grazing bifurcation of periodic orbits. They are labelled as DG and AG

respectively. Moreover, we detect also, a bifurcation from infinity at the line $y_E = 0$ where there appears a symmetric periodic orbit of cloud type whose stability depends on the sign of x_E. Accordingly, the complete bifurcation set in the parameter plane (x_E, y_E) appears in Figure 5.1, where we indicate with $C^{\{l,c\}}_{\{s,u\}}$ when a periodic orbit exists. As before, the subscript stands for the stability of such an orbit (s =stable, u =unstable), and the superscript indicates its shape (l =lens, c =cloud).

5.2 A chaos boundary crisis for positive real part complex eigenvalues

If one reviews the scientific literature on hysteretic systems, typically the different works have emphasized their ability for generating chaotic solutions when the involved dynamics are of focus type. However, only exceptionally, rigorous proofs for the existence of chaotic solutions have been given. Here, we will give a mathematical analysis justifying a instantaneous transition to chaotic behaviour by considering the hysteretic system (1.12) taking the modal parameter $\mu = i$. In particular, we will study only the case having repulsive real equilibria inside the hysteresis band, trying to analyze the existence of chaotic behaviour from a theoretical point of view.

Thus, we consider the hysteretic system S_U and S_L

$$\begin{cases} x' = 2\gamma(x \mp x_E) - (y \mp y_E), \\ y' = (\gamma^2 + 1)(x \mp x_E). \end{cases} \qquad \mp x \geqslant -1 \tag{5.9}$$

First, we compute as before the transition map U, taking an initial point $(-1, u_-)$ and following the orbit until it hits the straight line $x = 1$ in a point of the form $(1, u_+)$, so that $u_+ = U(u_-)$. Note that at the arrival point we must have $x' \geqslant 0$, and given that $x' = 0$ in the vertical nullcline $y = y_E + 2\gamma(x - x_E)$ we must have $u_+ \leqslant y_E + 2\gamma(1 - x_E)$. According to Definition 1.10, the ordinate of the *contact point* at the line Σ_+ is

$$u^c_+ = y_E + 2\gamma(1 - x_E),$$

so that we have $u_+ \leq u^c_+$. Similarly, for the point where there is a tangency at Σ_-, we define

$$u^c_- = y_E + 2\gamma(-1 - x_E) = y_E - 2\gamma(1 + x_E).$$

For initial points with $u_- > u^c_-$ we have $x' < 0$, while $x' > 0$ when $u_- < u^c_-$. By resorting to the corresponding matrix exponential, we can compute the

solution $(x(\tau), y(\tau))$ with initial point $(x(0), y(0)) = (-1, u_-)$ as

$$\begin{pmatrix} x(\tau) - x_E \\ y(\tau) - y_E \end{pmatrix} = e^{A\tau} \begin{pmatrix} -1 - x_E \\ u_- - y_E \end{pmatrix}, \tag{5.10}$$

where

$$e^{A\tau} = e^{\gamma\tau} \begin{pmatrix} \cos\tau + \gamma \sin\tau & -\sin\tau \\ (\gamma^2 + 1)\sin\tau & \cos\tau - \gamma\sin\tau \end{pmatrix}. \tag{5.11}$$

To get the transition map, we write

$$\begin{pmatrix} 1 - x_E \\ u_+ - y_E \end{pmatrix} = e^{A\tau} \begin{pmatrix} -1 - x_E \\ u_- - y_E \end{pmatrix}, \tag{5.12}$$

where the matrix exponential is given in (5.11). From the above equation, by assuming $\sin\tau \neq 0$, we get

$$\begin{aligned} u_-(\tau) &= y_E - \frac{e^{-\gamma\tau}(1 - x_E) + (1 + x_E)(\cos\tau + \gamma\sin\tau)}{\sin\tau}, \\ u_+(\tau) &= y_E - \frac{e^{\gamma\tau}(1 + x_E) + (1 - x_E)(\cos\tau - \gamma\sin\tau)}{\sin\tau}, \end{aligned} \tag{5.13}$$

so having a τ-parametric representation of the map U, provided we study the valid parameter domain $\mathcal{I}$.

We will take as reference the orbit that starts at $(-1, u_-^c)$ and study the conditions assuring that it arrives at Σ_+, see the left panel of Figure 5.3. From the first component of (5.10), we get the equality

$$x(\tau) = x_E - (1 + x_E)e^{\gamma\tau}\left(\cos\tau - \gamma\sin\tau\right),$$

so that the arrival condition $x(\tau) = 1$ is fulfilled whenever the *departure tangent orbit flight time determining equation*

$$\sigma := \frac{1}{\rho} = \frac{x_E - 1}{x_E + 1} = e^{\gamma\tau}\left(\cos\tau - \gamma\sin\tau\right) \tag{5.14}$$

is satisfied for a certain $\tau > 0$. Note that, regarding (1.25) we have now,

$$\begin{array}{rcll} 1 \leqslant & \sigma & < \infty, & \text{if} \quad x_E \leqslant -1, \\ -\infty \leqslant & \sigma & < -1, & \text{if} \quad -1 < x_E \leqslant 0, \\ -1 < & \sigma & < 0, & \text{if} \quad 0 < x_E < 1, \\ 0 < & \sigma & < 1, & \text{if} \quad 1 < x_E, \end{array} \tag{5.15}$$

and the case $x_E = -1$ should be separately considered. We must select the smaller positive value of τ if there are more than one value satisfying (5.14), because of the hysteretic mechanism that determine the admissible solutions, as indicated in Chapter 1.

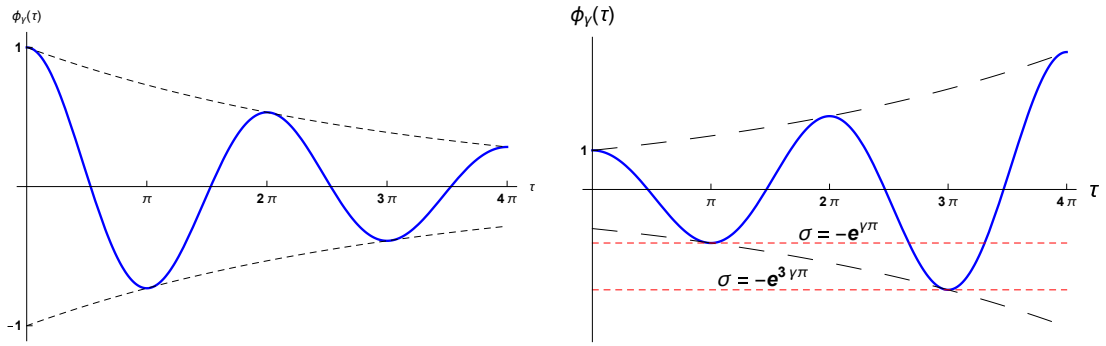

Figure 5.2: The graph of $\phi_\gamma(\tau)$ for $\gamma = -0.1$ (left), and $\gamma = 0.1$ (right).

The graph of the function

$$\phi_\gamma(\tau) = e^{\gamma\tau}\left(\cos\tau - \gamma\sin\tau\right),$$

with derivative

$$\phi'_\gamma(\tau) = -(1+\gamma^2)e^{\gamma\tau}\sin\tau,$$

appears in Figure 5.2, so that its critical points appear at $\tau = k\pi$, with $k \in \mathbb{N}$.

We note that for $\gamma = 0$ we have $\phi_0(\tau) = \cos\tau$. Regarding the value of σ, we see that there are no solutions for equation (5.14) when $\gamma \leq 0$ and $|\sigma| > 1$. When $\gamma > 0$, there always exists a solution, even there appear cases where the time τ is bigger than 2π, the time corresponding to a complete turn around the focus.

To avoid a long taxonomy, we will pay attention in what follows just to the case $\gamma > 0$, putting emphasis into the particular case $-e^{\gamma\pi} \leqslant \sigma < 0$, where $\phi_\gamma(\pi) = -e^{\gamma\pi}$ is the first relative minimum value for ϕ. Note that, from the right part of Figure 5.2, if otherwise $\sigma < -e^{\gamma\pi}$ then condition (5.14) requires a time $\tau > 2\pi$. From the above discussion, the following result clarifies the situation.

Lemma 5.4. *For system* (5.9) *with* $\gamma > 0$ *and* $x_E > -\tanh(\gamma\pi/2)$ *the orbit starting at* $(-1, u_-^c)$ *arrives at* Σ_+ *with a flight time* $\tau_-^c < \pi$. *Furthermore, any orbit starting at* Σ_- *spends a time* $\tau < \pi$ *to hit* Σ_+.

Proof. To show the first assertion, note that from the hypotheses, the condition $x_E > -1$ holds. Then the inequality $\sigma > -e^{\gamma\pi}$ is equivalent to

$$\frac{x_E - 1}{x_E + 1} > -e^{\gamma\pi},$$

that leads to

$$x_E(1 + e^{\gamma\tau}) > 1 - e^{\gamma\tau},$$

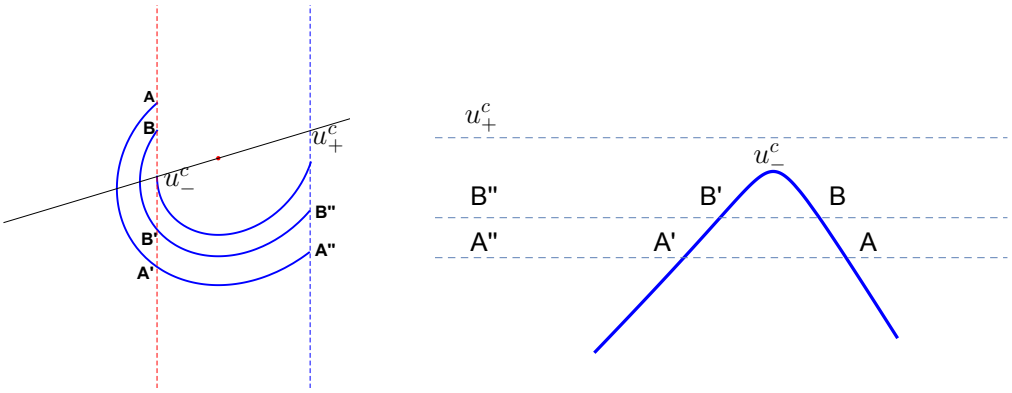

Figure 5.3: The orbits for $\gamma = 0.15$ and $x_E = -0.2 > -\tanh(\gamma\pi/2) \approx -0.231354$, determine a continuous transition map.

so that

$$x_E > \frac{1 - e^{\gamma\pi}}{1 + e^{\gamma\pi}} = -\tanh\left(\frac{\gamma\pi}{2}\right).$$

Therefore, we can assume that $\sigma > -e^{\gamma\pi}$. Since $x_E > -1$ we have $\sigma < 1$, so that equation (5.14) always produces a solution with $\tau_-^c < \pi$.

If we consider any point $(-1, u_-)$ with $u_- < u_-^c$ then it is easy to see that we need a time $\tau < \tau_-^c$ to pass from Σ_- to Σ_+. Effectively, by uniqueness of solutions such an orbit can be described by the graph of a function $y(x) < y_c(x)$ with $x \in [-1, 1]$, being $y_c(x)$ the function whose graph corresponds with the orbit starting at $(-1, u_-^c)$. Then, we see from (5.9) that the transition time of such an orbit is given by

$$\int_{-1}^{1} \frac{dx}{2\gamma(x - x_E) - (y(x) - y_E)} < \int_{-1}^{1} \frac{dx}{2\gamma(x - x_E) - (y_c(x) - y_E)} = \tau_-^c,$$

as claimed.

Regarding the left panel of Figure 5.3, we conclude that the above argument is not valid for the orbits starting at points $(-1, u_-)$ with $u_- > u_-^c$. In fact, as such orbits always are longer than the previously considered, which are in fact subsets of them, their flight time should be greater. In any case, by the continuous dependence on the initial conditions and having transversality at the section Σ_+, the flight time is a continuous function of the ordinate u_-. The conclusion of the lemma comes now by showing that the case $\tau = \pi$ is not possible. Effectively from (5.10) with $\tau = \pi$ we should get

$$1 - x_E = e^{\gamma\pi}(1 + x_E)$$

which is equivalent to $\sigma = -e^{\gamma\pi}$, getting a contradiction.

□

The above result guarantees that, under its hypotheses, the transition map U is well defined for all $u_- \in \mathbb{R}$, and that the flight time for all the orbits is always less than π, the time corresponding to a half-turn around the focus.

From (5.13), and under the hypotheses of Lemma 5.4, we can assure that $\tau \in \mathcal{I} = (0, \pi)$ for any orbit of the upper system, and therefore the transition map U is smooth. In fact, for $\gamma > 0$ we have

$$\lim_{\tau \to 0^+} u_-(\tau) = \lim_{\tau \to 0^+} u_+(\tau) = -\infty,$$

and

$$\lim_{\tau \to \pi^-} u_-(\tau) = +\infty, \quad \lim_{\tau \to \pi^-} u_+(\tau) = -\infty.$$

We will not study the possible bifurcations when using y_E as the bifurcation parameter, as it has been done in previous chapters. Anyway, we can anticipate that after a saddle-node bifurcation there appear a couple of symmetric periodic orbits.

Remark 5.5. *We can generalize the last argument in the proof of Lemma 5.4 as follows. Orbits with flight time $\tau = k\pi$ are only possible for some distinguished locations of the focus, namely it is needed $\sigma = (-1)^k e^{k\gamma\pi}$, that is*

$$x_E = -\tanh\left(\frac{k\gamma\pi}{2}\right)^{(-1)^{k+1}}.$$

Lemma 5.6. *For system* (5.9) *with $\gamma > 0$ and*

$$-1 < -\tanh\left(\frac{3\gamma\pi}{2}\right) < x_E < -\tanh\left(\frac{\gamma\pi}{2}\right) < 0, \tag{5.16}$$

the orbit starting at $(-1, u_-^c)$ arrives to Σ_+ after a flight time $\tau_-^c \in (2\pi, 3\pi)$. Such an orbit intersects Σ_- at two other points before arriving to Σ_+. Consequently, there exist three points at Σ_- with the same image at Σ_+, namely

$$(-1, u_-^c),\ (-1, u_-^1),\ (-1, u_-^2)$$

with flight times satisfying

$$\tau_2 < \pi < \tau_1 < 2\pi < \tau_-^c < 3\pi.$$

Proof. Condition (5.16) is equivalent to

$$-e^{3\gamma\pi} < \sigma < -e^{\gamma\pi}$$

and then the departure tangent orbit flight time determining equation (5.14) gives that its solution $2\pi < \tau_-^c < 3\pi$, see Figure 5.4. The corresponding orbit

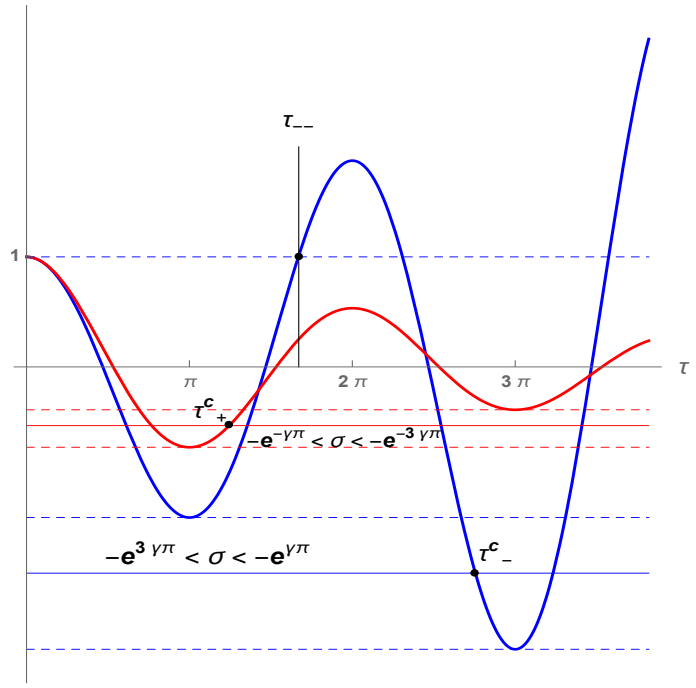

Figure 5.4: The graphs of $\phi_\gamma(\tau)$ (in blue) and $\phi_{-\gamma}(\tau)$ (in red) for $\gamma = 0.1$, where several relevant times are pointed out.

gives more than a complete turn around the focus, so that there exist two other points at Σ_-, as stated.

The first intersection point $(-1, u_-^1)$ is reached after a flight time τ_{--}, so that the time in going from $(-1, u_-^1)$ to Σ_+ is $\tau_1 = \tau_-^c - \tau_{--}$. To see that $\tau_1 > \pi$, it suffices to compute τ_{--} from (5.10) with $x(\tau) = -1$ and $u_- = u_-^c$, obtaining the condition

$$1 = \phi_\gamma(\tau_{--}),$$

where the solution $\tau_{--} \in (2\pi, 3\pi)$. Since

$$\phi_\gamma(\tau_{--} + \pi) = -e^{\gamma\pi}, \quad \phi_\gamma(\tau_-^c) < -e^{\gamma\pi},$$

and $\phi_\gamma(\tau)$ is decreasing for $\tau \in (2\pi, 3\pi)$, we conclude that $\tau_-^c > \tau_{--} + \pi$, and so $\pi < \tau_1 < 2\pi$. The condition $\tau_2 < \pi$ is obvious, and the Lemma follows.

□

Remark 5.7. *From Remark 5.5, we can assure that, under the hypotheses of Lemma 5.6 the transition map U has two discontinuities, see Figure 5.5. This fact introduces extra difficulties in the determination of the bifurcation set, which is excluded of the scope of this chapter, as previously mentioned.*

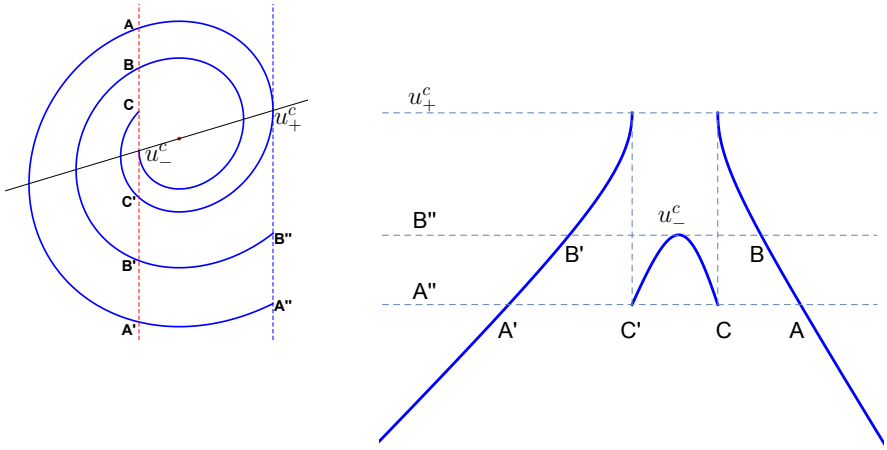

Figure 5.5: The orbits for $\gamma = 0.15$ and $x_E = -0.4 < -\tanh(\gamma\pi/2) \approx -0.231354$, determine a discontinuous transition map.

Our final task is to consider the case in between lemmas 5.4 and 5.6, that is

$$x_E = -\tanh\left(\frac{\gamma\pi}{2}\right).$$

As it will be shown, there exists one orbit with tangency points at the two lines Σ_- and Σ_+. Effectively, if we impose $u_- = y(0) = u^c_-$ and $u_+ = y(\tau) = u^c_+$, as defined above, we obtain the condition

$$\begin{pmatrix} 1 - x_E \\ 2\gamma(1 - x_E) \end{pmatrix} = e^{A\tau} \begin{pmatrix} -1 - x_E \\ -2\gamma(1 + x_E) \end{pmatrix}.$$

The first component gives the equation

$$1 - x_E = -e^{\gamma\tau}(1 + x_E)(\cos\tau - \gamma\sin\tau),$$

while the second component leads to

$$2\gamma(1 - x_E) = -e^{\gamma\tau}(1 + x_E)(2\gamma\cos\tau + (1 - \gamma^2)\sin\tau).$$

Assuming $|x_E| \neq 1$, and dividing the two above equations, we see that

$$2\gamma\cos\tau - 2\gamma^2\sin\tau = 2\gamma\cos\tau + (1 - \gamma^2)\sin\tau,$$

so concluding that

$$(1 + \gamma^2)\sin\tau = 0,$$

that is $\tau = k\pi$, with $k \in \mathbb{N}$. When k is odd, if we go back to the first component then we have

$$1 - x_E = e^{k\gamma\pi}(1 + x_E), \tag{5.17}$$

while for k even we obtain

$$1 - x_E = -e^{k\gamma\pi}(1 + x_E).$$

Here, we only deal with the case $k = 1$, getting from (5.17),

$$1 - x_E = e^{\gamma\pi}(1 + x_E) \iff x_E = \frac{1 - e^{\gamma\pi}}{1 + e^{\gamma\pi}} = -\tanh(\gamma\pi/2). \tag{5.18}$$

Note that for $\tau = \pi$ and the above choice for x_E, in the equality

$$\begin{pmatrix} 1 - x_E \\ u_+ - y_E \end{pmatrix} = e^{\gamma\pi} \begin{pmatrix} -1 & 0 \\ 0 & -1 \end{pmatrix} \begin{pmatrix} -1 - x_E \\ u_- - y_E \end{pmatrix} = e^{\gamma\pi} \begin{pmatrix} 1 + x_E \\ -u_- + y_E \end{pmatrix} \tag{5.19}$$

the first components are always equal, and from the second we deduce that an orbit starting at $(-1, u_-^c)$ arrives at $(1, u_+^c)$ after a time π, when the linear relation

$$u_+ - y_E = e^{\gamma\pi}(-u_- + y_E)$$

is satisfied. Clearly, according to the transition mechanism, we must consider only the values with

$$u_+ \le u_+^c = y_E + 2\gamma(1 - x_E) = y_E + 2\gamma e^{\gamma\pi}(1 + x_E),$$

where we have used (5.18), leading to

$$e^{\gamma\pi}(-u_- + y_E) \le 2\gamma e^{\gamma\pi}(1 + x_E),$$

that is

$$u_- \ge y_E - 2\gamma(1 + x_E) = u_-^c.$$

We can state the following result.

Proposition 5.8. *For $x_E = -\tanh(\gamma\pi/2)$ the upper system in (5.9) has an orbit which is tangent to the two lines $\Sigma_\mp$ at the points $(-1, u_-^c)$ and $(1, u_+^c)$ with a flight time $\tau = \pi$. The transition map U is a continuous function defined for all $u_- \in \mathbb{R}$ and has the following properties, see Figure 5.6.*

(a) For all $u_- \ge u_-^c$ the flight time is π and we have

$$u_+ = U(u_-) = y_E - e^{\gamma\pi}(u_- - y_E),$$

leading to a portion of its graph which, starting at the point

$$(u_-^c, u_+^c) = \left(y_E - \frac{4\gamma}{1 + e^{\gamma\pi}}, y_E + \frac{4\gamma e^{\gamma\pi}}{1 + e^{\gamma\pi}} \right),$$

is a straight line of slope $-e^{\gamma\pi}$.

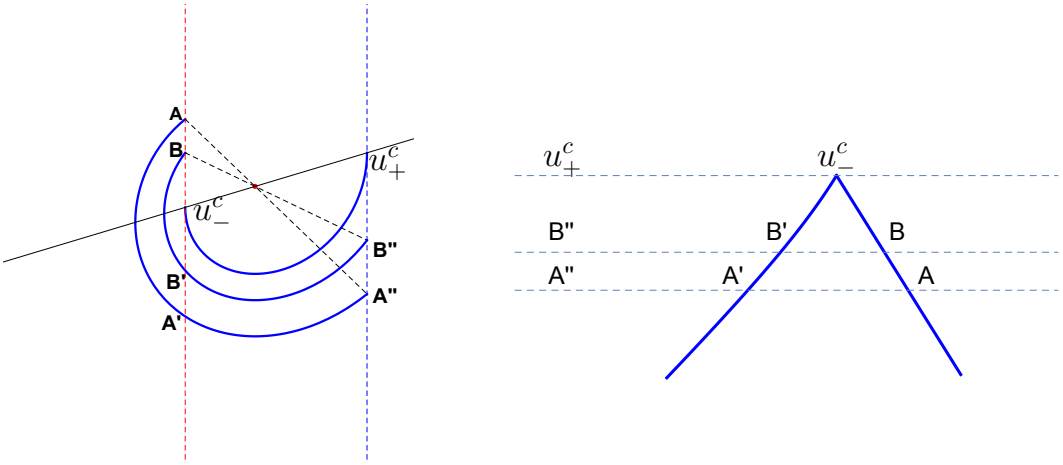

Figure 5.6: The orbits for $\gamma = 0.15$ and $x_E = -\tanh(\gamma\pi/2) \approx -0.231354$, determine a continuous transition map with a corner separating a concave from above curve and a straight line piece.

(b) For all $u_- < u_-^c$ the flight time satisfies $\tau < \pi$ and we have the parametric representation $u_+(\tau) = U(u_-(\tau))$, where

$$u_-(\tau) = y_E - 2\frac{e^{\gamma(\pi-\tau)} + \cos\tau + \gamma\sin\tau}{(1+e^{\gamma\pi})\sin\tau},$$
$$u_+(\tau) = y_E - 2\frac{e^{-\gamma(\pi-\tau)} + \cos\tau - \gamma\sin\tau}{(1+e^{\gamma\pi})\sin\tau}e^{\gamma\pi}, \tag{5.20}$$

so that

$$\lim_{\tau\to 0^+} u_-(\tau) = \lim_{\tau\to 0^+} u_+(\tau) = -\infty,$$
$$\lim_{\tau\to\pi^-} u_-(\tau) = u_-^c, \quad \lim_{\tau\to\pi^-} u_+(\tau) = u_+^c.$$

(c) By introducing the auxiliary function

$$\varphi_\gamma(\tau) = 1 + e^{\gamma(\pi-\tau)}(\cos\tau + \gamma\sin\tau)$$

with $\gamma \in \mathbb{R}$ and $\tau \in [0,\pi]$, we see that $\varphi_\gamma(0) = 1+e^{\gamma\pi}$, $\varphi_\gamma(\pi) = 0$ so that $\varphi_\gamma'(\tau) = -(1+\gamma^2)e^{\gamma(\pi-\tau)}\sin\tau < 0$ and $\varphi_\gamma(\tau) > 0$ for $\tau \in (0,\pi)$. We get

$$u_-'(\tau) = \frac{2\varphi_\gamma(\tau)}{(1+e^{\gamma\pi})\sin^2\tau}, \quad u_+'(\tau) = \frac{2\varphi_{(-\gamma)}(\tau)e^{\gamma\pi}}{(1+e^{\gamma\pi})\sin^2\tau},$$

so that

$$U'(u) = \frac{u_+'(\tau)}{u_-'(\tau)} = \frac{\varphi_{(-\gamma)}(\tau)}{\varphi_\gamma(\tau)}e^{\gamma\pi} > 0,$$

with

$$\lim_{\tau\to 0^+} U'(u_-(\tau)) = 1, \quad \lim_{\tau\to\pi^-} U'(u_-(\tau)) = e^{\gamma\pi},$$

(d) For the second derivative, we have $\operatorname{sign}(U''(u)) = \operatorname{sign}\gamma$ *for all* $\tau \in (0, \pi)$.

Proof. All the computations are direct from the above discussion. Statement (d) comes from the additional computation

$$\begin{aligned} U''(u) &= \frac{u''_+(\tau)u'_-(\tau) - u'_+(\tau)u''_-(\tau)}{u'_-(\tau)^3} = \\ &= \frac{\operatorname{sh}(\gamma(\pi-\tau)) - \gamma\sin\tau}{\varphi_\gamma(\tau)^3}(1+\gamma^2)(1+e^{\gamma\pi})e^{\gamma\pi}\sin^3\tau. \end{aligned}$$

□

Note that Proposition 5.8 is valid also for negative values of γ. For $\gamma = 0$ the graph of U is piecewise linear with two pieces. Hereafter we consider $\gamma > 0$, and we will take y_E as the only bifurcation parameter. Of course, as we are dealing with focus dynamics, the invariant manifold at infinity constitutes a 2π-periodic orbit which becomes attractive under such assumption $\gamma > 0$. This amounts that orbits starting at a point with sufficiently big values of u_- eventually approach such a periodic orbit at infinity.

From Proposition 5.8, we can state the following result, regarding the value

$$y_{BC}(\gamma) = 2\gamma\tanh\left(\frac{\gamma\pi}{2}\right), \tag{5.21}$$

where we advance that the subscript BC is to be reminiscent of boundary crisis. The following result is straightforward.

Lemma 5.9. *Consider system* (5.9) *for* $x_E = -\tanh(\gamma\pi/2)$ *with* $\gamma > 0$ *and the function* $y_{BC}(\gamma)$ *defined in* (5.21). *If* $y_E < y_{BC}(\gamma)$, *then there are no periodic orbits, while for* $y_E = y_{BC}(\gamma)$ *there appears a double tangent orbit symmetrical with respect to the origin.*

Finally, always under the hypothesis of $x_E = -\tanh(\gamma\pi/2)$, we consider the situation when $y_E > y_{BC}(\gamma)$ for $\gamma > 0$.

For the sake of convenience we will work with the map $Q(u) = U(-u)$ with the parametric representation $(-u_-(\tau), u_+(\tau))$.

Remark 5.10. *Note that fixed points of* Q *represent symmetric periodic orbits while period-2 points of* Q *will correspond to non-symmetric periodic orbits.*

Effectively, let $u^* = -u$. *We have symmetric periodic orbits for all values of* u *such that* $U(u)+u = 0$, *and this is equivalent to* $Q(u^*) = U(-u^*) = u^*$, *so that* u^* *is a fixed point for* Q. *Similarly, if* u *corresponds to a non-symmetric periodic orbit, we know that* $U(-U(u)) = -u$, *that is* $U(-U(-u^*)) = u^*$, *and so* $Q(Q(u^*)) = u^*$ *and* u^* *is a period-2 point of* Q.

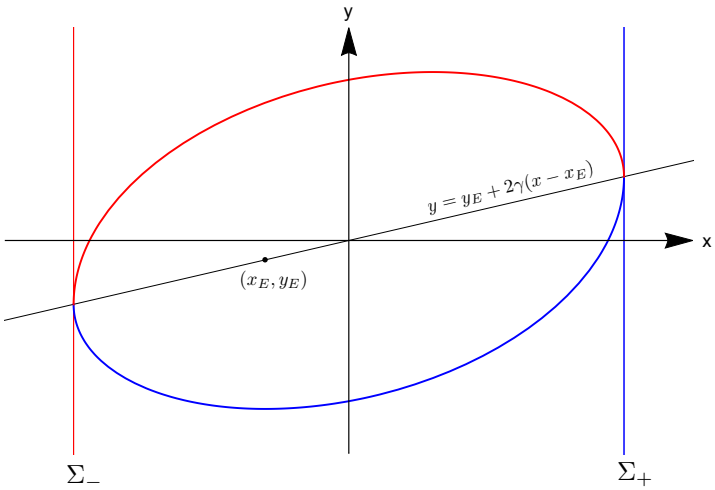

Figure 5.7: In this figure we see the double tangent orbit after a time π. The contact points ordinates u_-^c and u_+^c, are defined in Proposition 5.8.

The following result shows that the map Q can have two fixed point and other two points of period-2.

Proposition 5.11. *Consider system* (5.9) *for* $x_E = -\tanh(\gamma\pi/2)$ *with* $\gamma > 0$ *and the function* $y_{BC}(\gamma)$ *defined in* (5.21)*. Regarding the associated transition map* U*, the map* $Q(u) = U(-u)$ *for* $y_E > y_{BC}(\gamma)$ *has two fixed points and other two points of period-2. Consequently, system* (5.9) *has four periodic orbits, two of them are symmetric and the other two are non-symmetric periodic orbits but forming a symmetric pair. Moreover, the four periodic orbits are unstable.*

Proof. It is easy to see that for $y_E > y_{BC}(\gamma)$ there exist two fixed points of Q and that its corner is above the diagonal of the first quadrant. Without loss of generality, we take the origin to be at the smaller fixed point of Q, see figure 5.8, and use (x_P, y_P) for the coordinates of the corner.

We pay attention to the intervals

$$I_0 = [0, x_P], \quad I_1 = [x_P, x_R],$$

where x_R is a pre-image of the smaller fixed point of Q, and so $Q(x_R) = 0$ with $x_R \neq 0$. The greater fixed point of Q is denoted by x_F. We know that $Q'(x) = e^{\gamma\pi} > 1$ for all $x \in I_0 \backslash \{x_P\}$ and $Q'(x) < -1$ for all $x \in I_1 \backslash \{x_P\}$. Therefore, the corner (x_P, y_P) is above the straight line Γ passing through (x_F, x_F) with slope -1.

Let us introduce the function $Q_{-1}(x)$ as the inverse of the function Q in the interval I_1. Clearly, $Q_{-1}(x_F) = x_F$ and $-1 < Q'_{-1}(x) < 0$ for all $x \in [0, y_P]$. Thus, the point $(x_P, Q_{-1}(x_P))$ is below the line Γ.

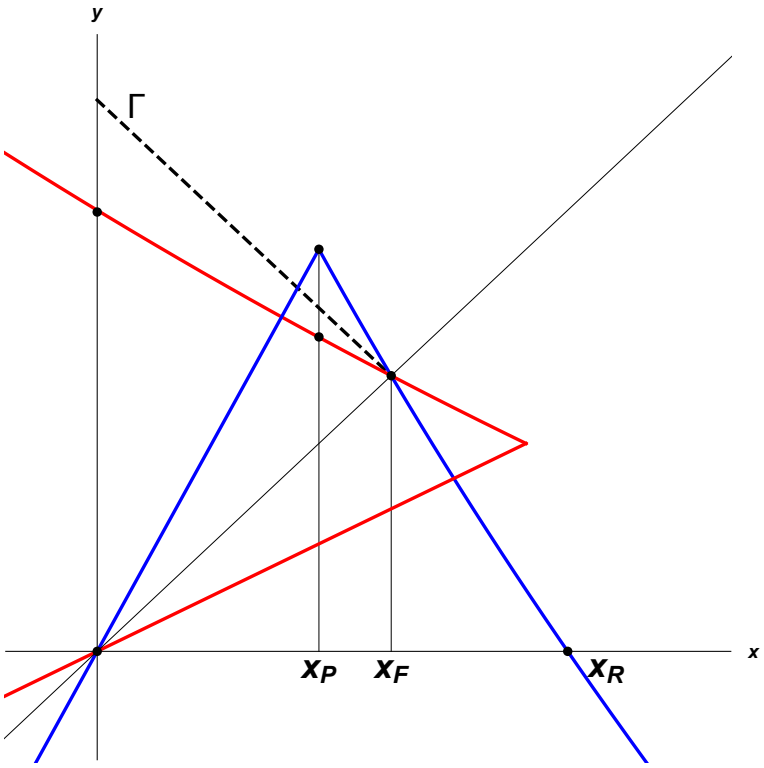

Figure 5.8: In this figure we show the map Q (in blue) and its symmetrical with respect to the diagonal of the first quadrant (in red). Each intersection between both maps represent a periodic orbit. Some remarkable points are indicated.

Using the intermediate value theorem in the interval I_0 for the function $Q_{-1}(x) - Q(x)$, we conclude the existence of a value $x^* \in I_0$ such that

$$Q_{-1}(x^*) = Q(x^*),$$

which leads to $Q^2(x^*) = x^*$. From this period-2 condition, all the assertion follows. The stability comes from the fact that the derivative $|Q'(x)| > 1$ for all $x \neq x_P$. □

Under the hypotheses of Proposition 5.11, we can say that at $y_E = y_{BC}(\gamma)$ there appears a degenerate bifurcation where a non-smooth saddle-node bifurcation of periodic orbits along with a non-smooth pitchfork bifurcation of periodic orbits take place passing from no periodic orbits to four of them.

We will see that under some additional restriction in the parameter γ, the same critical value leads to a rather more complex bifurcation. First, we introduce the following definition.

Definition 5.12. *Consider an interval $I \subset \mathbb{R}$. If $Q(I) \subset I$, then I is a* trapping interval *for the map Q.*

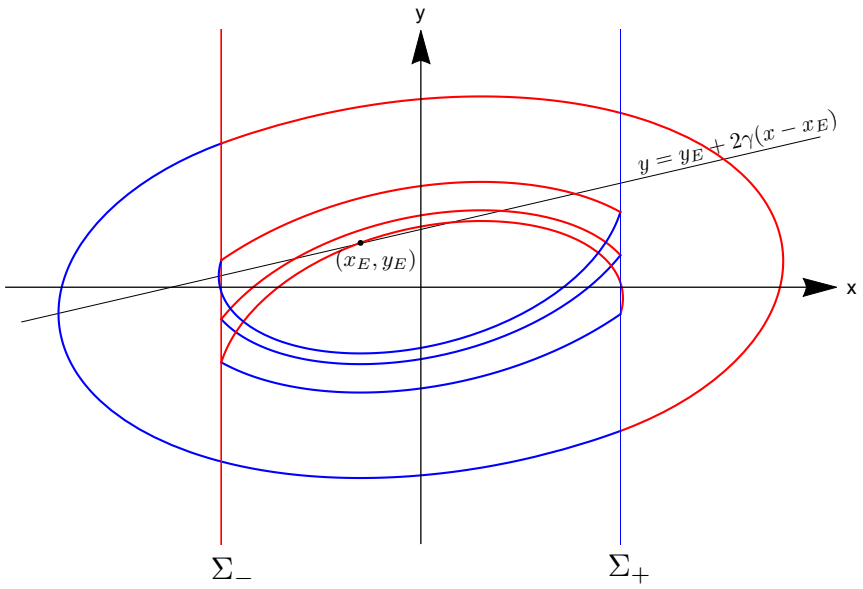

Figure 5.9: Here we show the four periodic orbits existing for $y_E > y_{BC}(\gamma)$ as Proposition 5.11 stated, where two of them are symmetric and the other two form a symmetric pair.

Lemma 5.13. *Whenever* $0 < \gamma\pi < \log 2$*, system* (5.9) *induces a map* Q *which has a trapping interval for all* $y_E > y_{BC}(\gamma)$*.*

Proof. The hypotheses $0 < \gamma\pi < \log 2$ is equivalent to $1 < e^{\gamma\pi} < 2$, and this implies that for the map Q the left part of its graph has a slope in the interval $(1, 2)$, while its right part has a slope in $(-2, -1)$.

Assume again for a given value of γ fulfilling the hypothesis, that the two fixed points of Q are the origin and (x_F, x_F) with $x_F > 0$, see Figure 5.10. Taking as reference the point (x_P, y_P) and using the notation $x_R > 0$ for the point where $Q(x_R) = 0$, we see that $Q([0, x_P]) = [0, y_P]$ and also $Q([x_P, x_R]) = [0, y_P]$. Thus, if $y_P < x_R$ then we can assure that the interval $[0, x_R]$ is invariant for the map Q, that is, $[0, x_R]$ would be a trapping interval, indeed the maximal one.

We claim that the condition for γ assures that $y_P < x_R$. Note that the value $x_R > 2x_P$; otherwise the slope of the right part of the map Q would be less than -2, contrary to our hypothesis. Now,

$$y_P = Q(x_P) = e^{\gamma\pi} x_P < 2x_P < x_R,$$

and the claim follows.

□

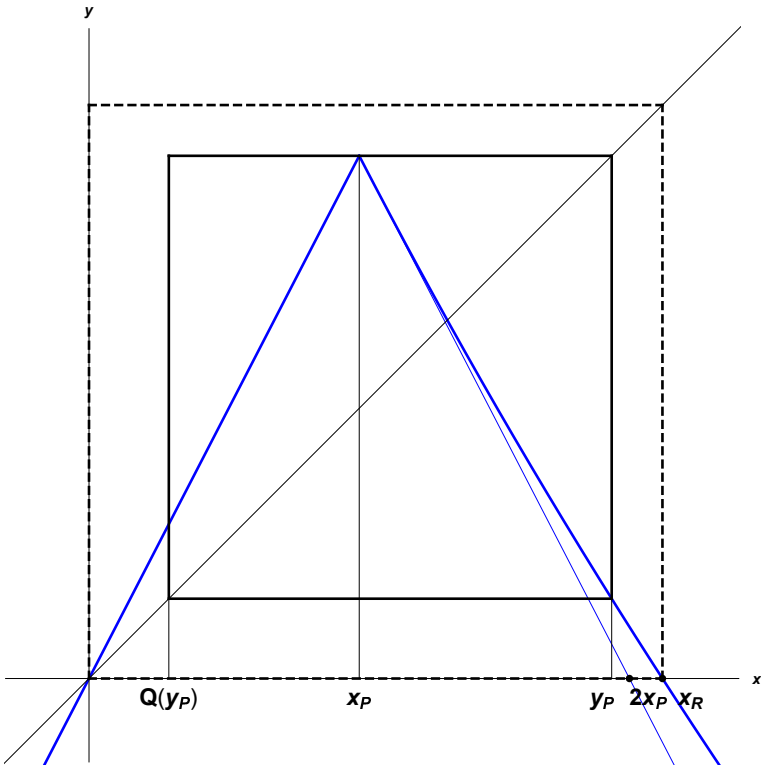

Figure 5.10: In this figure we show the maximal trapping interval $[0, x_R]$ and the optimal trapping interval $[Q(y_P), y_P]$ for the map Q, see Lemma 5.13. Some remarkable points are indicated.

Regarding the proof of Lemma 5.13, it is clear that the interval $[0, x_R]$ is not the optimal trapping interval. In fact, the minimal trapping interval is $[Q(y_P), y_P]$, see Figure 5.10. As a second remark, the restriction on γ in the lemma is somehow conservative, since what it is needed is simply the condition $y_P < x_R$.

Restricting our attention to the minimal trapping interval, that is $[Q(y_P), y_P]$, if we want to study the dynamics on such an invariant set, then we can do a translation and a scale to transform such an interval into the interval $[0, 1]$. In this setting, we can resort to the excellent analysis done by S. Bassein in [5], to show our final result. Other related references are [10] and [50]. We recall from [5] the definition of a chaotic map.

Definition 5.14. *A map $f : S \subset [0, 1] \to S$ is chaotic if the following statements hold.*

(a) The map f is topologically transitive*; that is, if I and J are open intervals, each of which contains a point in S, then there is an $n > 0$ such that $f^n(I \cap S)$ and $J \cap S$ have a point in common.*

(b) Periodic points are dense *in S; that is, if I is an open interval that contains a point of S, then it contains a periodic point in S.*

Theorem 5.15. *Consider system* (5.9) *for $x_E = -\tanh(\gamma\pi/2)$ with $0 < \gamma\pi < \log 2$. Then, the system has a chaos boundary crisis bifurcation at $y_E = y_{BC}(\gamma)$. More precisely, for $y_E > y_{BC}(\gamma)$ system* (5.9) *induces a transition map Q which has a trapping interval I, and it is chaotic in the whole interval or at least in a subset of I.*

Proof. Again we assume that for a given value of γ fulfilling the hypothesis, that the two fixed points of Q are the origin and (x_F, x_F) with $x_F > 0$, see Figure 5.10. The existence of the trapping interval for the associated map Q is guaranteed by Lemma 5.13. To study the dynamics on such a trapping interval, we can follow step by step all the arguments that appear for the piecewise linear map in [5]. Note that, although our map has a piece which is not linear, the key point is that the derivative of the map Q satisfies $|Q'(x)| > 1$ for all $x \in \mathbb{R} \setminus \{x_P\}$.

As in [5], two cases has to be considered, depending on the relative size of the ordinates of points $(Q(y_P), Q^2(y_P))$ and (x_F, x_F). When $Q^2(y_P) \leqslant x_F$, the dynamics of Q is chaotic in the whole trapping interval I, while for $Q^2(y_P) > x_F$, the chaotic behaviour is restricted to a subset of I. For a detailed reasoning, see Sections 3-4 and 5 of [5] respectively. Finally, the chaotic behaviour of the map Q can be translated to our system (5.9) by recalling that the global transition map is Q^2 and so proper fixed points of Q^{2n} with $n \in \mathbb{N}$ represent periodic orbits for our system.

□

Just to illustrate the phenomenon described in our last result, we consider two different cases that correspond to chaos in the whole trapping interval and chaos in a subset of it. Thus, for $\gamma = 0.2$ and $y_E = 0.621686 > y_{BC}(\gamma) \approx 0.121686$, we obtain a chaotic behaviour in the whole trapping interval, see Figure 5.11, which exhibits a symmetric chaotic attractors. However, for $\gamma = 0.2$ with $y_E = 1.12169$, we obtain a chaotic behaviour in a subset of the trapping interval, see Figure 5.12, which corresponds to a symmetric pair os chaotic attractors. In both cases, it should be noticed that in the attractors, the orbits spend a time less than π between any two consecutive jumps, a characteristic which is different from the chaotic attractors already known, see [35, 36] and [45–47].

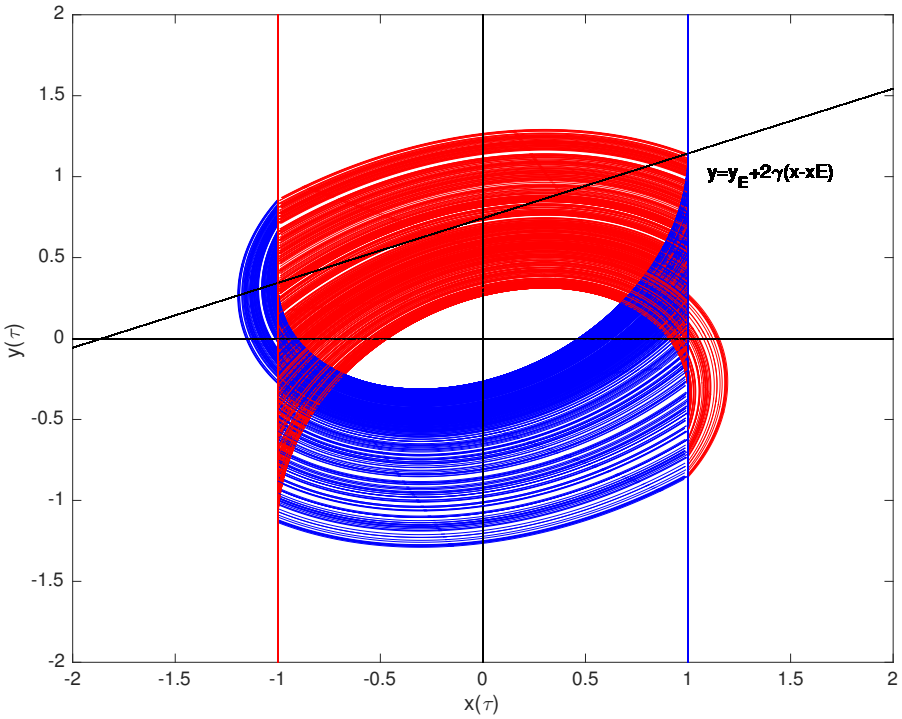

Figure 5.11: Symmetric chaotic attractor of system (5.9) for $\gamma = 0.2$, $x_E = -\tanh(\gamma\pi/2)$ and $y_E = 0.621686 > y_{BC}(\gamma)$.

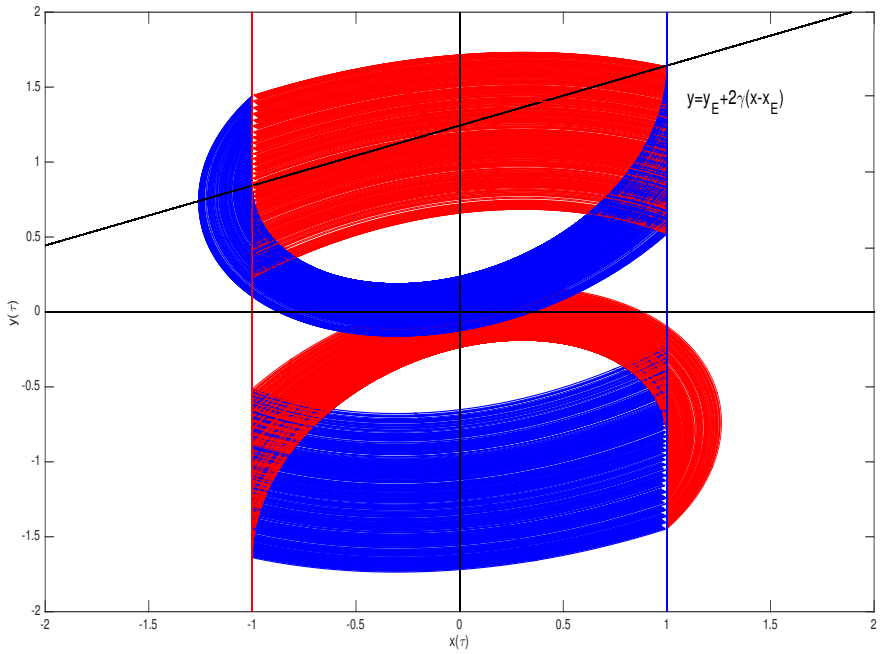

Figure 5.12: A symmetric pair of chaotic attractors of system (5.9) for $\gamma = 0.2$, $x_E = -\tanh(\gamma\pi/2)$ and $y_E = 1.12169 > y_{BC}(\gamma)$.

Chapter 6

Conclusions

In this thesis the study of some symmetric bidimensional linear systems with hysteresis associated to two switching lines has been done. After an introduction containing several preliminary results, four additional chapters include the main results and their proofs. Also, two appendices are offered, where some non-generic cases are considered.

We have investigated two dimensional hysteretic systems coming from a reduction, by using the relaxation hypothesis, of symmetric three dimensional slow-fast piecewise linear systems with three zones. We have shown that, under generic conditions, such hysteretic systems can be written in a Liénard canonical form. When the matrix is regular, an additional change of variables and time allows us to rewrite our systems in a normalized canonical form with only an essential parameter along with a modal parameter which discriminates the spectrum of the involved matrices. Accordingly, we have divided the study of the dynamics in separated chapters for each value of the modal parameter.

In Chapter 2, hysteretic systems with a zero eigenvalue have been studied and we have shown that the possible periodic orbits are always symmetric. Regarding the case corresponding to a double zero eigenvalue, we have studied the behaviour of the system near the invariant manifold at infinity, getting bifurcations leading to periodic orbits. In the most general cases, apart from the bifurcations associated to the behaviour near infinity, we have found a saddle-node bifurcation and other less well-known ones, as is the case for the grazing bifurcations. All the bifurcation curves have been analytically characterized. Finally, we have emphasized the usefulness of the analysis of hysteretic systems in the study of periodic orbits in 3D piecewise linear systems, by showing how the results obtained for the planar hysteretic systems can be transferred to such systems in $\mathbb{R}^3$. Here, we have been enforced to work with a Liénard canonical form that cannot be normalized, while in the rest of our work the number of parameters can be reduced. The material of this chapter is essentially the

same as in reference [17], submitted for publication.

In Chapter 3, the case of single non-zero real eigenvalues is studied. Here the situation is more involved and as in the remaining cases, we have taken advantage of the normalized canonical form. Next, to determine the existence of periodic orbits, we have studied the properties of the transition map, taking into account different locations and type of equilibria. In theses cases, it is remarkable how, dealing only with real eigenvalues, the achieved structure of periodic orbits is by no means trivial. Different bifurcations involving periodic orbits have been emphasized, and a precise mathematical characterization of all the corresponding parameter bifurcation values has been obtained. In particular, the existence of a saddle-node bifurcation of periodic orbits along with the pitchfork bifurcation of one of the two periodic orbits generated, provides a situation with four different periodic orbits, being stable only the two non-symmetric periodic orbits. The usefulness of the followed approach in detecting periodic orbits in the original 3D systems has been stressed. The material of this chapter is essentially the same as in reference [18], submitted for publication.

In Chapter 4, the same strategy is followed for the case of non-zero double eigenvalue. The complexity level of the structure of periodic orbits is basically the same as before.

In Chapter 5, we have studied the case of complex eigenvalues. In the case where the eigenvalues have zero real part, we have assured the existence of a continuum of periodic orbits when the equilibria are located on the y-axis, otherwise one symmetric periodic orbit can exist at most. On the contrary, when the real part of the eigenvalues is different from zero, the situation is more complex. Here, we have restricted our analysis to the special case where the equilibria are repulsive foci and there exists an orbit which is tangent to both switching lines. In this situation, we have found a parameter region where a chaos boundary crisis bifurcation has been shown.

In appendices A and B, some non-generic cases are considered. In Appendix A, we have studied the dynamics when the system cannot be transformed in the Liénard canonical form. In Appendix B, we have dealt with some cases where the eigenvalues take specific values, which facilitate the computation of the return map.

Appendix A

Canonical form for the Non-Liénard Case

The Liénard canonical form (1.5) can be obtained under the hypothesis $a_{12} \neq 0$ for the initial matrix A_0 in system (1.1). In this Appendix, we deal with the non-Liénard case, that is $a_{12} = 0$. Then, in the following we will study the global system S_U-S_L

$$\begin{cases} x' = a_{11}x \pm b_1, \\ y' = a_{21}x + a_{22}y \pm b_2, \end{cases} \qquad \pm x \leqslant 1, \tag{A.1}$$

which comes from (1.3)-(1.4) by assuming $\widetilde{a}_{12} = 0$ and by dropping the tildes.

Note that for an orbit of the upper system, the derivative of the variable x at the lines Σ_- and Σ_+ is

$$x'|_{x=\pm 1} = b_1 \pm a_{11},$$

so that it is constant along each line. According to the transition mechanism introduced in Chapter 1, to get a periodic orbit we need that an orbit of the upper system, which departs from the line Σ_- arrives at the falling line Σ_+. Then, we must have $x' > 0$ at both lines $\Sigma_\mp$, getting the condition $b_1 \pm a_{11} > 0$, or equivalently, $|a_{11}| < b_1$ for the existence of periodic orbits. Thus, we give the following result about the existence of periodic orbits.

Proposition A.1. *A necessary condition for the existence of periodic orbits for system* (A.1) *is* $|a_{11}| < b_1$. *Consequently, if* $b_1 \leqslant 0$, *then there are no periodic orbits.*

Remark A.2. *Hereafter, we assume the two inequalities* $b_1 > 0$ *and* $|a_{11}| < b_1$, *so that periodic orbits are possible in system* (A.1).

These conditions imply that the only type of orbits that exist are lens-type orbits, because cloud orbits require a change on the sign of the derivative x'.

In order to get a canonical form, we make the following change of variables

$$v = x, \quad w = \alpha x + y, ,$$

which transform the upper system in (A.1) into

$$\begin{array}{rcl} v' & = & a_{11}v + b_1, \\ w' & = & (\alpha(a_{11} - a_{22}) + a_{21})v + a_{22}w + \alpha b_1 + \beta b_2. \end{array} \tag{A.2}$$

The eigenvalues of the linear part of system (A.2) are $\lambda = a_{11}$ and $\mu = a_{22}$. Thus, different cases arise by considering the quoted eigenvalues.

(a) If $a_{11} = a_{22}$, then system (A.2) has a double eigenvalue λ and we distinguish the following three cases.

(a.1) If $a_{21} = 0$, then system (A.2) can be rewritten, after renaming the parameters, as

$$\left\{ \begin{array}{l} x' = \lambda x + b_1, \\ y' = \lambda y + b_2. \end{array} \right. \tag{A.3}$$

(a.2) If $a_{21} > 0$, then after the following change of variables

$$v = x, \quad w = a_{21}y,$$

and renaming the parameters, system (A.2) can be rewritten as

$$\left\{ \begin{array}{l} x' = \lambda x + b_1, \\ y' = x + \lambda y + b_2. \end{array} \right. \tag{A.4}$$

(a.3) If $a_{21} < 0$, then after the change of variables

$$v = x, \quad w = -a_{21}y,$$

and renaming the parameters, system (A.2) can be rewritten as

$$\left\{ \begin{array}{l} x' = \lambda x + b_1, \\ y' = -x + \lambda y + b_2. \end{array} \right. \tag{A.5}$$

(b) If $a_{11} \neq a_{22}$, then system (A.2) has two real eigenvalues. After an appropriated change of variables and renaming parameters if necessary, we can rewrite system (A.2) in the form

$$\left\{ \begin{array}{l} x' = \lambda x + b_1, \\ y' = \mu y + b_2. \end{array} \right. \tag{A.6}$$

Effectively, if $a_{21} = 0$, then system (A.1) is already written in the form (A.6). If $a_{21} \neq 0$, then it is enough to select

$$\alpha = \frac{a_{21}}{a_{22} - a_{11}},$$

in system (A.2).

Next, we will analyze the existence of periodic orbits in systems (A.3)-(A.6). Then according to Proposition A.1, we assume $|\lambda| < b_1$ and $b_1 > 0$.

Case (a.1). One double eigenvalue with $a_{21} = 0$.

When $a_{21} = 0$, our initial system can be written in the form (A.3). We consider the two cases $\lambda = 0$ and $\lambda \neq 0$.

If $\lambda = 0$, there is no equilibrium point and every straight line $y = b_2/b_1 x + C$ is a solution of the system. Then, there exists infinitely many periodic orbits of rectangular type.

If $\lambda \neq 0$, then, there is one equilibrium located at the point $(x_E, y_E) = (-b_1/\lambda, -b_2/\lambda)$ which is a stable star for $\lambda < 0$ and an unstable star if $\lambda > 0$. Thus, from the necessary condition for the existence of periodic orbits (see Proposition A.1), we need $x_E < -1$ for $\lambda > 0$ or $x_E > 1$ for $\lambda < 0$. By computing the solutions of system (A.3), we see that all the trajectories are the straight lines $y = y_E + (x - x_E) + C$. To obtain the transition map U, as in the Liénard case, we impose that the trajectories pass through the points $(-1, u_-)$ and $(1, u_+)$, then $U(u_-)$ is

$$U(u_-) = u_- + 2. \tag{A.7}$$

It is easy to see that there exists only one non-hyperbolic symmetric periodic orbit corresponding to the pair $(u_-, u_+) = (-1, 1)$. And there exist infinitely many non-symmetric periodic orbits because the global transition map verifies $L \circ U = (-U) \circ (-U) = id$.

Case (a.2). One double eigenvalue with $a_{21} > 0$.

In this case, our initial system can be written in the form (A.4).

For $\lambda = 0$, there is no equilibrium point. The solutions are the parabolas

$$y = \frac{x^2}{2b_1} + \frac{b_2}{b_1} x + C.$$

The transition map U is

$$U(u) = u + \frac{2b_2}{b_1}. \tag{A.8}$$

Then, there exists only one symmetric periodic orbit which is non-hyperbolic corresponding to the value $u = -b_2/b_1$, and infinitely many non-symmetric periodic orbits, because the global transition map $L \circ U = (-U) \circ (-U) = id$.

If $\lambda \neq 0$, then the system has one equilibrium at the point $(x_E, y_E) = (-b_1/\lambda, -b_2/\lambda + b_1/\lambda^2)$, which is an improper node, stable for $\lambda < 0$ and unstable for $\lambda > 0$. According to Proposition A.1, periodic orbits can exist only when $|x_E| > 1$. The solutions are

$$\begin{aligned} x(\tau) &= x_E + e^{\lambda\tau}(x_0 - x_E) \\ y(\tau) &= y_E + e^{\lambda\tau}[(x_0 - x_E)\tau + (y_0 - y_E)]. \end{aligned}$$

The transition map U satisfies

$$\rho U(u) = (\rho - 1)y_E + \frac{\log \rho}{\lambda}(x_E + 1) + u, \tag{A.9}$$

where the parameter ρ is defined in (1.24). This transition map verifies the condition $U(u) + u = 0$ only for

$$u = \frac{1-\rho}{1+\rho}y_E - \frac{\log \rho}{\lambda(1+\rho)}(x_E + 1).$$

This point represents a symmetric periodic orbit which is stable when $\rho > 1$, that is $x_E > 1$, and unstable for $\rho < 1$ that is $x_E < -1$. We can assure that non-symmetric periodic orbits do not exist for this case, because condition (a) of Proposition 1.7 is not satisfied.

Case (a.3). One double eigenvalue with $a_{21} < 0$.

In this case, our initial system can be written in the form (A.5).

Assume that $\lambda = 0$, then we do not have any equilibrium point and the solutions are

$$y = \frac{-x^2}{2b_1} + \frac{b_2}{b_1}x + C.$$

So that, the transition map U is given by (A.8). Then, we have only one non-hyperbolic symmetric periodic orbit and infinitely many non-symmetric periodic orbits.

When $\lambda \neq 0$, the system has one equilibrium at the point $(x_E, y_E) = (-b_1/\lambda, -b_2/\lambda - b_1/\lambda^2)$, which is an improper node, stable for $\lambda < 0$ and unstable for $\lambda > 0$. According to Proposition A.1, we need the condition $|x_E| > 1$ to get a periodic orbit. The solutions are

$$\begin{aligned} x(\tau) &= x_E + e^{\lambda\tau}(x_0 - x_E) \\ y(\tau) &= y_E + e^{\lambda\tau}\left(-(x_0 - x_E)\tau + (y_0 - y_E)\right) \end{aligned}$$

The transition map U is

$$\rho U(u) = (\rho - 1)y_E - \frac{\log \rho}{\lambda}(x_E + 1) + u, \tag{A.10}$$

where the parameter ρ defined in (1.24). This transition map U satisfies the condition $U(u) + u = 0$ only at the value

$$u = \frac{1-\rho}{1+\rho}y_E + \frac{\log \rho}{\lambda(1+\rho)}(x_E + 1).$$

This point represents a symmetric periodic orbit which is stable when $\rho > 1$, that is $x_E > 1$ and unstable when $\rho < 1$, that is $x_E < -1$. For this case, similarly with the previous one, condition (a) of Proposition 1.7 is not satisfied, so the existence of non-symmetric periodic orbits is not possible.

Case (b). Two real eigenvalues.

Finally, consider system (A.6). Assuming that the two eigenvalues are different from zero, the system has one equilibrium at the point $(x_E, y_E) = (-b_1/\lambda, -b_2/\mu)$, which is a node if $\lambda\mu > 0$ or a saddle if $\lambda\mu < 0$. According to Proposition A.1, the condition $|x_E| > 1$ must be satisfied to get periodic orbits. The solutions of system (A.6) are

$$\begin{aligned} x(\tau) &= x_E + e^{\lambda\tau}(x_0 - x_E), \\ y(\tau) &= y_E + e^{\mu\tau}(y_0 - y_E). \end{aligned}$$

Direct computations show that the transition map U is

$$U(u) = (1 - \rho^{-\mu/\lambda})y_E + \rho^{-\mu/\lambda}u,$$

where ρ is defined in (1.24). Then, the map U satisfies the equality $U(u)+u = 0$ only for the value

$$u = \frac{\rho^{-\mu/\lambda} - 1}{\rho^{-\mu/\lambda} + 1} y_E,$$

which represents a symmetric periodic orbit, stable for $|\rho^{-\mu/\lambda}| < 1$ and unstable for $|\rho^{-\mu/\lambda}| > 1$. In conclusion, on the one hand, if the equilibrium point is a saddle, that is $\lambda\mu < 0$, then there exists a stable symmetric periodic orbit only if $|\rho| < 1$ which is equivalent to $x_E < -1$. On the other hand, if the equilibrium point is a node, that is $\lambda\mu > 0$, then we must have $|\rho| > 1$ to get a periodic orbit, or equivalently, $x_E > 1$.

From Proposition 1.7(a), we deduce that the existence of non-symmetric periodic orbits is not possible in the case of two real eigenvalues different from zero.

Assume now one zero eigenvalue, let us say $\lambda = 0$ and $\mu \neq 0$. The upper system is

$$\begin{cases} x' = b_1 \\ y' = \mu y + b_2 \end{cases} \tag{A.11}$$

which has not equilibria. The solutions are

$$\begin{aligned} x(\tau) &= b_1\tau + x_0, \\ y(\tau) &= -\frac{b_2}{\mu} + \left(y_0 + \frac{b_2}{\mu}\right) e^{\mu\tau}. \end{aligned}$$

The transition map U is

$$U(u) = \frac{b_2}{\mu}(e^{\frac{2\mu}{b_1}} - 1) + e^{\frac{2\mu}{b_1}}u.$$

From Proposition 1.7(a), it follows that non-symmetric periodic orbits do not exist. The transition map U satisfies the condition $U(u) + u = 0$ only at the value

$$u = \frac{b_2 \left(1 - 2\mathrm{ch}\left(\frac{2\mu}{b_1}\right)\right)}{\mu\,\mathrm{sh}\left(\frac{2\mu}{b_1}\right)}.$$

Such a point represents a symmetric periodic orbit, which is unstable for $\mu > 0$ and stable for $\mu < 0$.

When $\mu = 0$ and $\lambda \neq 0$, the upper system is

$$\begin{cases} x' = \lambda x + b_1, \\ y' = b_2, \end{cases} \tag{A.12}$$

which has no equilibria. The solutions are

$$\begin{aligned} x(\tau) &= -\frac{b_1}{\lambda} + \left(x_0 + \frac{b_1}{\lambda}\right) e^{\lambda\tau}, \\ y(\tau) &= b_2\tau + y_0. \end{aligned}$$

The transition map U is

$$U(u) = \frac{b_2}{\lambda} \log\left(\frac{\lambda + b_1}{-\lambda + b_1}\right) + u.$$

A non-hyperbolic symmetric periodic orbit appears for the value

$$u = -\frac{b_2}{2\lambda} \log\left(\frac{\lambda + b_1}{-\lambda + b_1}\right).$$

The global transition map is the identity, so there exist infinitely many non-symmetric periodic orbits for the case $\mu = 0$.

Appendix B

Algebraically computable cases

In general, the τ-parametric expressions of the transition map U are transcendental ones, so that it is not possible to eliminate the parameter τ for obtaining direct explicit expressions that guarantee the existence of periodic orbits. However, when dealing with single real non-zero eigenvalues, it is possible to choose specific values for the parameter γ so that the problem of existence of periodic orbits can be transformed in an algebraic problem. The idea is to get real eigenvalues whose ratio is a rational number as done in some previous works, see [31, 40, 41]. In fact, as we show below, every rational value of γ can be analyzed following this approach. We only will treat in detail a couple of cases for illustrating such possibility.

B.1 Node cases

In stable node cases, the two real eigenvalues, say λ_1 and λ_2, have the same (negative) sign. Let us consider $p, q \in \mathbb{N}$ such that $\gcd(p, q) = 1$ and take $a > 0$, so that $\lambda_1 = -pa < 0$ and $\lambda_2 = -qa < 0$. We know that the entries of the corresponding exponential matrix can be written in terms of the exponentials

$$e^{-pa\tau}, \quad e^{-qa\tau},$$

so that if we introduce the auxiliary variable

$$v = e^{-a\tau} \in (0, 1)$$

then we see that

$$e^{-pa\tau} = v^p, \quad e^{-qa\tau} = v^q,$$

and so the exponential matrix can be written in terms of rational functions in the new time-like variable $v \in (0, 1)$. Since the trace of the matrix of the system will be $t = -(p+q)a$, in our canonical form for the node case we must

have $2\gamma = -(p+q)a$. Also, for the determinant of the matrix we must have $\gamma^2 - 1 = \lambda_1\lambda_2 = pqa^2$. We have so

$$\frac{(q+p)^2a^2}{4} - 1 - pqa^2 = 0,$$

Finally, we obtain

$$\frac{(q-p)^2a^2}{4} - 1 = 0.$$

$$a = \frac{2}{|p-q|}, \quad \gamma = -\frac{p+q}{|p-q|}.$$

For instance, the simplest case $(p,q) = (2,1)$ leads to $a = 2$, $\lambda_1 = -pa = -4$, $\lambda_2 = -qa = -2$ and $\gamma = -3$.

For unstable nodes, we can assume $a > 0$, $\lambda_1 = pa > 0$ and $\lambda_2 = qa > 0$. As before, p, $q \in \mathbb{N}$ such that $\gcd(p,q) = 1$ and $v = \exp(-a\tau)$, so that

$$e^{pa\tau} = v^{-p}, \quad e^{qa\tau} = v^{-q}.$$

Everything is similar, and we get

$$a = \frac{2}{|p-q|}, \quad \gamma = \frac{p+q}{|p-q|}.$$

Let us consider in more detail the simplest unstable node case $(p,q) = (2,1)$, which leads to $a = 2$, $\lambda_1 = pa = 4$, $\lambda_2 = qa = 2$ and $\gamma = 3$. We know that

$$\begin{pmatrix} 1 - x_E \\ u_+ - y_E \end{pmatrix} = e^{A\tau} \begin{pmatrix} -1 - x_E \\ u_- - y_E \end{pmatrix},$$

We obtain that

$$e^{A\tau} = \exp\left[\begin{pmatrix} 2\gamma & -1 \\ \gamma^2 - 1 & 0 \end{pmatrix}\tau\right] = \frac{1}{2}\begin{pmatrix} -2e^{2\tau} + 4e^{4\tau} & e^{2\tau} - e^{4\tau} \\ -8e^{2\tau} + 8e^{4\tau} & 4e^{2\tau} - 2e^{4\tau} \end{pmatrix},$$

and defining $v = \exp(-2\tau) \in (0,1)$, we get that the matrix exponential in terms of v is

$$\frac{1}{2v^2}\begin{pmatrix} 4 - 2v & v - 1 \\ 8 - 8v & 4v - 2 \end{pmatrix}.$$

Thus,

$$\begin{pmatrix} 1 - x_E \\ u_+ - y_E \end{pmatrix} = \frac{1}{2v^2}\begin{pmatrix} 4 - 2v & v - 1 \\ 8 - 8v & 4v - 2 \end{pmatrix}\begin{pmatrix} -1 - x_E \\ u_- - y_E \end{pmatrix},$$

and solving for $u_-(v)$ and $u_+(v)$ we get

$$u_-(v) = y_E + 2\frac{(1+x_E)(2-v) + (1-x_E)v^2}{v-1} \tag{B.1}$$

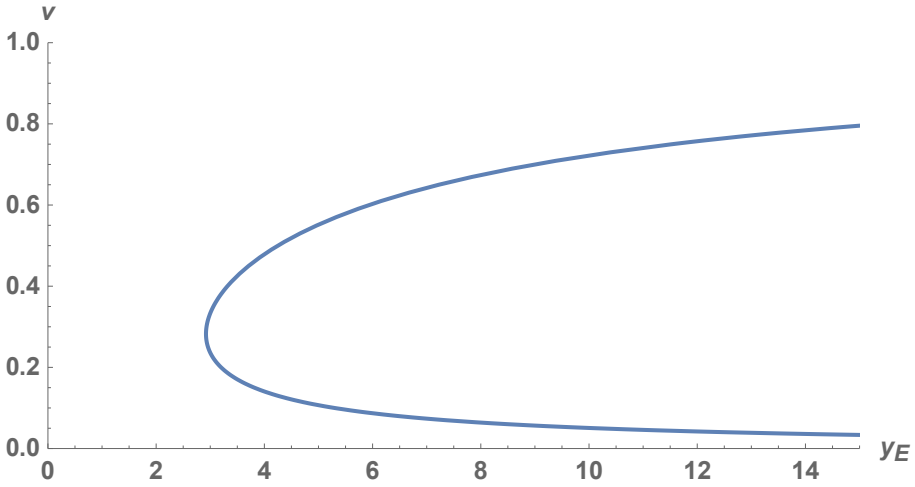

Figure B.1: The bifurcation set for symmetric periodic orbits in the case of unstable node with $\gamma = 3$ and $x_E = -1/2$. We can observe a saddle node bifurcation at $y_E \approx 2.92107$, a value which can be computed by solving a polynomial equation.

and

$$u_+(v) = y_E + 2\frac{(1+x_E)+(1-x_E)(2v+1)v}{v(v-1)} \tag{B.2}$$

so that the condition $u_-(v)+u_+(v) = 0$, for having a symmetric periodic orbit, becomes

$$y_E = \frac{(1+x_E)(v^2-2v-1)-(1-x_E)v(v^2+2v-1)}{v(v-1)}. \tag{B.3}$$

Therefore, once fixed the value of x_E, we get an algebraic expression that allows to plot in terms of the auxiliary variable v the bifurcation diagram telling us the number of symmetric periodic orbits depending on the value of y_E, see Figure B.1.

In the case of non-symmetric periodic orbits, we must solve for two different times τ_1 and τ_2 the two equations

$$\begin{aligned} u_-(\tau_1) + u_+(\tau_2) &= 0, \\ u_-(\tau_2) + u_+(\tau_1) &= 0, \end{aligned} \tag{B.4}$$

where we can introduce two auxiliary variables $v = \exp(-a\tau_1) \in (0,1)$ and $w = \exp(-a\tau_2) \in (0,1)$ to get an algebraic system of equations. For our detailed case $\gamma = 3$, from the expressions in (B.1)-(B.2), after removing a

constant factor 2, we get the system

$$y_E + \frac{(1+x_E)(2-v)+(1-x_E)v^2}{v-1} + \frac{(1+x_E)+(1-x_E)(2w+1)w}{w(w-1)} = 0,$$

$$y_E + \frac{(1+x_E)(2-w)+(1-x_E)w^2}{w-1} + \frac{(1+x_E)+(1-x_E)(2v+1)v}{v(v-1)} = 0,$$

which, after multiplying by $(v-1)w(w-1)$ and $v(v-1)(w-1)$ respectively, leads to a pair of polynomial equations, namely

$$\begin{aligned}(v-1)w(w-1)y_E + (1+x_E)\Phi_+(v,w) + (1-x_E)\Phi_-(v,w) = 0,\\ v(v-1)(w-1)y_E + (1+x_E)\Phi_+(w,v) + (1-x_E)\Phi_-(w,v) = 0,\end{aligned}$$

with

$$\Phi_+(v,w) = -vw^2 + vw + v + 2w^2 - 2w - 1$$

and

$$\Phi_-(v,w) = w\left(v^2w - v^2 + 2vw - v - 2w + 1\right).$$

Computing now the resultant of the polynomials in the left hand side, to eliminate w, we get the expression

$$-2(v-1)^3 E_1(v,x_E,y_E)E_2(v,x_E,y_E) = 0,$$

where

$$E_1(v,x_E,y_E) = (1+x_E)(1-2v-v^2) + (1-x_E)v\left(v^2+2v-1\right) + v(v-1)y_E$$

and

$$E_2(v,x_E,y_E) = 4x_E\left(v^2x_E - v^2 + v - x_E - 1\right) - (v-1)(vx_E - v + x_E + 1)y_E.$$

We can observe that the condition $E_1(v,x_E,y_E) = 0$ reproduces the known solution (B.3) for y_E corresponding to symmetric periodic orbits, but now the condition $E_2(v,x_E,y_E) = 0$ (whenever it provides admissible values for v and w) leads to non-symmetric periodic orbits satisfying

$$y_E = 4x_E\frac{(v^2x_E - v^2 + v - x_E - 1)}{(v-1)(vx_E - v + x_E + 1)}. \tag{B.5}$$

For instance, when $x_E = -1/2$ we conclude from (B.3) that there appears a symmetric periodic orbit for

$$y_E = \frac{3v^3 + 5v^2 - v + 1}{2(1-v)v},$$

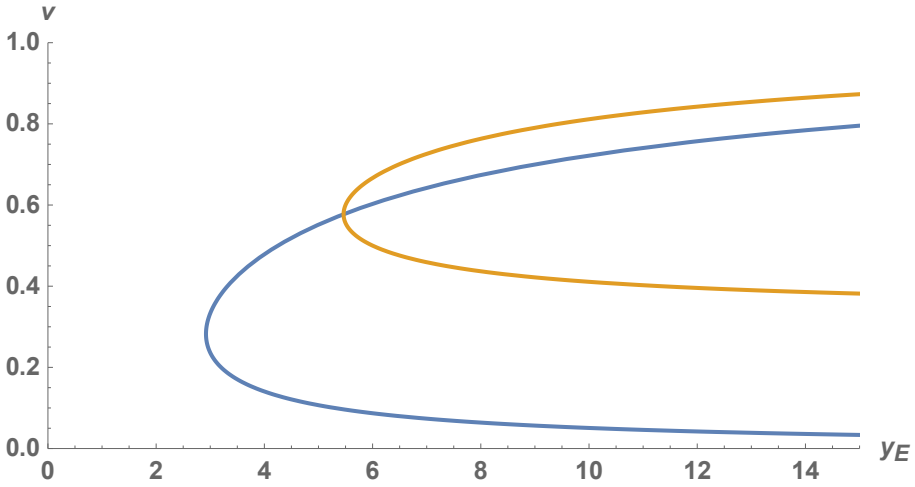

Figure B.2: The complete bifurcation diagram for symmetric periodic orbits in the case of unstable node with $\gamma = 3$ and $x_E = -1/2$. We can observe that, apart from the saddle node bifurcation of periodic orbits at $y_E \approx 2.92107$, there appears a pitchfork bifurcation of periodic orbits for $y_E = 2(1+\sqrt{3})$. Both values can be computed by solving polynomial equations. For $y_E > 2(1+\sqrt{3})$ we have 4 periodic orbits, two of them are symmetric and the other two form a symmetric pair of non-symmetric periodic orbits.

and from (B.5) we can assure the appearance of a non-symmetric periodic orbit for

$$y_E = 2\frac{3v^2 - 2v + 1}{(1-v)(3v-1)},$$

leading to the bifurcation diagram of Figure B.2. These computations are in perfect agreement with statement (b) of Theorem 3.7, where the stability of different periodic orbits is also determined. Even if we could determine such stability from the above algebraic expressions, we will not do it for the sake of brevity, as we already have such information and our goal was to show how is posible in these cases to compute algebraically the bifurcation diagram.

B.2 Saddle cases

As in the node case, it is possible to choose some values of the parameter γ for which we are able to get algebraic expressions for the parametric representation of the transition map U. In a saddle system, we will take $a > 0$, $\lambda_1 = pa > 0$ and $\lambda_2 = -qa < 0$. As before, p, $q \in \mathbb{N}$ such that $\gcd(p,q) = 1$ and we take $v = \exp(-a\tau)$, so that

$$e^{pa\tau} = v^{-p}, \quad e^{-qa\tau} = v^q.$$

Thus, the trace of the matrix of the system will be $2\gamma = (p-q)a$, and for the determinant of the matrix we will have $\gamma^2 - 1 = \lambda_1\lambda_2 = -pqa^2$. We have so

$$\frac{(p-q)^2a^2}{4} - 1 + pqa^2 = 0,$$

Finally, we obtain

$$\frac{(p+q)^2a^2}{4} - 1 = 0,$$

so that

$$a = \frac{2}{p+q}, \quad \gamma = \frac{p-q}{p+q}.$$

For instance, the simplest cases $(p,q) = (1,2)$ and $(p,q) = (2,1)$ lead to $\gamma = -1/3$ and $\gamma = 1/3$, respectively.

We consider in detail the case $(p,q) = (2,1)$, that is $\gamma = 1/3$. We obtain that

$$\exp\left[\begin{pmatrix} 2\gamma & -1 \\ \gamma^2 - 1 & 0 \end{pmatrix}\tau\right] = \frac{1}{18}\begin{pmatrix} 6e^{-2\tau/3} + 12e^{4\tau/3} & 9e^{-2\tau/3} - 9e^{4\tau/3} \\ 8e^{-2\tau/3} - 8e^{4\tau/3} & 12e^{-2\tau/3} + 9e^{4\tau/3} \end{pmatrix},$$

and defining $v = \exp(-2\tau/3) \in (0,1)$, we get that the matrix exponential in terms of v is

$$\frac{1}{18v^2}\begin{pmatrix} 6\left(v^3+2\right) & 9(v-1)\left(v^2+v+1\right) \\ 8(v-1)\left(v^2+v+1\right) & 6\left(2v^3+1\right) \end{pmatrix}.$$

After solving for $u_-(v)$ and $u_+(v)$ we get

$$u_-(v) = y_E + \frac{(x_E+1)(2v^3+4) - 6v^2(x_E-1)}{3(v-1)\left(v^2+v+1\right)} \tag{B.6}$$

and

$$u_+(v) = y_E - \frac{(x_E-1)(4v^3+2) - 6v(x_E+1)}{3(v-1)\left(v^2+v+1\right)} \tag{B.7}$$

so that the condition for having a symmetric periodic orbit becomes

$$2y_E + \frac{(x_E+1)(2v^3+6v+4) - (x_E-1)(4v^3+6v^2+2)}{3(v-1)\left(v^2+v+1\right)} = 0,$$

that is

$$y_E = \frac{(x_E-1)(2v^3+3v^2+1) - (x_E+1)(v^3+3v+2)}{3(v-1)\left(v^2+v+1\right)}. \tag{B.8}$$

Taking again the value $x_E = -1/2$ as an interesting case of reference, we conclude that there appears a symmetric periodic orbit whenever

$$y_E = \frac{7v^3+9v^2+3v+5}{6(1-v)\left(v^2+v+1\right)},$$

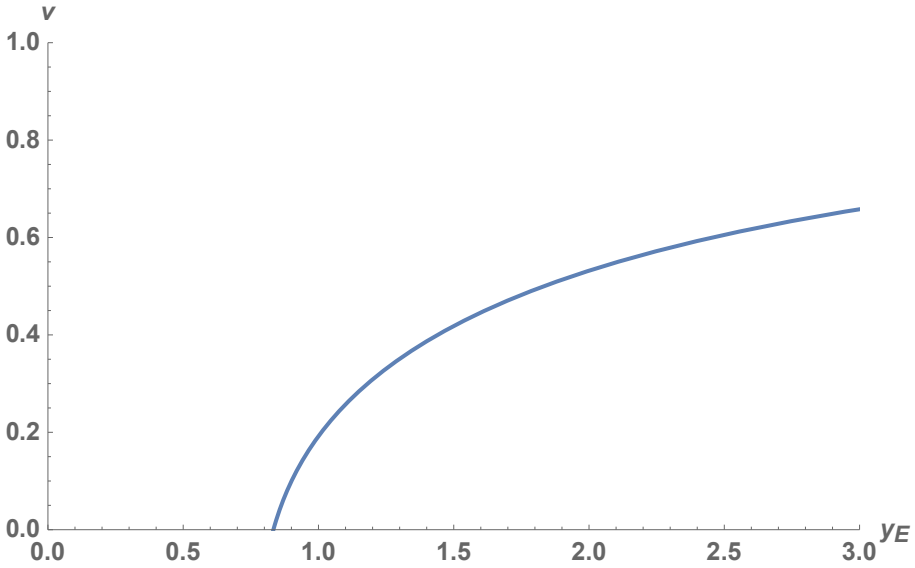

Figure B.3: The bifurcation set for symmetric periodic orbits in the case of a saddle with $\gamma = 1/3$ and $x_E = -1/2$. We can observe that the branch of periodic orbits starts in a homoclinic bifurcation at $y_E = 5/6$, corresponding to the limit value $v = 0$.

see Figure B.3. We observe that for $v = 0$ we have $y_E = 5/6$, so that there exists one symmetric periodic orbit for all $y_E > 5/6$. Furthermore, as $v = 0$ is the limit value when $\tau \to \infty$, the existence of these periodic orbits start from a homoclinic bifurcation, according to Theorem 3.9.

We repeat the procedure for solving (B.4) in looking for non-symmetric periodic orbits. After defining $v = \exp(-2\tau_1/3) \in (0, 1)$ and $w = \exp(-2\tau_2/3) \in (0, 1)$, we can take advantage of (B.6)-(B.7) to pass to a pair of polynomial equations, whose resultant is

$$-162(1 + 3x_E^2)(-1 + v)^5(1 + v + v^2)^4 F_1(v, x_E, y_E)F_2(v, x_E, y_E) = 0,$$

where

$$F_1(v, x_E, y_E) = (1 - x_E)(1 + 3v^2 + 2v^3) + (1 + x_E)(2 + 3v + v^3) - 3(1 + v^3)y_E,$$

and

$$F_2(v, x_E, y_E) = 4x_E(1 + v + v^2) + 3(-1 + v)(-1 - 3x_E + v - 3x_E v)y_E.$$

Clearly, the condition $F_1(v, x_E, y_E) = 0$ reproduces the branch of symmetric periodic orbits already obtained in (B.8), but we have also another possibility,

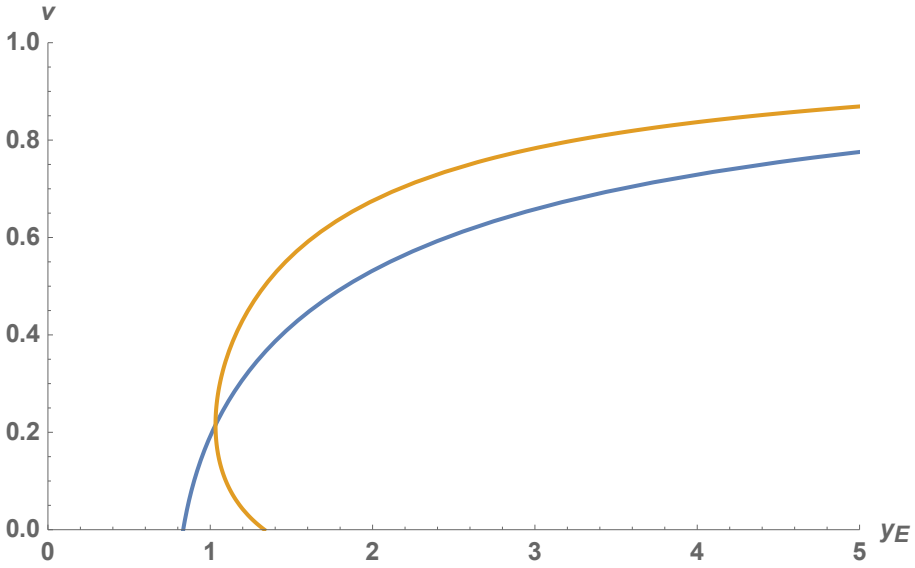

Figure B.4: The bifurcation set for symmetric and non-symmetric periodic orbits in the case of a saddle with $\gamma = 1/3$ and $x_E = -1/2$. We can observe that the two branches of non-symmetric periodic orbits start in a pitchfork bifurcation at $y_E = \frac{2}{9}\left(2+\sqrt{7}\right) \approx 1.03239$ and they end in a homoclinic bifurcation at $y_E = 4/3$, corresponding to the limit value $v = 0$.

as is the condition $F_2(v, x_E, y_E) = 0$. Thus, non-symmetric periodic orbits appear at

$$y_E = 4x_E \frac{1+v+v^2}{3(1-v)(-1-3x_E+v-3x_E v)}. \tag{B.9}$$

In our particular case $x_E = -1/2$, we have a non-symmetric periodic orbit for

$$y_E = -\frac{4\left(v^2+v+1\right)}{3(v-1)(5v+1)},$$

and we observe that this branch appears in a pitchfork bifurcation at the value $y_E = \frac{2}{9}\left(2+\sqrt{7}\right)$ leading to two new periodic orbits that disappear in a homoclinic connection ($v = 0$) for $y_E = 4/3$. We complete the bifurcation diagram of this case in Figure B.4, where it should be remarked that the upper non-symmetric periodic orbits branch is not relevant for $y_E > 4/3$, since then, although $v < 1$, the value of w becomes negative.

Bibliography

[1] A. A. Andronov, A. A. Vitt, and S. È. Khaĭkin. *Theory of oscillators*. Dover Publications, Inc., New York, 1987. Translated from the Russian by F. Immirzi, Reprint of the 1966 translation.

[2] J. C. Artés, J. Llibre, J. C. Medrado, and M. A. Teixeira. Piecewise linear differential systems with two real saddles. *Math. Comput. Simulation*, 95:13–22, 2014.

[3] I. Babaa, T. Wilson, and Yuan Yu. Analytic solutions of limit cycles in a feedback-regulated converter system with hysteresis. In *IEEE Transactions on Automatic Control*, volume 13, pages 524–531, 1968.

[4] B. C. Bao, Q. D. Li, N. Wang, and Q. Xu. Multistability in Chua's circuit with two stable node-foci. *Chaos*, 26(4):043111, 9, 2016.

[5] S. Bassein. The dynamics of a family of one-dimensional maps. *Amer. Math. Monthly*, 105:118 – 130, 1998.

[6] V. Carmona, E. Freire, E. Ponce, J. Ros, and F. Torres. Limit cycle bifurcation in 3D continuous piecewise linear systems with two zones. Application to Chua's circuit. *Internat. J. Bifur. Chaos Appl. Sci. Engrg.*, 15(10):3153–3164, 2005.

[7] V. Carmona, E. Freire, E. Ponce, and F. Torres. Invariant manifolds of periodic orbits for piecewise linear three-dimensional systems. *IMA J. Appl. Math.*, 69(1):71–91, 2004.

[8] V. Carmona, E. Freire, E. Ponce, and F. Torres. Bifurcation of invariant cones in piecewise linear homogeneous systems. *Internat. J. Bifur. Chaos Appl. Sci. Engrg.*, 15(8):2469–2484, 2005.

[9] V. Carmona, E. Freire, E. Ponce, and F. Torres. The continuous matching of two stable linear systems can be unstable. *Discrete Contin. Dyn. Syst.*, 16(3):689–703, 2006.

[10] K. Cheng and K.J. Palmer. On the dynamics os skew tent maps. *arXiv:1710.10880*.

[11] L. O. Chua, C. W. Wu, A. Huang, and G.Q. Zhong. A universal circuit for studying and generating chaos. I. Routes to chaos. *IEEE Trans. Circuits Systems I Fund. Theory Appl.*, 40(10):732–744, 1993.

[12] S. Coombes. Neuronal networks with gap junctions: a study of piecewise linear planar neuron models. *SIAM J. Appl. Dyn. Syst.*, 7(3):1101–1129, 2008.

[13] M. Desroches, S. Fernández-García, M. Krupa, R. Prohens, and A. Teruel. Piecewise-linear (PWL) canard dynamics : Simplifying singular perturbation theory in the canard regime using piecewise-linear systems. In *Nonlinear Systems*, volume 1 of *Mathematical Theory and Computational Methods*. Springer, September 2018.

[14] M. Desroches, A. Guillamon, E. Ponce, R. Prohens, S. Rodrigues, and A. E. Teruel. Canards, folded nodes, and mixed-mode oscillations in piecewise-linear slow-fast systems. *SIAM Rev.*, 58(4):653–691, 2016.

[15] M. di Bernardo, C. J. Budd, A. R. Champneys, and P. Kowalczyk. *Piecewise-smooth dynamical systems: theory and applications*. Applied Mathematical Sciences. Springer, 2008.

[16] M. Esteban, E. Ponce, and F. Torres. Bifurcation analysis of hysteretic systems with saddles. *Applied Mathematics and Nonlinear Science*, 2(2):449–464, 2017.

[17] M. Esteban, E. Ponce, and F. Torres. Periodic orbit in planar hysteretic systems without equilibria. *Submitted for publication*, 2018.

[18] M. Esteban, E. Ponce, and F. Torres. Periodic orbits in hysteretic systems with real eigenvalues. *Submitted for publication*, 2018.

[19] S. Fernández-García, M. Krupa, and F. Clément. Mixed-mode oscillations in a piecewise linear system with multiple time scale coupling. *Physica D: Nonlinear Phenomena*, 332:9 – 22, 2016.

[20] E. Freire, E. Ponce, and J. Ros. The focus-center-limit cycle bifurcation in symmetric 3D piecewise linear systems. *SIAM J. Appl. Math.*, 65(6):1933–1951, 2005.

[21] E. Freire, E. Ponce, and J. Ros. Bistability and hysteresis in symmetric 3D piecewise linear oscillators with three zones. *Internat. J. Bifur. Chaos Appl. Sci. Engrg.*, 18(12):3633–3645, 2008.

[22] E. Freire, E. Ponce, and F. Torres. A general mechanism to generate three limit cycles in planar Filippov systems with two zones. *Nonlinear Dynam.*, 78(1):251–263, 2014.

[23] F. Giannakopoulos and K. Pliete. Closed trajectories in planar relay feedback systems. *Dynamical Systems: An International Journal*, 17:343–358, 2002.

[24] J. M. Gonçalves, A. Megretski, and M. A. Dahleh. Global stability of relay feedback systems. *IEEE Trans. Automat. Control*, 46(4):550–562, 2001.

[25] J. Guckenheimer and P.J. Holmes. *Nonlinear Oscillations, Dynamical Systems, and Bifurcations of Vector Fields*, volume 42 of *Applied Mathematical Sciences*. Springer-Verlag, New York, first edition, 1983.

[26] M. P. Kennedy. Three steps to chaos. II. A Chua's circuit primer. *IEEE Trans. Circuits Systems I Fund. Theory Appl.*, 40(10):657–674, 1993.

[27] C. Kuehn and C. Münch. Generalized play hysteresis operators in limits of fast-slow systems. *SIAM J. Appl. Dyn. Syst.*, 16(3):1650–1685, 2017.

[28] Y. A. Kuznetsov. *Elements of applied bifurcation theory*, volume 112 of *Applied Mathematical Sciences*. Springer-Verlag, New York, third edition, 2004.

[29] J. Llibre and E. Ponce. Global first harmonic bifurcation diagram for odd piecewise linear control systems. *Dynamics and Stability of Systems*, 11(1):49–88, 1996.

[30] J. Llibre and E. Ponce. Bifurcation of a periodic orbit from infinity in planar piecewise linear vector fields. *Nonlinear Analysis*, 36:623–653, 1999.

[31] J. Llibre, E. Ponce, and J. Ros. Algebraic determination of limit cycles in a family of three-dimensional piecewise linear differential systems. *Nonlinear Anal.*, 74(17):6712–6727, 2011.

[32] J. Llibre and A. Teruel. *Introduction to the Qualitative Theory of Differential Systems*. Birkhäuser Advanced Texts Basler Lehrbücher. Springer Basel, 2014.

[33] R. Lupini, F. Bizzarri, and M. Storace. Discontinuities in a one-dimensional map describing a hysteretic chaotic circuit. In *Proceedings of the Third World Congress of Nonlinear Analysts, Part 8 (Catania, 2000)*, volume 47, pages 5253–5264, 2001.

[34] R.N. Madan. *Chua's Circuit: A Paradigm for Chaos.*, volume 1 of *World Scientific Series in Nonlinear Science (Book 1)*. World Scientific Pub Co Inc, 1993.

[35] U. F. Moreno, P. L. D. Peres, and I. S. Bonatti. Contributions to the analysis of second order piecewise linear systems with chaotic oscillations. volume I, pages 715–718, 2000.

[36] U. F. Moreno, P. L. D. Peres, and I. S. Bonatti. Analysis of piecewise-linear oscillators with hysteresis. *IEEE Trans. Circuits Systems I Fund. Theory Appl.*, 50(8):1120–1124, 2003. Special issue on switching and systems.

[37] K.A. Morris. What is hysteresis? *ASME Applied Mechanics Reviews.*, 64(5), 2011.

[38] R. W. Newcomb and N. El-Leithy. Chaos generation using binary hysteresis. *Circuits Systems Signal Process.*, 5(3):321–341, 1986.

[39] K. Pliete. *Closed Trajectories in Planar Piecewise-Smooth Systems of Liénard-Type with a Line of Discontinuity.* PhD thesis, Köln University, 2003.

[40] E. Ponce and J. Ros. On periodic orbits of 3D symmetric piecewise linear systems with real triple eigenvalues. *Internat. J. Bifur. Chaos Appl. Sci. Engrg.*, 19(7):2391–2399, 2009.

[41] E. Ponce, J. Ros, and E. Vela. Algebraically computable piecewise linear nodal oscillators. *Appl. Math. Comput.*, 219(9):4194–4207, 2013.

[42] E. Ponce, J. Ros, and E. Vela. Unfolding the fold-Hopf bifurcation in piecewise linear continuous differential systems with symmetry. *Phys. D*, 250:34–46, 2013.

[43] N. S. Postnikov. Dynamic chaos in relay systems with hysteresis. *Comput. Math. Model.*, 8(1):62–72, 1997. Nonlinear dynamical systems: qualitative analysis and control, No. 2.

[44] R. Prohens, A.E. Teruel, and C. Vich. Slowfast n-dimensional piecewise linear differential systems. *Journal of Differential Equations*, 260(2):1865 – 1892, 2016.

[45] T. Saito. The hysteresis chaos generator family. In *IEEE International Symposium on Circuits and Systems*, pages 15–18, 1988.

[46] T. Saito. An approach toward higher-dimensional hysteresis chaos generators. *IEEE Trans. Circuits and Systems*, 37(3):399–409, 1990.

[47] T. Saito and K. Mitsubori. Control of chaos from a piecewise linear hysteresis circuit. *IEEE Trans. Circuits and Systems*, 42(3):168–172, 1995.

[48] B. K. Shivamoggi. *Nonlinear dynamics and chaotic phenomena: an introduction*, volume 103 of *Fluid Mechanics and its Applications*. Springer, Dordrecht, second edition, 2014.

[49] D.J.W. Simpson. Dimension reduction for slow-fast, piecewise-smooth, continuous systems of odes. *Submitted for publication. arXiv:1801.04653*, 2018.

[50] I. Sushko, V. Avrutin, and L. Gardini. Bifurcation structure in the skew tent map and its application as a border collision normal form. *J. Difference Equ. Appl.*, 22(4):582–629, 2016.

[51] R. Thul and S. Coombes. Understanding cardiac alternans: a piecewise linear modeling framework. *Chaos*, 20(4):045102, 13, 2010.

[52] A. Tonnelier. McKean caricature of the FitzHugh-Nagumo model: traveling pulses in a discrete diffusive medium. *Phys. Rev. E (3)*, 67(3):036105, 9, 2003.

[53] A. Tonnelier and W. Gerstner. Piecewise linear differential equations and integrate-and-fire neurons: insights from two-dimensional membrane models. *Phys. Rev. E (3)*, 67(2):021908, 16, 2003.

[54] E. Vela. *Piecewise linear differential systems: limit cycles and analysis of bifurcations*. PhD thesis, University of Seville, 2013.

[55] A. Visintin. *Differential models of hysteresis*, volume 111 of *Applied Mathematical Sciences*. Springer-Verlag, Berlin, 1994.